USDA UNITED STATES DEPARTMENT OF AGRICULTURE

Agricultural Research Service

National Sedimentation Laboratory
Channel and Watershed Processes Research Unit
Oxford, Mississippi 38655

Erodibility of Cohesive Streambeds in the Yalobusha River System

By Andrew Simon, Robert E. Thomas, Andrew J. C. Collison and Wendy Dickerson with Appendix II by Carlos V. Alonso.

Research Report No. 26 **February 2002**

EXECUTIVE SUMMARY

The general objective of this study was to provide the U.S. Army Corps of Engineers, Vicksburg District with erodibility, erosion rates, and knickpoint migration rates for the cohesive streambeds of the Yalobusha River system. Specifically, the USDA-ARS National Sedimentation Laboratory was charged with:

1. Determining bed-material characteristics, incipient-motion criteria, and erosion rates of the clay beds in reaches targeted by the Corps of Engineers (CoE) for grade control and knickpoint areas previously identified by 1997 CoE surveys and the ARS in Simon (1998);
2. Determining the spatial distribution of the erodibility, incipient-motion criteria, and erosion rates of the clay beds;
3. Developing predictive technology for rates of erosion and knickpoint migration for the clay beds; and
4. Identifying and prioritizing clay-bed reaches in most need of erosion control;

Erosion of streambed materials in the Yalobusha River system is controlled by the nature of the two dominant geologic formations: Naheola and Porters Creek Clay. These are expressed in terms of two parameters: critical shear stress and an erodibility coefficient. Maps of the distribution of these parameters throughout the Yalobusha River system are provided in the body of the report. In general, Porters Creek Clay is extremely resistant to erosion by hydraulic stresses, requiring shear stresses in the hundreds of Pa to initiate downcutting. Given the range of representative flow depths and bed slopes, shear stresses of this magnitude probably do not occur on a frequent basis. This resistance to hydraulic erosion apparently also plays an important role in limiting knickpoint migration in two key ways. Firstly, the potential for geotechnical failure is reduced because of a lack of downcutting needed to produce a knickpoint face of sufficient height to create instability; and secondly, secondary scour, caused by pressure reduction and flow acceleration close to the brink, is reduced. Erosion of streambeds cut into the Naheola formation, however, can occur over a range of commonly occurring shear stresses. These differences lead to stark contrasts in knickpoint migration rates between the two formations, notwithstanding that the geotechnical shear strength of Naheola beds are greater than those composed of the Porters Creek Clay.

Tables are provided that classify erosion resistance (in Pascals) and erodibility (in $cm^3/N\text{-}s$) for every study site. For every site, an estimate of the amount of erosion that would occur for one-day storms at a range of shear stresses is provided as a guide. In addition, shear stress-exceedance series for the intensively monitored sites, and associated erosion estimates have also been provided. These have been compared to the erosion observed in surveys and a hydraulic analysis has been performed to account for discrepancies.

That migration of some knickpoints or knickzones, particularly those cut into the Porters Creek Clay formation, has been severely limited is directly related to the hydraulic resistance of these clay beds. More than 30 years after the completion of the most recent channel dredging on the Yalobusha River main stem (1967), the major erosion zone is still just upstream of the upstream terminus of the channel work (river kilometer 27.8). With maximum critical shear stress values reaching more than 400 Pa, erosion of knickpoints cut into the Porters Creek Clay formation is marginal.

ACKNOWLEDGMENTS

The material presented here was developed as part of a program of applied research in geomorphology and erodibility of unstable river systems cut into cohesive streambeds. Funds for this work were provided by the U.S. Army Corps of Engineers, Vicksburg District under Reimbursable Agreement 00-OA-6408-008 (ARS Project No. 6408-13000-010-08R) and carried out in cooperation with the USDA Agricultural Research Service, National Sedimentation Laboratory. We would like to thank Brian Bell, Bret Bledsoe, Kari Christman, Mark Griffith, Tony Layzell, Rob Neely and Geoff Waite for assisting with fieldwork and database development. Finally, we would also like to thank Messrs. John Smith and Phillip Haskins (CoE) for supporting this research.

TABLE OF CONTENTS

LIST OF FIGURES

LIST OF TABLES

INTRODUCTION AND BACKGROUND

Thousands of kilometers of cohesive-bed stream channels in the Midwestern United States are incised and eroding at accelerated rates due to human disturbances imposed near the turn of the 20th century (Simon and Rinaldi, 2000). The Yalobusha River of north-central Mississippi (upstream of Grenada Lake) is one of these systems and poses particular concerns to river managers because of downstream flooding problems in the vicinity of Calhoun City. The U.S. Army Corps of Engineers (CoE), Vicksburg District is charged with alleviating the downstream flooding problems resulting from a massive debris dam (see Simon, 1998) while protecting middle and upper reaches from further streambed and streambank erosion. Before the CoE can consider removing the debris dam or re-routing downstream flows, they are protecting reaches upstream from this zone by constructing grade-control and other structures. Prediction of future channel responses and the effects of potential mitigation measures are difficult, however, because of an incomplete knowledge of erodibility and erosion mechanisms in cohesive streams.

The detachment and erosion of cohesive (silt- and clay-sized) material by gravity and/or flowing water is controlled by a variety of physical, electrical, and chemical forces. Identification of all of these forces and the role they play in determining detachment, incipient motion, and erodibility of cohesive materials is incomplete and, at least, still poorly understood. The behavior of cohesive materials in flowing water is important in estimating erosion and sedimentation in a variety of types of waterways, and in the associated transport of adsorbed constituents. Sub-aerial behavior of cohesive materials is important in determining soil detachment and erosion from channels, upland areas (by overland flow or raindrop impact), and with regards to mass movements on hillslopes and channel banks.

Assessing erosion resistance of cohesive materials by flowing water is complex due to the difficulties in characterizing the strength of the electro-chemical bonds that define the resistance of cohesive materials. The many studies that have been conducted on erodibility of cohesive materials have observed that numerous soil properties influence erosion resistance including antecedent moisture, clay mineralogy and proportion, density, soil structure, organic content, as well as pore and water chemistry (Grissinger, 1982). Furthermore, field evidence indicates that cohesive streambeds erode by a variety of mechanisms including particle-by-particle detachment, geotechnical failure of knickpoint faces, and possibly, by upward-directed seepage forces. Studies of streambank stability in cohesive materials have led to recognition of the importance of positive and negative pore-water pressures in accurate numerical analysis of mass-wasting processes and channel widening (Casagli *et al*., 1997; Simon and Curini, 1998; Rinaldi and Casagli, 1999; Simon *et al*., 1999). Negative pore-water pressures increase the shear strength of unsaturated, cohesive materials by providing tension between particles. These studies led to the idea that positive and negative pore-water pressures may play an important role in the entrainment and erosion of cohesive streambed particles or aggregates (Simon and Collison, 2001).

The need for evaluation of cohesive streambed erodibility in the incised channels of the Midwestern United States led to initial field testing of the hydraulic stresses required to erode cohesive streambeds (critical-shear stresses; Hanson and Simon, 2001). As part of this effort, a number of sites in the Yalobusha River system were tested during the spring of 1998. The preliminary results from several streams in the Yalobusha River basin along with the location and size of major knickzones were reported to the CoE in Simon (1998) and showed that some of

the streambeds were extremely resistant to erosion by flowing water. Measured critical shear stresses in the range of 32-393 Pa (mean = 158 Pa) indicated that on average, erosion of the tested clay beds was equivalent to eroding a non-cohesive particle with a diameter of 330 mm. The large range of critical shear stress values severely limits the application of such criteria to predict the erosion of these clay beds, the migration of knickpoints, and further bed incision. However, if these preliminary estimates are valid, then rates of erosion and knickpoint migration may be very low in specific reaches of the Yalobusha River system, which may serve as "natural" grade control. Given the plans of the CoE to construct grade control structures at critical knickzones in the basin, it was important to determine the distribution of erodibility, erosion rates, and knickpoint migration rates in the Yalobusha River system. This information will serve to assist the CoE in developing their Technical Work Plan and designs for grade control. To address these issues, a research plan was developed to evaluate the erodibility of cohesive streambeds and migration rates of critical knickpoints in the Yalobusha River system.

OBJECTIVES AND SCOPE

The general objective of the study was to provide the U.S. Army Corps of Engineers, Vicksburg District with erodibility, erosion rates, and knickpoint migration rates for the cohesive streambeds in the Yalobusha River system. Specific objectives included:

1. Determine bed characteristics, incipient-motion criteria, and erosion rates of the clay beds in reaches targeted by the Corps of Engineers for grade control, and knickzone areas previously identified by 1997 CoE surveys and the ARS in Simon (1998);
2. Determine the spatial distribution of the erodibility, incipient-motion criteria, and erosion rates of the clay beds;
3. Develop predictive technology for rates of erosion and knickpoint migration for the clay beds;
4. Identify and prioritize clay-bed reaches most in need of erosion control;
5. Establish a technique that determines the critical link between knickpoint migration, subsequent channel incision and widening, and delivery of woody vegetation to the channel to reduce the likelihood of renewed accumulation of large woody debris.

The latter objective was addressed in a separate report (Downs and Simon, 2001) and is, therefore, not reported here.

To realize the five specific objectives and to deliver a working tool to the CoE, Vicksburg District, the methods employed in this study are separated into several units, each of which is dependent on and complementary to the others. These include:

1. Field testing of hydraulic and geotechnical characteristics of clay-bed materials in all major (critical) knickzone reaches and in areas of proposed grade-control structures in order to develop erodibility relationships, critical shear stress values, and *in situ* rates of erosion;
2. Field measurement of erosion rates of knickpoints (ten sites) combined with flow-level monitoring over a period of three years using survey and hydraulic measurements; and

3. Numerical modeling of clay beds and knickpoints to analytically test field observations of erosion processes and to develop criteria for incipient-motion and knickpoint migration.

SITE SELECTION

Two basic types of sites were identified, and erodibility data were collected at both types. "Intensive" sites were located in the vicinity of existing major knickpoints (Figure 1). The purpose of the "intensive" sites was to monitor knickpoint migration and to collect stage data to calculate water-surface slope and shear stress for a range of flow events. This was accomplished with a set of four pressure transducers mounted on fence posts and placed longitudinally along the reach containing the knickzone. "General" sites were located in the vicinity of proposed grade-control structures and were sited for the sole purpose of erodibility testing of the cohesive streambeds (Figure 1). No topographical survey or stage information was collected at these sites. A site list corresponding to the numerical scheme of Figure 1 is provided in Table 1.

The majority of sites were selected by the Corps of Engineers. Additional sites were added by the National Sedimentation Laboratory (NSL) to provide a more comprehensive view of the basin. The initial criteria for site selection were based on the 1997 longitudinal profile surveys completed by the CoE. Sites that appeared to have a significant drop in bed elevation were assigned to an NSL reconnaissance team for determination of dominant formation, bed-material type and the nature of the change in bed elevation. The reconnaissance team discovered that some of the rapid local decreases in bed elevations were due to beaver and debris dams. Those sites that had head cutting were scheduled for erodibility testing.

A total of 88 sites were selected in the Yalobusha River basin as a part of this study (Table 2). Of those sites, 75 were actually tested, 10 were un-testable, and estimates of erodibility were made at three sites. Sites where data were estimated were due to problems with equipment accessibility or uncooperative landowners. The 10 un-testable sites varied from beaver/debris dams to depositional areas. A total of 172 jet-tests were performed on 2 types of material; 105 on streambeds consisting of the Naheola formation and 67 on streambeds consisting of the Porters Creek Clay formation.

METHODS

The methods employed in this study can be conveniently separated into field and analytical techniques, each of which were used to evaluate (1) surface erosion by hydraulic shear stresses and (2) mass failure and upstream migration of knickpoints. Methods to evaluate surface erosion were conducted at all of the sites while evaluation of knickpoints was conducted at the ten "intensive" sites only.

Field Methods

Several field instruments were used to characterize the *in situ* mechanical properties and erodibility of the cohesive streambeds. Surface erodibility by flowing water was quantified with a submerged jet-test device (Hanson, 1990), substrate pore-water pressure was recorded *in situ*

with a miniature, digital tensiometer, while the geotechnical resistance to mass failure of the streambeds was evaluated with a borehole shear tester (BST; Lutenegger and Hallberg, 1981).

Jet-Test Device - Development & Background

A submerged jet-test has been developed by the Agricultural Research Service (Hanson, 1990) for testing the *in situ* erodibility of surface materials in the laboratory and in the field (ASTM, 1995). This device has been developed based on knowledge of the hydraulic characteristics of a submerged jet and the characteristics of soil-material erodibility. In an attempt to remove empiricism and to obtain direct measurements of the critical shear stress parameter (τ_c) and the erodibility coefficient (k), Hanson and Cook (1997) developed analytical procedures for determining soil k based on the diffusion principles of a submerged circular jet and the corresponding scour produced by the jet. These procedures are based on analytical techniques developed by Stein *et al*. (1993) for a planar jet at an overfall and extended by Stein and Nett (1997). Stein and Nett (1997) validated this approach in the laboratory using six different soil types.

Stein and Nett (1997) showed that as the scour hole increases with time, the applied shear stress decreases due to increasing dissipation of jet energy within the plunge pool. Detachment rate is initially high and asymptotically approaches zero as shear stress approaches the critical shear stress of the bed material. The difficulty in determining equilibrium scour depth is that the length of time required to reach equilibrium can be large. Blaisdell *et al*. (1981) observed during studies on pipe outlets that scour in cohesionless sands continued to progress even after 14 months. They developed a function to compute the equilibrium scour depth that assumes that the relation between scour and time follows a logarithmic-hyperbolic function. Fitting the jet-test data to the logarithmic-hyperbolic method described in Hanson and Cook (1997) can predetermine the parameter τ_c. k is then determined by curve fitting measured values of scour depth versus time and minimizing the error of the measured time versus the predicted time. Both k and τ_c are treated as soil properties and the former does not generally correlate well with standard soil mechanical indices such as Atterberg limits. Instead, k is dependent on the physio-chemical parameters that determine the inter-particle forces characteristic of cohesive sediment (Parchure and Mehta, 1985; Mehta, 1991).

Jet-Test Device - *In Situ* Field Techniques

In situ jet-tests were performed at each of the study sites. In general, at least one test each was conducted on perennially wet and intermittently dry areas of the bed. The jet-test apparatus consists of a pump, adjustable head tank, jet submergence tank, jet nozzle, delivery tube, and point gauge (Figure 2). Water is pumped directly from the stream into an adjustable head tank designed to supply shear stresses between 4 and 200 Pa. Stresses up to 1500 Pa can be applied using a direct connection from the jet tube to the pump. A rounded 6.4 mm-diameter nozzle forms the jet. The nozzle is submerged within a cylindrical tank that is driven into the streambed. The initial height of the nozzle above the streambed is noted and can be easily adjusted prior to initiating a test. Changes in maximum bed scour are measured using a point gauge at specific time increments. With relatively hard material, maximum scour measurements were taken at ten-minute intervals over a period of 120 minutes. With relatively soft material, maximum scour measurements were taken at five-minute intervals over a period of 60 minutes at

a lower pressure setting. To ensure that the point gauge is not pushed down into the bed, the operator places their hand near the scour location and feels when the rod just touches the bed material.

Initiation of a jet-test requires placement of the submergence tank by driving it 40 mm into the bed. Once the submergence tank is set in the bed, the jet tube and adjustable head tank are attached. The head tank controls the pressure delivered to the jet nozzle and, in turn, the jet velocity. Once the jet nozzle is set, the initial jet height is measured precisely using the point gauge. Following a determination of the bed elevation relative to the jet nozzle, the head is set by holding a deflection plate downstream of the jet nozzle to divert the impinging jet. Once the head is set, testing can begin by removing the deflection plate and allowing the jet to impinge on the bed.

Borehole Shear Test (BST) - Field Techniques

The borehole shear tester (Figure 3) measures drained, direct-shear geotechnical parameters (cohesion and angle of internal friction) *in situ*. An 80 mm × 400 mm-deep hole is bored into the channel bed. The shear head is placed in the borehole to a depth of about 0.3 m and expanded out under a known initial pressure (generally about 40 kPa) to the walls of the borehole. Depending on the formation, Porters Creek or Naheola, an initial consolidation time of 90 minutes or 60 minutes is used, respectively. An axial stress is then applied and measured on the shearing gauge until failure beyond the walls of the borehole occurs. The axial stress is released, the normal pressure is raised in increments of about 10 kPa, an additional 30 minutes of consolidation is provided and the axial stress is applied again. In this way a series of data points are obtained providing the shear stress required to fail the material for each associated normal stress that was applied to the walls of the borehole. A linear regression between shear stress (y-axis) and normal stress (x-axis) then provides apparent cohesion (y-intercept) and friction angle (slope of the regression line). Figure 4 is provided as an example.

As with the jet-tests, where possible, wet and dry tests were performed at each site to test for differences in strength characteristics. The wet tests were conducted on perennially wet areas of the bed by placing a cofferdam into the material and establishing a waterproof seal prior to augering into the streambed.

Pore-Water Pressure - Field Techniques

Total cohesion includes both the inherent cohesion (effective) due to the soil skeleton and any additional cohesion provided by matric suction. To obtain values of effective cohesion, measurements of pore-water pressures below the surface of the streambeds were required. Pore-water pressure was recorded *in situ* with a miniature, digital tensiometer that provided measurements of either positive or negative (matric suction or tension) pore-water pressure. A 5 mm hole was bored or drilled into the surface to a depth of about 60 mm. The tensiometer was immediately placed in the hole and readings were recorded every 15 seconds for a minimum of 6 minutes. If the readings had not stabilized during the first 6 minutes additional readings were taken until the readings stabilized. The resulting pore-water pressure data are then plotted against time to assure that the readings have equilibrated. In cases where they have not, a power regression function is applied to obtain the asymptotic, equilibrium value of pore-water pressure (Figure 5). Values of effective cohesion are then obtained using the following formula:

$$c' = c_a - \psi(\tan \phi^b) \quad (1)$$

where c' = effective cohesion, in kPa; c_a = apparent cohesion (measured with the BST), in kPa; ψ = matric suction (tension), in kPa; and ϕ^b = rate of increase of shear strength with increasing matric suction (negative pore-water pressure) and assumed to be about 10-15 degrees.

Streambed Sampling

Samples of cohesive streambed materials were obtained at all sites to perform a number of analytic laboratory tests. Samples for particle-size analysis were obtained with an auger from the boreholes where BST tests were conducted. Surface materials were also sampled in the vicinity of the jet-tests for particle-size analysis. Undisturbed cores were obtained by driving a hammer sampler into the bed from the surface. The resulting 50 mm × 50 mm soil cores were extruded and sealed in the field then returned to the laboratory for evaluation of bulk unit weight, moisture content and, at "intensive sites", saturated hydraulic conductivity (permeability, k_{sat}).

Saturated Hydraulic Conductivity (permeability, k_{sat})

Permeability rates were determined utilizing a laboratory falling head permeameter (Figure 6). Sufficient readings were taken to enable calculation of k_{sat} by the equation:

$$k_{sat} = \left(\frac{\left(d_P^{\,2} + d_{PT}^{\,2}\right)L}{\left(d_{SC}^{\,2}\right)t} \right) \ln\left(\frac{H_1}{H_2} \right) \quad (2)$$

where k_{sat} = permeability, in m/s; d_P = diameter of permeameter, in m; d_{PT} = diameter of permeameter reading tube, in m; L = depth of soil core, in m; d_{SC} = diameter of soil core, in m; t = time step, in seconds; H_1 = starting head of water in permeameter, in m; and H_2 = finishing head of water in permeameter. Equation (2) was modified from Watts and Halliwell (1996).

Monitoring of Flow and Knickpoint Migration Rates

Surveys of "Intensive" Sites

Up to twelve repetitive surveys were conducted between 1999 and 2002 at the ten "intensive" sites in the basin. Surveys of the channel thalweg were conducted noting any changes in slope. Where knickpoints have discrete lips, leading to steeply inclined faces, planimetric surveys of the form of the knickpoint were made. Survey data obtained during this study was "tied" into the 1997 CoE surveys to provide a longer record of change in the knickpoints. At all locations except Bear Creek this effort was successful.

Water Stage and Shear Stress

Calibrated pressure transducers were installed to measure stage variations with time. The transducers were set to take measurements every 30 minutes to give an almost continuous record

(Figure 7a). This record was then compared to that for the USGS gauging station 07283000, Skuna River at Bruce, in order to verify peak stages (see Figure 7b). Verified peaks were used to evaluate the magnitude and duration of excess shear stresses for assessing rates of erosion due to hydraulic stresses, and as input to finite-element software for the purpose of modeling the movement and distribution of pore-water pressure within the streambed. Stage data were also required for use with the finite-element stability software used to model failure of knickpoint faces. As a means of comparing the relative magnitude of flows during the study period with the long-term historical record, flow frequency plots were produced for the Skuna River at Bruce for the periods 1948-2001 and 1999 to 2001 (Figure 7c).

An average boundary shear stress is calculated from:

$$\tau_o = \gamma R S \tag{3}$$

where γ = unit weight of water, (9810 N/m^3); R = hydraulic radius (which is, for a wide open channel, equal to the flow depth), in m; and S = channel gradient, in m/m. Because of irregularities in the bed profiles, regression analyses were used to approximate the bed slopes. As an example, the channel bed in the vicinity of the major knickpoint on Big Creek is shown in Figure 8. Flow depths were used in lieu of hydraulic radius and were obtained by subtracting the elevation of the channel bed from the measured flow stage.

EROSION RESISTANCE AND ERODIBILITY OF STREAMBED MATERIALS BY HYDRAULIC FORCES

To address the problem of estimating critical shear stresses, potential erosion of streambeds and migration of knickzones, erosion tests on representative clay beds in the Yalobusha River system were conducted between 1998 and 2001 with the submersible jet-test device described earlier.

Jet-Test Results

Results of 176 jet-tests (105 in the Naheola; 67 in the Porters Creek Clay; and 4 in other materials) indicate that there is a wide variation in the erosion resistance of the streambeds (Table 3). Values of τ_c span almost four orders of magnitude from near 0.0 to greater than 400 Pa (mean = 87.8 Pa; standard error = 9.3 Pa). Values of k span about three orders of magnitude (mean = 0.12 cm^3/N-s; standard error = 0.02 cm^3/N-s). Exceptionally low values of τ_c (less than 0.01) were recorded during 22 jet-tests, in most cases due to the jet impinging on weaker layers or pockets of sand within the streambed. These low values were adjusted to a minimum value of 0.062 Pa to approximate a critical shear stress required to erode very fine sand or silt.

To provide a concise picture of the distribution of τ_c values throughout the Yalobusha River system, an average τ_c (and k) for each site were calculated from the data in Table 4. These data were then assigned an erodibility class modified from the five classes developed by Hanson and Simon (2001). The four erodibility classes for τ_c and their corresponding color codes shown in Table 4 and Figure 9 are:

- <1.99 = very erodible, red

- 2.00 to 9.99 = erodible, yellow
- 10 to 99.9 = resistant, blue
- >99.9 = very resistant, gray

Each of the tested sites was then mapped according to its τ_c class using GIS software. Reaches between sites within a similar geologic formation and τ_c class are assumed to be in the same class. For example, note the lengthy reaches (shaded gray) of very resistant materials along upper Topashaw Creek that extend up lower Buck Creek and Topashaw Tributary 1. These reaches, in contrast to the middle reaches of the Yalobusha River main stem and lower Dry and Little Topashaw Creeks, are extremely resistant to erosion by hydraulic forces (Figure 9).

The CD Rom accompanying this preliminary report contains the project maps shown in Figures 1, 9 and 10 that were generated using ArcView GIS software. By clicking on a specific site, average values of τ_c, k, and information such as stationing for that site, become highlighted within the associated data table. This feature has been enhanced to include additional information and digital photographic imagery of all of the sites. The CD Rom also contains a "Help" file containing instructions for utilizing the map features (Appendix I).

Similar classes for the erodibility coefficient k were also created and mapped in Figure 10:

- >0.199 = very erodible, red
- 0.091 to 0.199 = erodible, yellow
- 0.011 to 0.090 = resistant, blue
- <0.011 = very resistant, gray.

Erodibility by Formation

Distinct differences in susceptibility to erosion by hydraulic stresses exist for the two dominant formations. The Porters Creek Clay formation is clearly much more resistant to erosion by hydraulic forces than the Naheola formation. Table 5 shows mean and median values for τ_c and k sorted by formation. Values were obtained from all tests and from average site values. Median values are shown to provide a better estimate of the central tendency of the data distribution since they are not normally distributed. Frequency histograms for τ_c are shown in Figure 11 as an example. The histograms show that resistance of the Naheola formation is quite variable, with almost equal frequencies of occurrence across all class intervals but with a reduction in occurrence with increasing shear stress. In contrast τ_c values for the Porters Creek Clay formation are almost exclusively in the highest class, attesting to its much greater resistance to hydraulic forces.

To relate τ_c and k values to the relative potential for flows to erode cohesive beds in the Yalobusha River system, and in the absence of local shear stress data, an average boundary shear stress is calculated (Eq. (3)). Shear stresses are generated for a range of slopes (0.001-0.004) and flow depths of (1, 2, 4, and 8 m) (Table 6).

Clearly, most flows will be competent to erode streambeds composed of the Naheola formation (τ_c = 1.53 Pa). In contrast, only the deepest (8 m) flows with profiles steeper than 0.003 m/m generate average boundary shear stresses great enough to erode streambeds

composed of the Porters Creek Clay formation (τ_c = 183 Pa). Slopes this steep are probably only found in knickzones (Table 6).

Critical Shear Stress and Equivalent Particle Diameter

We can better visualize the detachment threshold for cohesive sediments by calculating the diameter of a cohesionless particle that would be eroded with the same shear stress. This is accomplished using the Shields criterion for the measured critical shear stresses:

$$\tau_* = \frac{\tau_0}{(\gamma_s - \gamma)d} \tag{4}$$

where τ_* = critical dimensionless shear stress (commonly 0.03, 0.047, or 0.06); γ_s = unit weight of sediment, in N/m^3; and d = a representative particle diameter, in m.

To account for the differences between the two primary materials making up the streambeds, the median τ_c value for each of the two formations (1.53 and 183 Pa) are used along with τ_* values of 0.03, 0.047, and 0.06. Equivalent particle diameters are calculated using Equation (4) and by assuming (γ_s - γ) = 1,650 kg/m^3 × 9.81 m/s^2. Results range from 188-377 mm and from 1.6-3.2 mm for the Porters Creek Clay and Naheola formations, respectively. Erosion of streambeds composed of the Porters Creek Clay formation is, therefore, equivalent to entraining particles with diameters between 188 and 377 mm. This is significant in that clasts of this equivalent size are often used as rip rap to protect streambeds from erosion.

Streambed-erodibility (expressed in terms of τ_c) characteristics of the Yalobusha River system are highly skewed, representing the two dominant material types (Figure 11a). As one might expect, a similar skewed distribution is shown for equivalent particle diameters in Figure 12a. The upper class of Figure 12a represents the Porters Creek Clay formation while the lowest classes represent the overlying Naheola formation, both belonging to the Midway Group of Paleocene age (Parks, 1961). Order of magnitude variation of τ_c within each material type is believed to be a function of varying degrees of sub-aerial exposure, weathering, and the amount of cracking along bedding planes and other planes of weakness. Under most conditions, the Porters Creek Clay is extremely resistant as evidenced by the great majority of test results falling in the highest classes of τ_c and equivalent diameter (Figures 11c and 12c). In contrast, τ_c data from streambeds composed of the Naheola formation are quite variable, bridging all data classes (Figures 11b and 12b).

Erodibility by Wet Versus Dry Conditions

The effect of continuous wetting in contrast to intermittently dry conditions on surface erodibility was compared for each of the two formations because of the drastic differences in the parameters τ_c and k between formations (Table 7). Based on median values of τ_c, intermittent drying of Porters Creek Clay streambeds results in a decrease in erosion resistance of 46%. A similar effect is shown by the 40% increase in median k values for the Porters Creek Clay formation under dry-bed conditions. However, both the τ_c and k data for the Naheola formation show an opposite effect, with τ_c values increased by 117% and k reduced by 25%. This

illustrates stark contrasts in the way the two materials react under wetting and drying scenarios. Under intermittently dry conditions, Porters Creek Clay beds tend to desiccate and crack extensively, forming flakes of material in the clay size range, which are easily entrained when flows return. Conversely, when dried, Naheola clay beds tend to form resistant pans on the bed surface, which are relatively unerodible by hydraulic shear.

Erosion Rates by Hydraulic Shear

In this study, jet-test results were used to develop a relation between critical shear stress (τ_c) and the erodibility coefficient (k) by which to estimate erosion rates of cohesive streambeds. One of the more commonly used functions is (Partheniades, 1965):

$$\varepsilon = k\,(\tau_o - \tau_c)^a \qquad (\text{for } \tau_o > \tau_c)$$
$$\varepsilon = 0 \qquad (\text{for } \tau_o \le \tau_c) \qquad (5)$$

where ε = erosion rate, in m/s; k = erodibility coefficient, in m^3/N-s; $\tau_o - \tau_c$ = excess shear stress, in Pa; τ_o = average boundary shear stress, in Pa; τ_c = critical shear stress, in Pa; and a = an exponent (often assumed = 1.0).

An inverse relationship between τ_c and k was observed, where soils exhibiting a low τ_c have a high k and soils having a high τ_c tend to have a low k. Because those sites with the greatest values of τ_c maintain the lowest erodibility coefficients (Figure 13), they can be expected to erode by *hydraulic stresses* at the lowest rates. This is not to say that erosion by other processes such as *geotechnical failure* of knickpoint faces follows this relation. Based on these observations, k can be estimated as a function of τ_c ($r^2 = 0.58$; Figure 13):

$$k = 0.08\ \tau_c^{\,-0.45} \qquad (6)$$

This relation is very similar to the one developed by Hanson and Simon (2001) for cohesive streambeds in the Midwestern United States (some sites from the Yalobusha River system were included) and to observed trends reported by Arulanandan *et al.* (1980) in laboratory flume testing of soil samples from streambeds across the United States. We can, therefore, provide a general expression for the relation between critical shear stress (τ_c) and erodibility coefficient (k):

$$k \approx 0.1\ \tau_c^{\,-0.5} \qquad (7)$$

This expression can then be utilized to estimate the parameters required to calculate erosion rates using Equation (5).

A "representative" average boundary shear stress of 78 Pa is calculated for non-knickzone reaches assuming an 8 m-deep flow at a bed slope of 0.001. Although this shear stress is insufficient to erode an "average" cohesive streambed cut into the Porters Creek Clay formation, local shear stresses as great as 225 Pa have been measured in the vicinity of knickzones. Based on τ_c data obtained from jet-testing, shear stresses of this magnitude are apparently capable of eroding some of the knickzone areas, particularly those cut into the Naheola formation. Table 6 provides a range of combinations of flow depth and bed slope that

are capable of generating high shear stresses, particularly in the vicinity of knickzones where bed slopes are steeper.

Rates of erosion in mm/s were calculated by Equation (5) for all study sites in the Yalobusha River system using average τ_c and k values obtained from jet-testing and by assuming a range of steady-flow conditions with boundary shear stresses of 50, 100, 150, 200, 250 and 300 Pa (Table 8). Values in this table provide an estimate of the rates of downwearing that would occur at a given site under the given range of shear stress conditions. However, due to limits imposed by channel depth and slope, all sites will not necessarily be capable of passing flows over the entire range of shear stresses used. Table 6 can be used somewhat as a guide to the general range of available shear stresses for a given set of flow depth and bed slope conditions.

Median values are again used as a measure to differentiate between sites with streambeds composed of the two different formations. As indicated previously, streambeds composed of the Porters Creek Clay formation are shown to be non-erodible until flows of about 250 Pa are encountered. At this shear stress, these beds can erode via particle-by-particle detachment at a rate of about 0.0004 mm/s (Table 8). Streambeds composed of the Naheola formation are readily eroded over the entire range of shear stresses at rates of 0.0047 to 0.032 mm/s (Table 8). Further separation of the data is to differentiate between wet and dry test conditions for both formations. The use of median values for τ_c and k provides estimates for the full range of estimated shear stresses (Figure 14).

Erosion Amounts by Hydraulic Shear

An evaluation of the amount of erosion that is likely to occur by hydraulic stresses at a given site requires knowledge of the duration of flows that will attain and exceed given shear stress values. Because flow data are not available at the "general" sites, only a rough estimate can be provided. Table 9 shows the amount of erosion (in m) that is likely to occur during a one-day storm event of a given shear stress at all study sites. Caution should be exercised in evaluating these results because of the uncertainty in predicting the magnitude and frequency of given shear stress values. Still, order of magnitude estimates are possible that can be used for planning purposes at the "general" sites. This is particularly true for sites cut into the Porters Creek Clay formation where extremely low rates and amounts of predicted erosion can be used to prioritize the siting of grade-control structures. Median values of erosion amounts are shown for each formation at the bottom of Table 9 and again clearly demonstrate the more resistant character of the Porters Creek Clay formation.

KNICKPOINT EROSION AND MIGRATION

Network-wide thalweg profiles surveyed by the U.S. Army Corps of Engineers (CoE) in 1997, combined with extensive field and aerial reconnaissance, identified a total of ten major knickpoints in the Yalobusha River system (Simon, 1998). The simplest and most commonly quoted definition of knickpoints is that of Brush and Wolman (1960). They state, *"knickpoints are points of abrupt change in the longitudinal profile of a stream"* (p.60). Special cases of the more general term 'knickpoint' include headcuts, which occur where the change in profile is a nearly vertical drop in the elevation of the channel (Begin *et al.*, 1980); and knickzones (resembling ramps), steeper reaches of channel representing a headward migrating zone of

incision (Schumm *et al.*, 1984; Schumm *et al.*, 1987). Knickzone locations generally represent the upstream terminus of channel-adjustment processes and many of the largest ones seem to be almost equidistant from the lower end of the river system, in the vicinity of river kilometer 28-30 (Figure 1; and Simon, 1998). Since the CoE 1997 survey, repeated surveys (starting in February 1999) of individual knickpoints were conducted after major flow events. Because of (1) some uncertainty in establishing the exact location of certain 1997 survey monuments, and (2) excessive distance between some 1997 thalweg-survey points, knickpoint-migration rates based on an initial time (t_0) of 1997 survey points are not as accurate as those based on the initial 1999 survey points.

Knickpoint Migration Rates: Field Evidence

Knickpoint migration rates were obtained from analysis of the repeated surveys. Cross-sectional and planimetric views of knickpoint migration for each of the ten "intensive" sites are provided in Figures 15-24. Migration rates vary from about 0.4 m/y to about 11 m/y over periods ranging to 60 months (except Bear Creek = 30 months). These rates must be viewed in context: knickpoint migration does not occur constantly; rather, it occurs as bursts separated by periods of little change. Over the study period (1997 to 2002), several knickpoints cut into the Naheola formation migrated 30 m or more (Table 10). Their average rate of migration over the period was 6.6 m/y. Those cut into the Porters Creek Clay formation migrated at significantly slower rates, with an average rate of migration of 1.0 m/y. The difference in knickpoint movement for streambeds cut into the Naheola and Porters Creek Clay formation are shown with bar charts in Figure 25 using both 1997 and 1999 as initial points of time. Additionally, amounts of knickpoint migration over the study period (using 1997 and 1999 as the initial time) are shown for each of the critical knickpoint areas in Figures 26-35. In Table 10, the "knickpoint" on North Topashaw Creek has been set apart because the site was, in fact, the location of a logjam, which was removed by flows during the monitoring period.

It is important to keep in mind that flows over the period of monitoring 1999-2001 have been relatively low in comparison to historical values, indicating that knickpoint migration rates would have been greater in "normal" flow years. This can be seen by comparing the frequency of occurrence of mean-daily flows over the periods 1948-2001 and 1999-2001 for the Skuna River at Bruce gauge (Figure 7c). In fact, the period 1999-2000 was exceptionally dry, but 2000-2002 was somewhat wetter. The cumulative graphs of knickpoint migration using 1997 as the initial point (Figures 26-35) do indeed show somewhat of a deceleration of rates during the period 1999-2000, followed by another burst of migration during 2000-2002, indicating that more migration occurs during higher flow years.

Measurements of τ_c and erodibility rates for cohesive bed materials in the Yalobusha basin suggest a discrepancy between observed knickpoint retreat rates and available hydraulic shear stress. This suggests that other mechanisms are causing some of the knickpoint retreat. We have identified four main mechanisms for erosion and migration of cohesive knickpoints:

1. Where streambeds become partially exposed during low-flow periods, the result is weathering and the formation of cracks, enhanced by tension cracking of the headwall related to pressure release and stress-induced deformation. Field observations of Porters Creek Clay beds confirm that these streambeds erode in aggregates or chips where bedding planes, fractures, and tension cracking are extensive. Generally, particle-by-particle erosion forms a 'slot' up to several meters wide along a plane of weakness during

a high flow event in an area of the bed that was previously sub-aerially exposed. The slot expands longitudinally as well as laterally, concentrating low and moderate flows into the zone and leaving other areas of the bed to dry and desiccate. The main erosion pathway can then shift to this dried area of the bed during a subsequent flood event;

2. Detachment of aggregates of flocculated particles may be instigated by upward-directed seepage forces on the falling limb of hydrographs (Simon and Collison, 2001). Upward-directed seepage forces result from pressure imbalance at the bed surface, and are caused by the inability of a streambed to dissipate a build up of excess pore-water pressure;
3. Where there is very little jointing, upward-directed seepage forces may cause static liquefaction in cohesive streambeds. Strong upward-directed seepage forces may increase the distance between cohesive particles resulting in reduced cohesion and a "super-saturated" or almost fluidized state (Simon and Collison, 2001);
4. Observations of failed blocks at the toe of knickpoints indicate that more rapid erosion and migration may occur by a cyclical mass failure mechanism. The cycle can be represented by:

    i. Hydraulic stresses linked to the development of a marked hydraulic jump and turbulence in the plunge-pool undercut and heighten the knickpoint face through a combination of vortex and splash erosion (Piest *et al.*, 1975; De Ploey, 1989; Bennett *et al*., 2000);
    ii. The face fails via a mass-failure mechanism, such as cantilever or planar failure, with deposition of the failed material in the plunge pool; and
    iii. This debris is removed, and is followed by further scour in the plunge pool, thereby preparing the knickpoint for subsequent failure (Simon *et al*., 2000).

A similar cycle was noted by Robinson and Hanson (1996a). Opinion is divided as to whether knickpoint failure occurs during flow events, or because of weathering when much of the knickpoint is exposed between events. Research on bank instability and bed erosion suggests that internal pore-water pressure and the balance of surcharge and confining pressure due to head- and tail-water plays an important role in controlling mass failure processes in channels. In order to assess the scope for mass failure to cause knickpoint retreat, we have used a combination of hydrological and slope-stability modeling, the methodology and results of which are presented below.

A qualitative example, from a knickpoint cut into the Naheola formation on Big Creek, is provided that aids in demonstrating the cycle of knickpoint erosion and migration. The survey of February 1, 1999 shows a scoured area at the base of the knickpoint face (Figure 16a). Three flows between February 15 and March 6 resulted in failure of the knickpoint face and deposition of the failed material in the scoured area beneath the face (Figure 16a). By Equation (3), maximum average boundary shear stresses during these flows were about 15 Pa (average τ_c = 50.8 Pa), resulting in little downwearing at the knickpoint threshold. The flow of 20 Pa on June 27, 1999 again resulted in little downwearing but did remove the failed debris, further scoured the toe, and caused failure of the knickpoint face and consequent deposition of debris (Figure 16a). Flows during Spring 2000 again removed debris and caused failure of the face.

The relative dominance of the four identified mechanisms is partly a function of the hydraulic and geotechnical resistance of the cohesive materials as well as the form of the nappe and the relative tailwater depth (Bennett *et al*., 2000). At a knickpoint with a deeply scoured toe,

it is likely that during periods of low tailwater, relatively steep hydraulic gradients within the knickpoint aid in initiating undercutting and mass failure of the face. In cases where high tailwater elevations occur, knickpoint erosion by mass failure is probably less likely because of the confining pressure afforded to the knickpoint face. In this case, erosion is probably dominated by particle-by-particle erosion enhanced by upward-directed seepage forces, while moderate tailwater heights are associated with a combination of both. In all cases, the active process is probably also a function of flow stage.

Influence of Hydraulic Stresses on Knickpoint Migration

As mentioned earlier, an evaluation of the amount of erosion that is likely to occur by hydraulic stresses at a given site requires knowledge of the duration of flows that will attain and exceed given shear stress values. Utilizing stage records constructed from transducer data and Equation (3), charts of the shear stress duration series for the nine remaining intensive sites have been produced, and can be seen in Figures 36-44. Of all the sites, only those with beds composed of the Naheola formation experience shear stresses greater than the critical shear stress for any period of time. The one exception to this is Topashaw Tributary 1A, where τ_c was exceeded only once, during the 15-year storm event of 06/27/99. During this event, the excess shear stress approach (Eq. (5)) predicts a scour amount of 57 mm. Due to the small size of this prediction, this cannot be confirmed by surveys. The site at Bear Creek moved from a substrate composed of the Naheola formation to one composed of Porters Creek Clay over the study period. This change occurred around June 2000. The predicted erosion amount before this date is 489 mm, while after this date, only 2 mm of erosion is predicted. This is in spite of the fact that the second half of the year 2000 and the year 2001 experienced more large storm events than in 1999 and the first half of 2000. However, field evidence (see Figure 15a) suggests a much greater amount of erosion than this. At Big Creek, only two storm events over the period of record exceeded the critical shear stress and were capable of causing bed erosion. Surveys indicate that about 500 mm of vertical erosion did occur upstream of the knickpoint face over this period, despite the fact that our predicted erosion amount for the survey period (one storm event fewer) is only 2 mm.

It was noted above that the excess shear stress approach tended to underestimate the amount of erosion occurring upstream of knickpoints. There may be many reasons for this. Of particular importance may be the changing form of the water surface over the knickpoint at various stages. At all locations, the pattern appears to be one of draw down over the knickpoint with low to medium tailwater elevations during low flows, with a radical change as stage increases (e.g. Figure 45). At medium flows, the water surface elevation increases immediately downstream of the knickpoint brink, so that tailwater heights are higher than the stage height upstream of the knickpoint. This occurs at all locations where the downstream transducers are relatively near to the knickpoint and hence are affected by changing flow patterns and the formation of waves or a hydraulic jump. These waves have been documented by Martín Vide (1994), who noted the occurrence of a downstream surface jet associated with supercritical flow and an undular jump. He noted that this was relatively long lasting, and served to smooth the scour hole (Martín Vide, 1994). Bennett (1999) documented the formation of two wall jets due to plunging water, one upstream and one downstream of the plunging jet focus. Each wall jet formed a counter-rotating eddy, the downstream one becoming three-dimensional, distorted and diffuse with distance from the knickpoint. This has also been noted by other authors, including

Lee and Hwang (1994) and Robinson and Hanson (1996b). However, at the highest stages, knickpoints are drowned out, and the conditions causing the hydraulic jump subside (e.g. Figure 45). Clearly, stages in the middle range, those affected most by the effects of hydraulic jumps, turbulent waves and rollers, should be the most hydraulically and geomorphologically important. In fact, Robinson and Hanson (1996b) have shown experimentally that it is during these discharge ranges that the shear stresses on the bed and on the knickpoint face are highest. In addition, our calculation of boundary shear stress is merely an average and hence tends to underestimate the maximum shear stress. For a constructed headcut in plexiglass, Robinson (1989) found that minimum and maximum shear stresses were nearly zero and 15 times the average shear stress respectively (1989). Robinson also found that maximum stresses on the knickpoint face are at least an order of magnitude lower than the maximum stresses on the floor (1989).

Observations of the bed upstream of knickpoints (see Figures 15-24) indicate that a repeatable form is present. In this area, the bed is scoured to such an extent as to produce a second step or ledge of variable size. This secondary scour is initially the result of increased bed shear stresses in the region immediately upstream of the knickpoint brink. The analysis presented in Appendix II shows that increasing flow acceleration and decreasing pressure at the bed are equally responsible for the increase in shear stress. In this way, planes of weakness, or areas of lower resistance are exploited. Once a small cavity is formed, a recirculation pattern acts to deepen the cavity or generate a new knickpoint. This newly forming step has a similar upstream effect, which then propagates upstream until the hydraulic effects of the knickpoint diminish. Such a form can be seen especially clearly in the thalweg profiles of Bear Creek (Figure 15a; also Figure 46) and Mud Creek (Figure 20a), although it is present at almost all locations (excepting those with exceptionally resistant streambeds). These observations are important, since the migration of knickpoints in the laboratory has been shown to be episodic and complex, with some knickpoints migrating very quickly and others very slowly, while others merely die out or coalesce, making measurements of migration rates extremely difficult (Schumm *et al.*, 1987). The formation of a series of steps in the thalweg profile in the manner discussed above explains such phenomena in the field setting. The migration of knickpoints may not be linear (due to the role of mass-wasting processes- see later in this report), but will be relatively constant until the upstream edge of the wedge of material is reached. After this, a burst of migration will occur until the next ledge upstream is met, when a relatively constant rate of retreat (this rate will be dependent upon substrate properties) will restart. Such a scenario can be seen in the thalweg plots (Figures 15a-24).

Knickpoint Failures and Migration by Geotechnical Processes

The significantly slower rates of knickpoint migration in the Porters Creek Clay formation (Table 10) highlight several hypotheses regarding the factors that control erosion processes in knickpoints in this geologic unit:

1. That very low hydraulic-erosion rates result in minimal increases in the height of the knickpoint face and, consequently, a reduced tendency for failure of the face during storm events, and
2. That geotechnical failure in the Porters Creek Clay is less likely due to greater shear strengths.

Hypothesis 2 is not borne out by the shear strength data in Table 11 that shows that on average, both cohesive and frictional strengths are greater in the Naheola formation than in the Porters Creek Clay formation. These results indicate that the lower migration rates (including the amount by geotechnical failure) in the Porters Creek Clay are directly related to its enhanced resistance to erosion by hydraulic shear. A list of all BST results is provided in Table 12. Of course, this has important implications if, for instance, there is only a thin layer of resistant Porters Creek Clay overlying weaker materials that could scour more easily.

To further test interpretations made from field evidence and analyses of repeated surveys of knickpoint migration processes, numerical analysis of controlling variables such as pore-water pressures and cohesive strengths were undertaken using finite-element hydrologic (SEEP/W; GeoSlope International 1998a), and limit equilibrium method slope-stability software (SLOPE/W; GeoSlope International 1998b). Geotechnical investigations yielded data on the soil mechanical properties (unit weight, cohesion, friction angle, permeability) of the remaining nine intensive knickpoints. SEEP/W is a two-dimensional finite-element hydrology model that simulates the movement of water and the resulting pore-water pressures for both saturated and unsaturated conditions using Richards' equation (Richards, 1931) and Darcy's law. The inputs are a finite-element mesh of the slope (or in this case, knickpoint), pressure vs. permeability and pressure vs. moisture content characteristic curves, and hydrologic boundary conditions.

Method

Thalweg survey data were used to construct a series of finite-element meshes based on cross-sections of the knickpoints as they retreated and as scour altered the bed geometry. The permeability function was derived from k_{sat} testing, while the pressure-moisture function was estimated using the permeability value and the SEEP/W function library (GeoSlope International 1998a). Obtained k_{sat} values can be seen in Table 13. The lower and lateral perimeters of the meshes were fixed as zero-flux boundaries. Though some seepage probably occurs through these boundaries under field conditions, it was assumed that over the course of the simulations (1-2 days) the amounts would be negligible compared with movement across the upper boundary. The upper boundary (water/ bed boundary) was simulated as a series of time-dependent variable heads of water. The head boundary was derived from stage data that were logged every 30 minutes from above and below the knickpoints to give head and tailwater elevations.

An initial steady-state simulation was carried out to bring the bed pore-water conditions to those observed in the field before events (unsaturated bed profile). The model was then run dynamically for the duration of each observed flow event. The principal output from the SEEP/W modeling was a spatial and temporal distribution of pore-water pressures (positive and negative) in the streambed (a typical finite-element mesh and pore-water pressure output are shown in Figures 47a and b for the knickpoint at Big Creek). These pore-water pressures were passed over to a Limit Equilibrium Method stability model (SLOPE/W) for calculation of Factor of Safety (F_s). In these simulations SLOPE/W performs an Ordinary Method rotational limit equilibrium analysis. This was used rather than the slightly more accurate Bishop's Simplified Method as it is able to analyze shear surfaces with gradients that are very high relative to friction angle, which tends to be the case with knickpoint failures in cohesive beds. The Ordinary Method is generally less conservative than Bishop's Method, with predicted F_s approximately

5% higher on identical shear surfaces. Average geotechnical property values for the two formations were used in the modeling. Input values are shown in Table 11.

In addition to soil-mechanical properties and pore-water pressure, the analysis takes account of surcharge (weight of water above the knickpoint) and confining pressure (weight of tailwater acting on the toe of the knickpoint). For comparison, the F_s of the knickpoints have been calculated using the initial observed condition (unsaturated) and also assuming complete saturation but no head of water. For the case of Big Creek, a sensitivity analysis has also been performed to identify the critical stage required to cause knickpoint mass failure.

Results

Table 14 summarizes the findings of the modeling. Of all the sites, only three (Big Creek, Buck Creek and the Yalobusha River) exhibited mass failures. The analysis of the major knickpoint on Big Creek (Figure 1) is provided to illustrate the mass failure cycle. Throughout the study period, the knickpoint has been stable under non-flood conditions. The inherent F_s is approximately 2.1-2.4 when observed ambient suction values are applied. If we assume that the knickpoint is saturated and that water pressure is hydrostatically distributed, F_s drops to 1.4-1.8. This indicates that knickpoint failure requires some type of flow event, and suggests that knickpoint failure is unlikely to occur as a result of sub-aerial weathering processes between flows, as has been suggested by some investigators.

To simulate flow events, every observed event with a flow depth greater than 0.3 m has been extracted from the stage record from January 1999 to June 2000. The sensitivity analysis (Figure 48) shows that stages lower than 0.5 m are unlikely to cause mass failure. Events have been simulated using the finite element mesh derived from the survey preceding the event. Where a mass failure is indicated (F_s close to, or below one) the predicted failed distance has been recorded for comparison with the observed knickpoint retreat distance at the next survey. In some cases there is more than one possible event between two successive knickpoint surveys. In this case the cumulative failed distance for each event is compared with the observed distance. The results (Table 15, Figure 49) show a close agreement between modeled and observed retreat rates.

A typical example is described in more detail below (Figure 50). As stage rises, pore-water pressure in the bed responds. Combined with increasing surcharge, this reduces the factor of safety to almost one. However, as tailwater height rises, it drowns out the knickpoint. The resulting confining pressure supports the knickpoint, raising F_s during the peak flow. As both headwater and tailwater levels decline, the knickpoint re-emerges from flow and confining pressure falls faster than surcharge and pore-water pressure, resulting in a second period of low F_s. The modeling and field data suggest that two failures occurred during this event, one before and one after the peak stage.

Knickpoint Migration Processes: Summary

This research has allowed a tentative formulization of the processes active at knickpoints with different forms. Generally, it has been found that knickpoints with homogeneous substrata tend to migrate with a ramp form via hydraulic shear stress and upward-directed seepage force-induced entrainment, irrespective of their erodibility. Such knickpoints generally exhibit extremely slow rates of migration (e.g. Cane Creek, formed in Porters Creek Clay, has a τ_c of

almost 400 pa and barely moved while the Yalobusha River, formed in the Naheola formation, has a τ_c of 18 Pa and equally barely moved over the study period). Geotechnical modeling suggests that very shallow (< 0.1 m) shear failures may also play a role in migration. Indeed, Mehta (1991) suggested this as a potential mechanism at the micro scale.

Porters Creek Clay knickpoints that are exposed during drier periods tend to crack, weather and erode via blocks when flows get large enough. Numerical modeling (Simon and Collison, 2001), suggests that upward-directed seepage forces may play a significant role in promoting entrainment, while it is hypothesized that hydraulic forces operating within cracks may also be important. Porters Creek Clay knickpoints that are perennially submerged tend to migrate via chipping of the face, promoted by upward-directed seepage forces and tension cracking.

One knickpoint (Big Creek) migrates via a mass-wasting cycle documented here and elsewhere (Simon *et al*., 2000). This knickpoint was formed in the relatively erodible Naheola formation. However, this knickpoint exhibited a distinguishing feature that made it different to all the others: it had a cap, of around 0.3 m in depth, which had a critical shear stress of almost an order of magnitude larger than the underlying strata. This allowed it to retreat via parallel retreat, since the underlying layer was eroded more readily, undercutting the cap and eventually causing cantilever failure.

In the intensively studied knickpoints, there was a characteristic deepening upstream of the knickpoint caused by accelerated scour (Appendix II). Increasing flow acceleration and decreasing pressure at the bed are equally responsible for an increase in shear stress. In this way, planes of weakness, or areas of lower resistance are exploited. Once a small cavity is formed, a recirculation pattern acts to deepen the cavity or generate a new knickpoint. In some cases (e.g. Big, Johnson and Mud Creeks), the upward-migrating mechanism met this deepening to wash through the knickpoint and move upstream to the next resistant wedge of material or this newly formed knickpoint. Such phenomena help to explain laboratory observations of knickpoint migration.

CONCLUSIONS

Erosion of streambed materials in the Yalobusha River system is controlled by the nature of the two dominant formations: Naheola and Porters Creek Clay. These are expressed in terms of two parameters: critical shear stress and an erodibility coefficient. Maps of the distribution of these parameters throughout the Yalobusha River system are provided in the body of the report. In general, the Porters Creek Clay formation is extremely resistant to erosion by hydraulic stresses, requiring shear stresses in the hundreds of Pa to initiate downcutting. Given the range of representative flow depths and bed slopes, shear stresses of this magnitude probably do not occur on a frequent basis. This resistance to hydraulic erosion apparently also plays an important role in limiting knickpoint migration in two key ways. Firstly, the potential for geotechnical failure is reduced because of a lack of downcutting needed to produce a knickpoint face of sufficient height to create instability; and secondly, secondary scour, caused by pressure field distortion and flow acceleration close to the brink, is reduced or prevented. Erosion of streambeds cut into the Naheola formation can, however, occur over a range of commonly occurring shear stresses. These differences lead to stark contrasts in knickpoint migration rates between the two formations, notwithstanding that the shear strength of Naheola beds are greater

than those composed of the Porters Creek Clay. That migration of some knickpoints or erosion zones, particularly those cut into the Porters Creek Clay formation has been severely limited is directly related to the hydraulic resistance of these clay beds. More than 30 years after the completion of the most recent channel dredging on the Yalobusha River main stem (1967), the major erosion zone is still just upstream of the upstream terminus of the channel work (river kilometer 27.8). With maximum τ_c-values reaching more than 400 Pa, erosion of knickpoints cut into the Porters Creek Clay formation is marginal.

REFERENCES

ASTM, 1995, Annual Book of ASTM Standards: Section 4, Construction, v. 04-09, *American Society for Testing and Materials*, West Conshohocken, PA: ASTM.

Arulanandan, K., Gillogley, E., and Tully, R., 1980, Development of a quantitative method to predict critical shear stress and rate of erosion of natural undisturbed cohesive soils, Technical Report GL-80-5, Vicksburg: U.S. Army Engineers Waterways Experiment Station.

Begin, Z. B., Meyer, D. F., and Schumm, S. A., 1980, Knickpoint migration due to base level lowering, *Journal of the Waterway, Port, Coastal and Ocean Division, Proceedings of the American Society of Civil Engineers* 106 (3), 369-388.

Bennett, S. J., 1999, Effect of slope on the growth and migration of headcuts in rills, *Geomorphology* 30 (3), 273-290.

Bennett, S. J., Robinson, K. M., Simon, A., Hanson, G. J., 2000, Stability of knickpoints formed in cohesive sediments, *In:* R. H. Hotchkiss, and M. Glade (eds.), *ASCE Joint Conference on Water Resources Engineering and Water Resources Planning & Management, Minneapolis, July 30 - August 2, 2000 [On CD]*, Reston: American Society of Civil Engineers.

Blaisdell, F. W., Clayton, L. A., and Hebaus, G. G., 1981, Ultimate dimension of local scour, *Journal of the Hydraulics Division, Proceedings of the American Society of Civil Engineers* 107 (HY3), 327-337.

Brush Jr., L. M., and Wolman, M. G., 1960, Knickpoint behavior in noncohesive material: a laboratory study, *Geological Society of America Bulletin* 71, 59-74.

Casagli, N., Curini, A., Gargini, A., Rinaldi, M., Simon, A., 1997, Effects of pore pressure on the stability of streambanks: Preliminary results from the Sieve River, Italy, *In:* S. S. Y. Wang, E. J. Langendoen, and F. D. Shields Jr. (eds.), *Management of Landscapes Disturbed by Channel Incision*, University: University of Mississippi, 243-248.

Chow, V. T., 1959, *Open-Channel Hydraulics*, New York: McGraw-Hill.

De Ploey, J., 1989, A model for headcut retreat in rills and gullies. *In:* A. Yair, and S. Berkowicz, (eds.), *Arid and Semi-Arid Environments, Catena Supplement 14*, Catena Verlag: Cremlingen-Destedt; 81-86.

Downs, P. W., and Simon, A., 2001, Fluvial geomorphological analysis of the recruitment of large woody debris in the Yalobusha River network, Central Mississippi, USA, Geomorphology 37 (1-2), 65-91.

GeoSlope International Ltd. 1998a, *SEEP/W Users Guide Version 4,* Calgary: GeoSlope International.

GeoSlope International Ltd. 1998b, *SIGMA/W Users Guide Version 4,* Calgary: GeoSlope International.

Grissinger, E. H., 1982, Bank erosion of cohesive materials, *In:* R. D. Hey, J. C. Bathurst, and C. R. Thorne (eds.), *Gravel-bed Rivers*, Chichester: John Wiley and Sons, 273-287.

Hanson, G. J., 1990, Surface erodibility of earthen channels at high stress, Part II - Developing an in situ testing device, *Transactions of the American Society of Agricultural Engineers* 33 (1), 132-137.

Hanson, G. J., and Cook, K. R., 1997, Development of excess shear stress parameters for circular jet testing, ASAE Paper No. 97-2227, St. Joseph: American Society of Agricultural Engineers.

Hanson, G. J., and Simon A., 2001, Erodibility of cohesive streambeds in the loess area of the midwestern USA, *Hydrological Processes* 15 (1), 23-38.
Lee, H-Y, and Hwang, S-T, 1994, Migration of a backward-facing step, *Journal of Hydraulic Engineering* 120 (6), 693-705.
Lutenegger, J. A., and Hallberg, B. R., 1981, Borehole shear test in geotechnical investigations. *ASTM Special Technical Publication 740*, 566-578.
Martín Vide, J. P., 1994, Mechanics of jet scour downstream of a headcut by O. R. Stein, P. Y. Julien, and C. V. Alonso: Discussion, *Journal of Hydraulic Research* 32 (6), 951-957.
Mehta, A. J., 1991, Review notes on cohesive sediment erosion, *In:* N.C. Kraus, K. J. Gingerich, and D. L. Kriebel (eds.), *Coastal sediment '91, Proceedings of Specialty Conference on Quantitative Approaches to Coastal Sediment Processes*, New York: American Society of Civil Engineers, 40-53.
Parchure, T. M., and Mehta, A. J., 1985, Erosion of soft cohesive sediment deposits, *Journal of Hydraulic Engineering* 111 (10), 1308-1326.
Parks, W. S., 1961, *Calhoun County geology and ground-water resources, Mississippi Geological Survey Bulletin 92,* University: Mississippi Geological Survey.
Partheniades, E., 1965, Erosion and deposition of cohesive soils, *Journal of the Hydraulics Division, Proceedings of the American Society of Civil Engineers* 91 (1), 105-139.
Piest, R. F., Bradford, J. M., and Wyatt, G. M., 1975, Soil erosion and sediment transport from gullies, *Journal of the Hydraulics Division, Proceedings of the American Society of Civil Engineers* 101 (1), 65-80.
Rajaratnam, N., and Muralidhar, D., 1968, Characteristics of the rectangular free overfall, Journal of Hydraulic Research, 6 (3), 233-258.
Richards, L. A., 1931, Capillary conductance of liquids in porous mediums, *Physics* 1, 318-333.
Rinaldi, M., and Casagli, N., 1999, Stability of streambanks in partially saturated soils and effects of negative pore water pressures: the Sieve River (Italy), *Geomorphology* 26 (4), 253-277.
Robinson, K. M., 1989, Stress distribution at an overfall, *Transactions of the American Society of Agricultural Engineers* 32 (1), 75-80.
Robinson, K. M., and Hanson, G. J., 1996a, Gully headcut advance, *Transactions of the American Society of Agricultural Engineers* 39 (1), 33-38.
Robinson, K. M., and Hanson, G. J., 1996b, Influence of backwater on headcut advance, *In:* C. T. Bathala (ed.), *ASCE North American Water and Environment Congress, Anaheim, CA, June 22, 1996 [On CD],* Reston: American Society of Civil Engineers.
Rouse, H., 1936, Discharge characteristics of the free overfall, *Civil Engineering,* ASCE, 6 (4), 257-260.
Rouse, H., 1937, Pressure distribution and acceleration at the free overfall, *Civil Engineering,* ASCE, 7 (7), 518.
Schumm, S. A., Harvey, M. D., and Watson, C. C., 1984, *Incised Channels, Morphology, Dynamics, and Control*, Littleton: Water Resources Publications.
Schumm, S. A., Mosley, M. P., and Weaver, W. E., 1987, *Experimental Fluvial Geomorphology*, New York: John Wiley & Sons.
Simon A., 1998, *Processes and forms of the Yalobusha River system: a detailed geomorphic evaluation, National Sedimentation Laboratory Research Report No. 9*, Oxford: U. S. Department of Agriculture, Agricultural Research Service.

Simon A., and Collison, A. J. C., 2001, Pore-water pressure effects on the detachment of cohesive streambeds: seepage forces and matric suction, *Earth Surface Processes and Landforms* 26 (13), 1421-1442.

Simon, A., and Curini, A., 1998, Pore pressure and bank stability: The influence of matric suction, *In:* S. R. Abt, J. Young-Pezeshk, and C. C. Watson (eds.), *Water Resources Engineering '98, Proceedings of the International Water Resources Engineering Conference, Memphis, August 3-7, 1998,* Reston: American Society of Civil Engineers, 358-363.

Simon, A., Curini, A., Darby, S. E., and Langendoen, E. J., 1999, Streambank mechanics and the role of bank and near-bank processes in incised channels, *In:* S. E. Darby and A. Simon (eds.), *Incised River Channels: Processes, Forms, Engineering and Management***,** Chichester: John Wiley and Sons, 123-152.

Simon, A., Bennett, S. J., and Griffith, M. K., 2000, Knickpoint Erosion and Migration in Cohesive Streambeds, *In:* R. H. Hotchkiss and M. Glade (eds.), *ASCE Joint Conference on Water Resources Engineering and Water Resources Planning & Management, Minneapolis, July 30 - August 2, 2000 [On CD]*, Reston: American Society of Civil Engineers.

Simon, A., and Rinaldi, M., 2000, Channel instability in the loess area of the Midwestern United States, *Journal of the American Water Resources Association*, 36 (1), 133-150.

Stein O. R., Julien, P. Y., and Alonso, C. V., 1993, Mechanics of jet scour downstream of a headcut, *Journal of Hydraulic Research* 31 (6), 723-738.

Stein, O. R., and Nett, D. D., 1997, Impinging jet calibration of excess shear sediment detachment parameters, *Transactions of the American Society of Agricultural Engineers* 40 (6), 1573-1580.

Watts, S., and Halliwell, L., 1996, Essential Environmental Science: Methods and Techniques. London: Routledge.

FIGURES

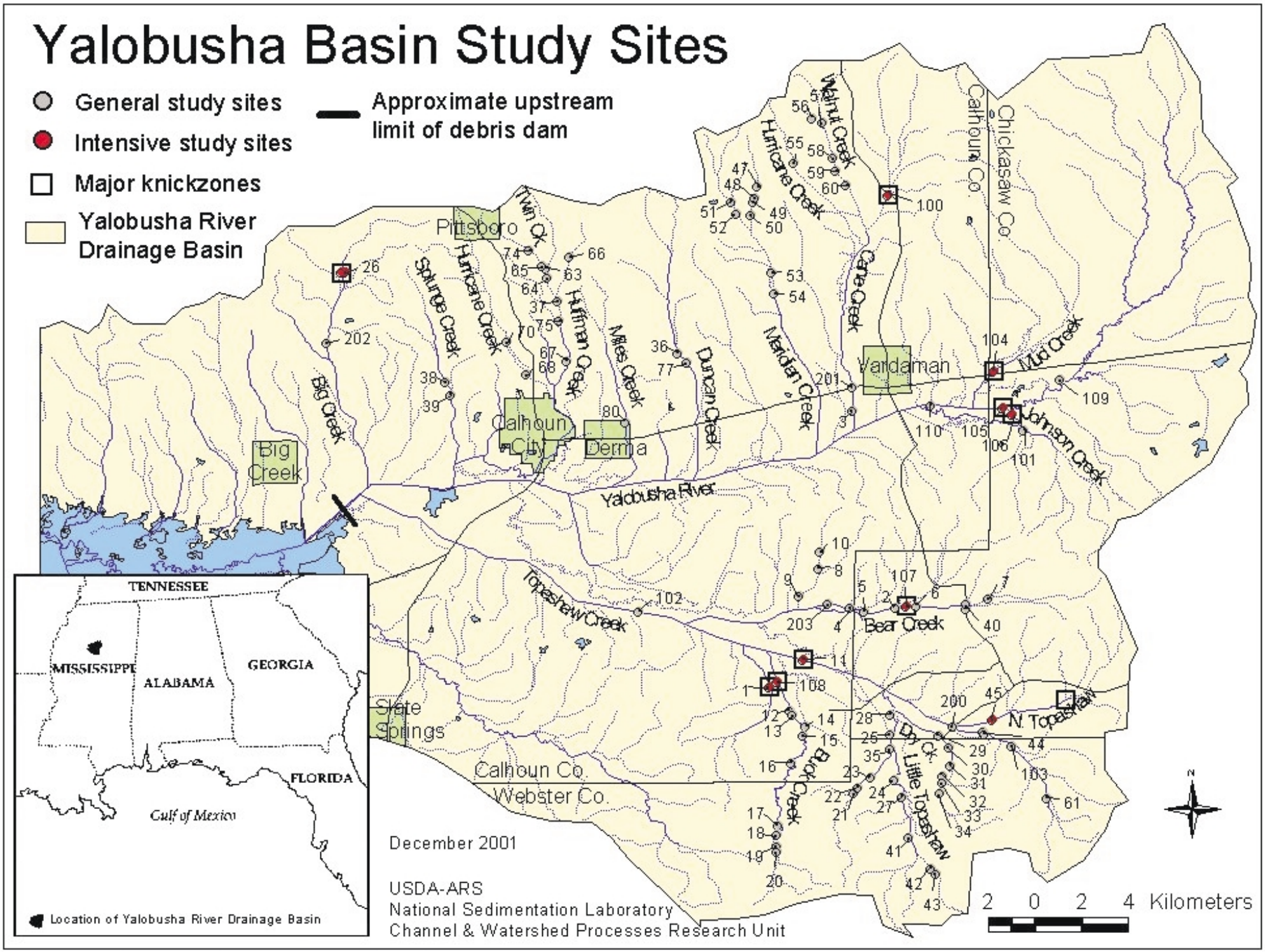

Figure 1 -- Yalobusha River Drainage Basin Study Sites

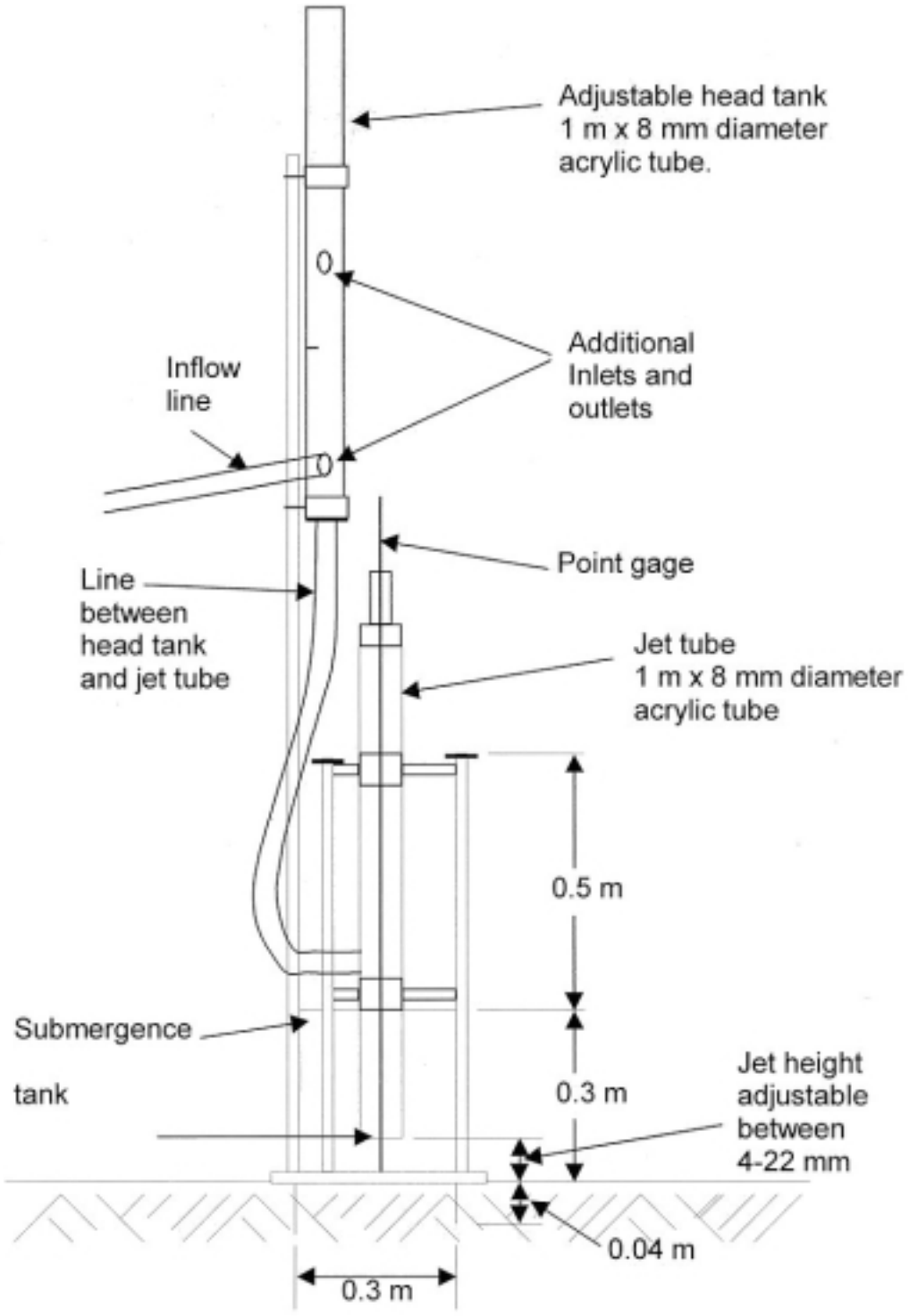

Figure 2 - Schematic of jet-test device.

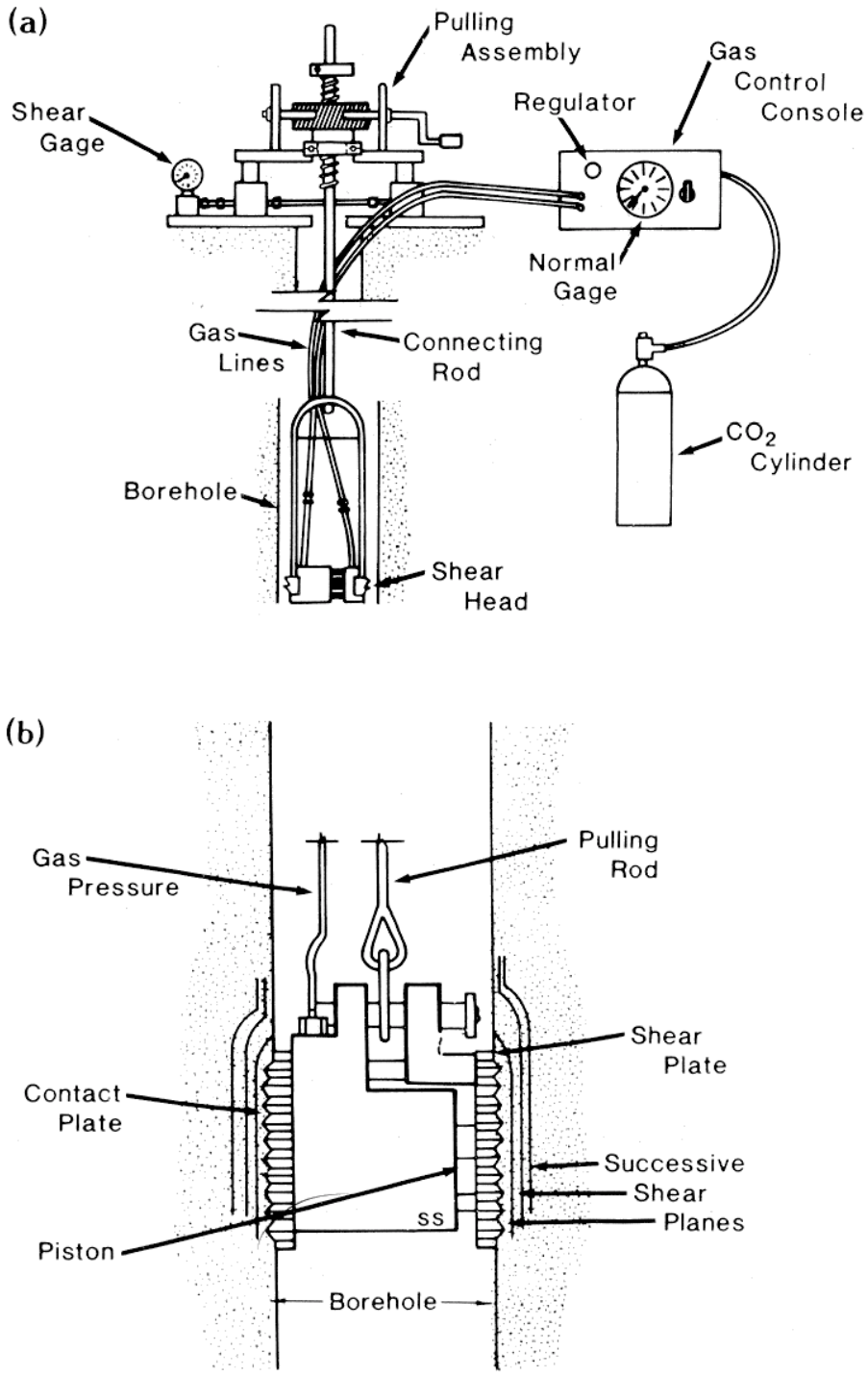

Figure 3 A - Schematic of borehole shear test (BST) assembly and
B - Detail of shear head in borehole.

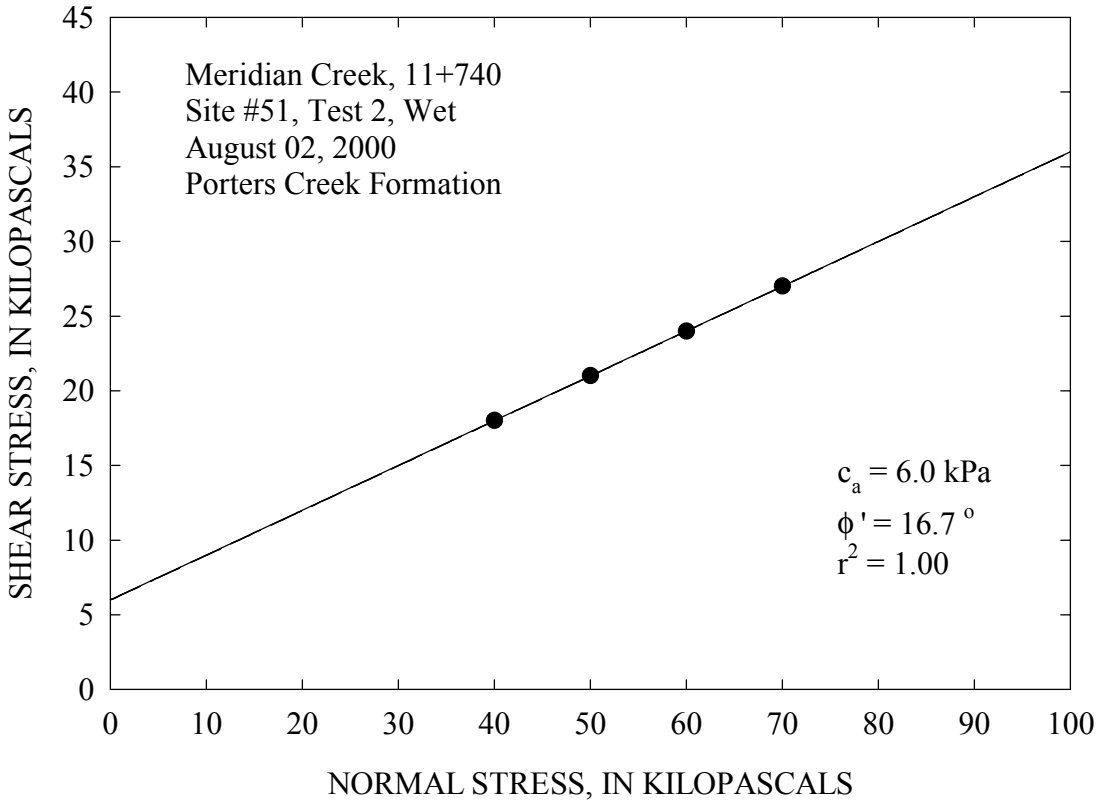

Figure 4 - Calculation of apparent cohesion (c_a) and effective friction angle (ϕ') from BST data.

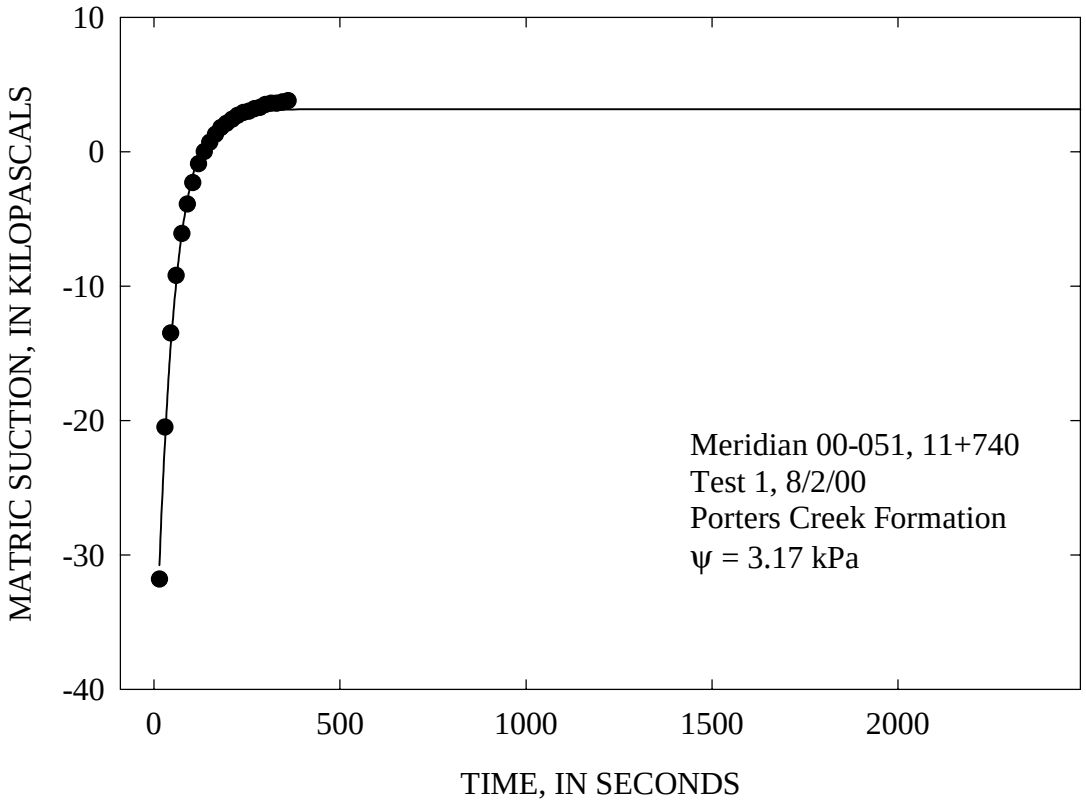

Figure 5 - Calculation of equilibrium matric suction (ψ) from field data.

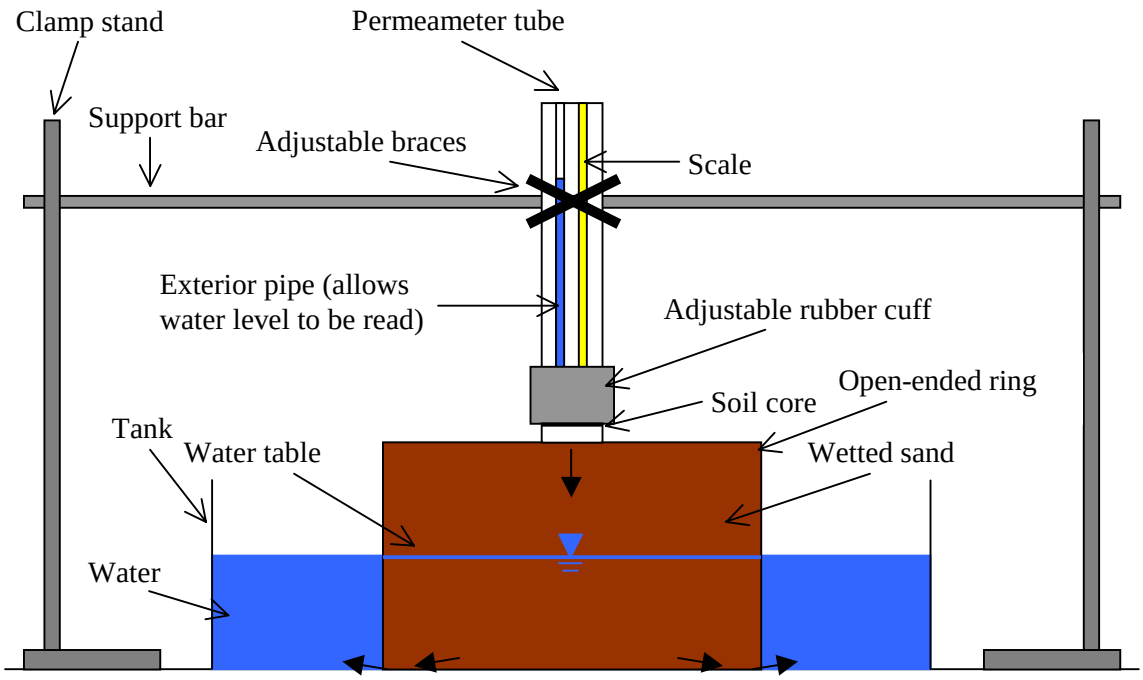

Figure 6 - Experimental setup for falling-head permeameter.

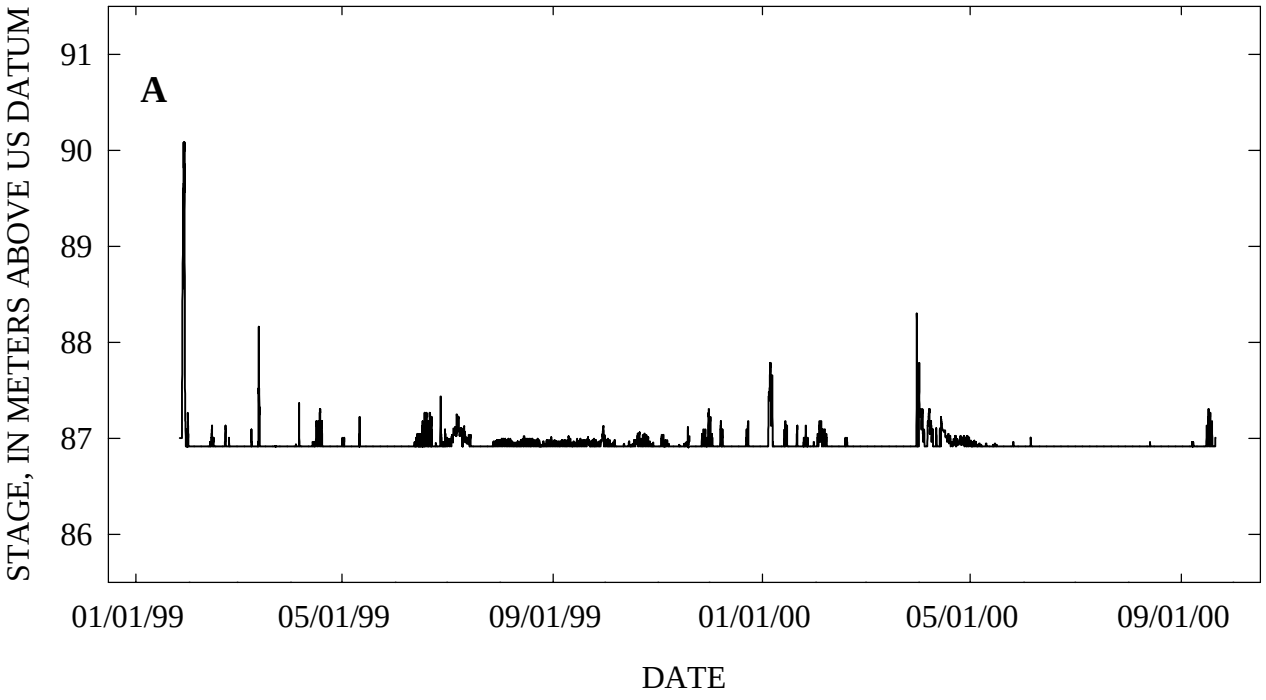
A
STAGE, IN METERS ABOVE US DATUM
91
90
89
88
87
86
01/01/99
05/01/99
09/01/99
01/01/00
05/01/00
09/01/00
DATE

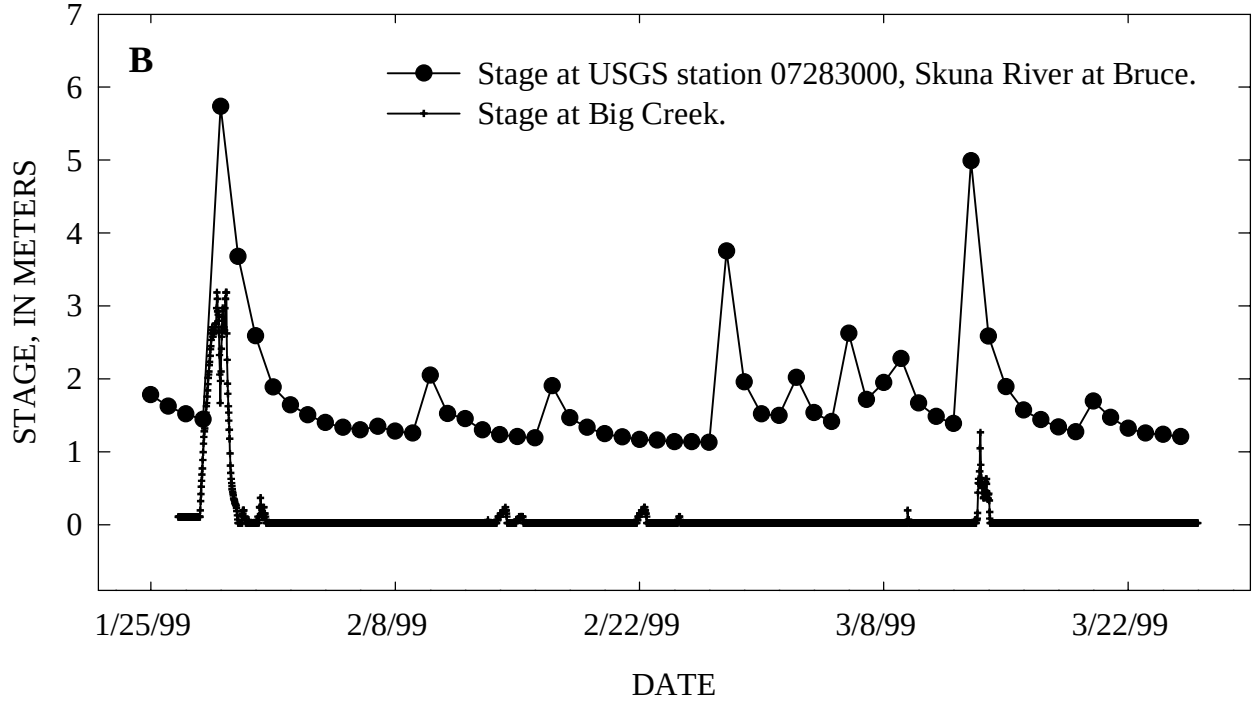
B
Stage at USGS station 07283000, Skuna River at Bruce.
Stage at Big Creek.
STAGE, IN METERS
7
6
5
4
3
2
1
0
1/25/99
2/8/99
2/22/99
3/8/99
3/22/99
DATE

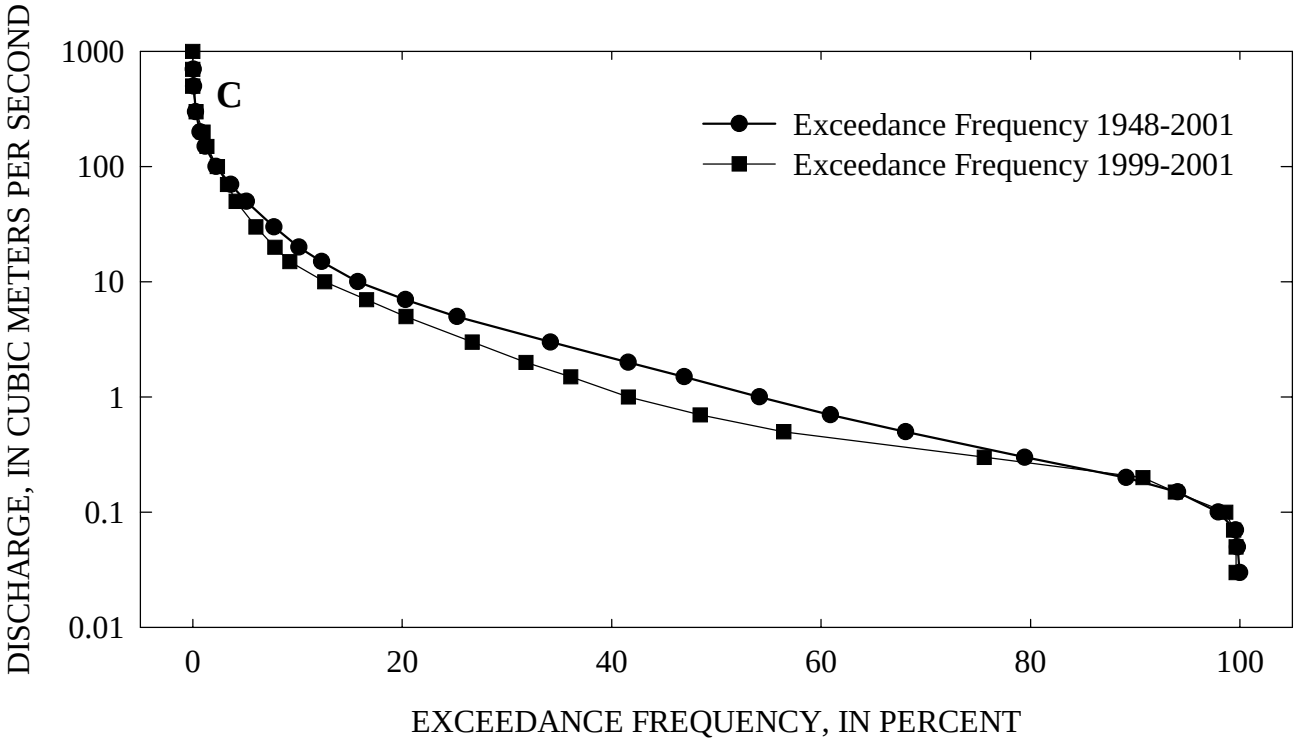

Figure 7 A - Example stage record from Big Creek,
B - Comparison of stage records between Skuna River and Big Creek and
C - Exceedance frequencies of mean daily discharges on the Skuna River, 1948-2001 and 1999-2001.

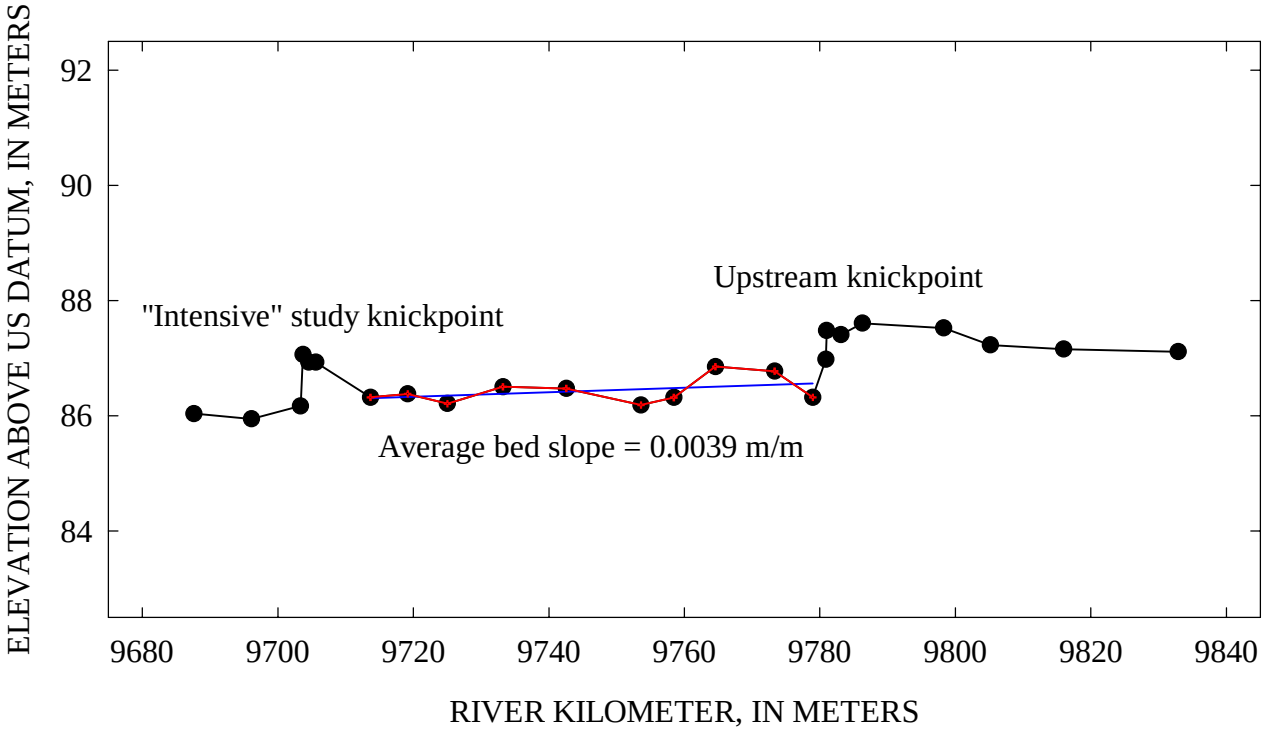

Figure 8 - Bed slope regression calculation for Big Creek knickzone.

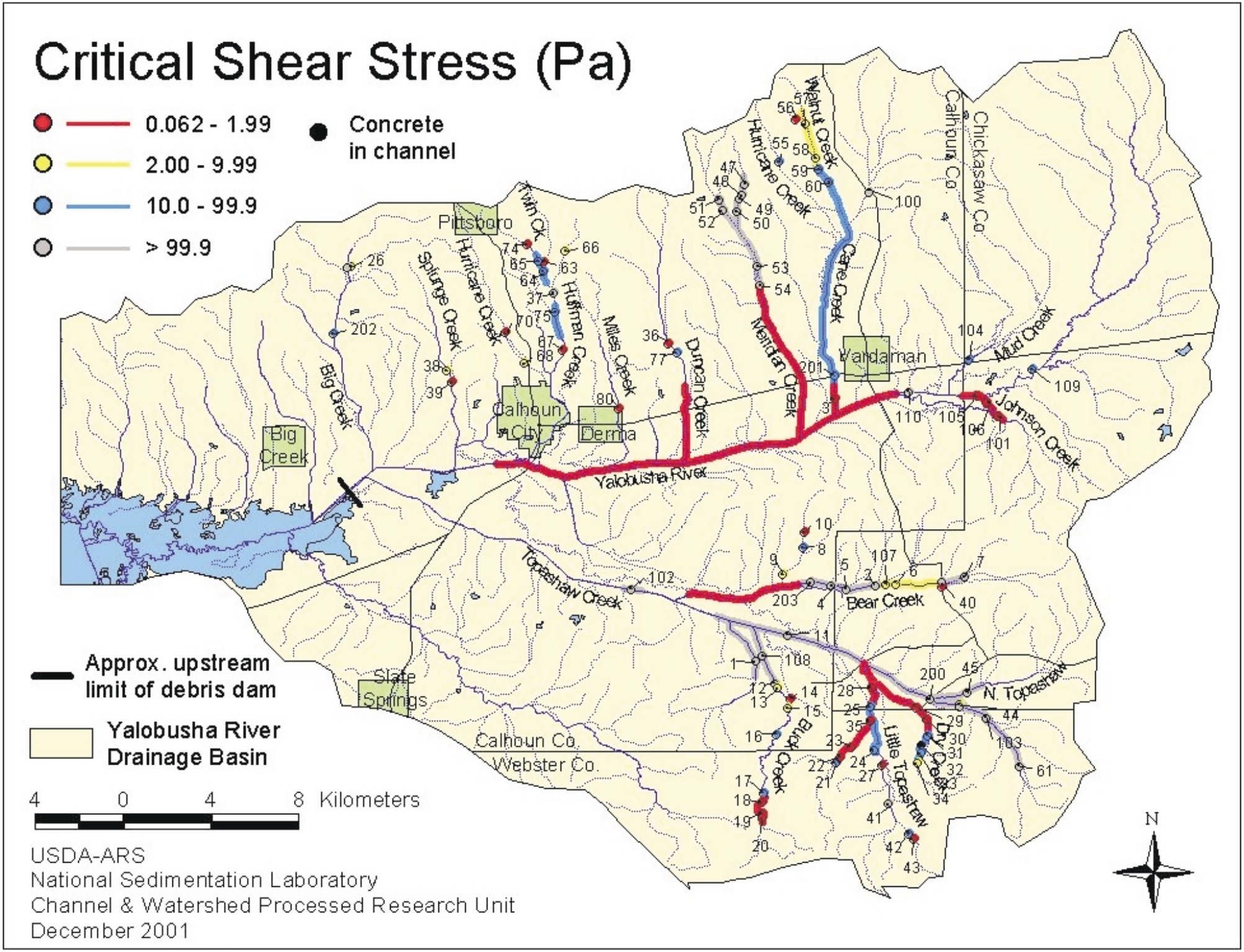

Figure 9 -- Critical Shear Stress

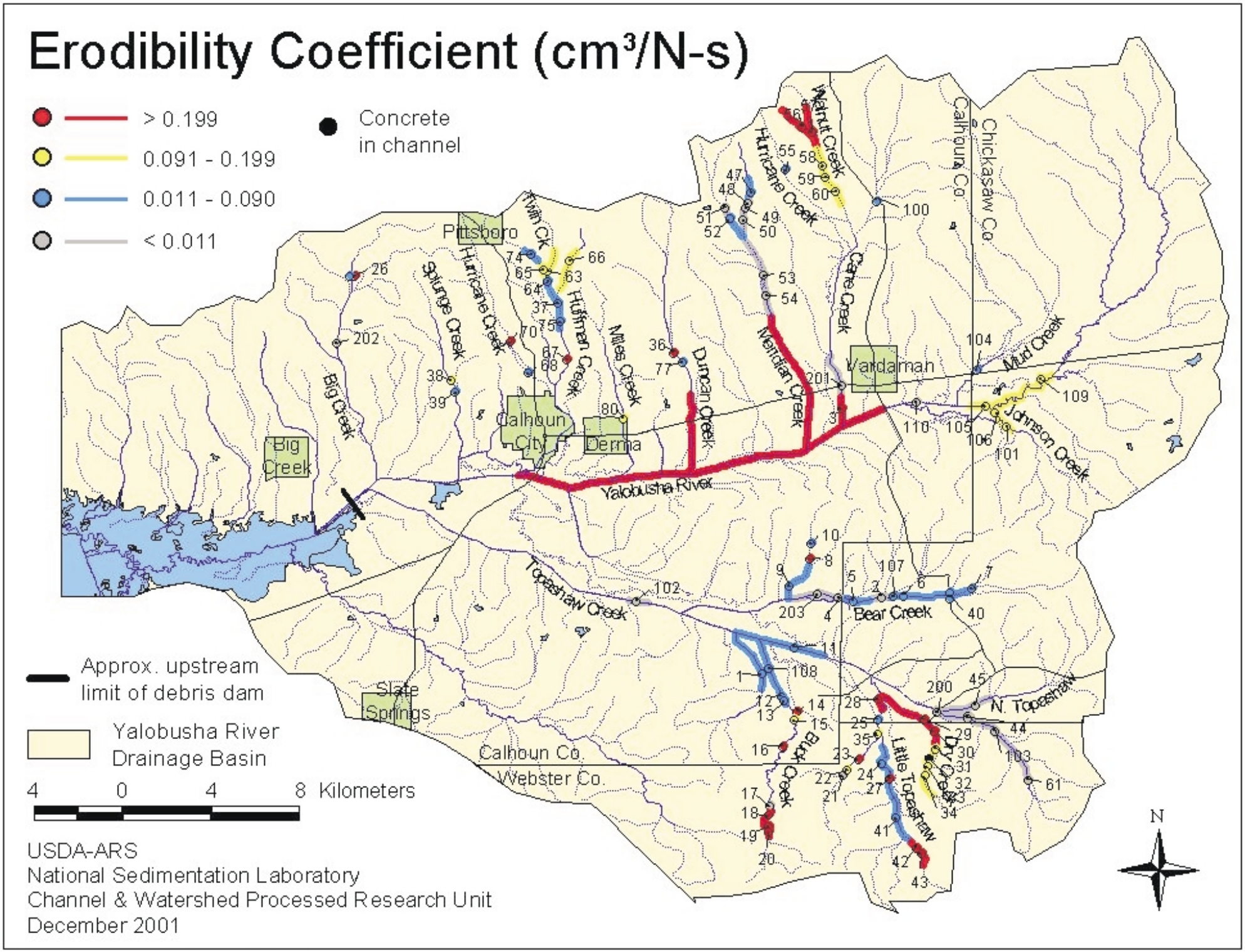

Figure 10 -- Erodibility Coefficient

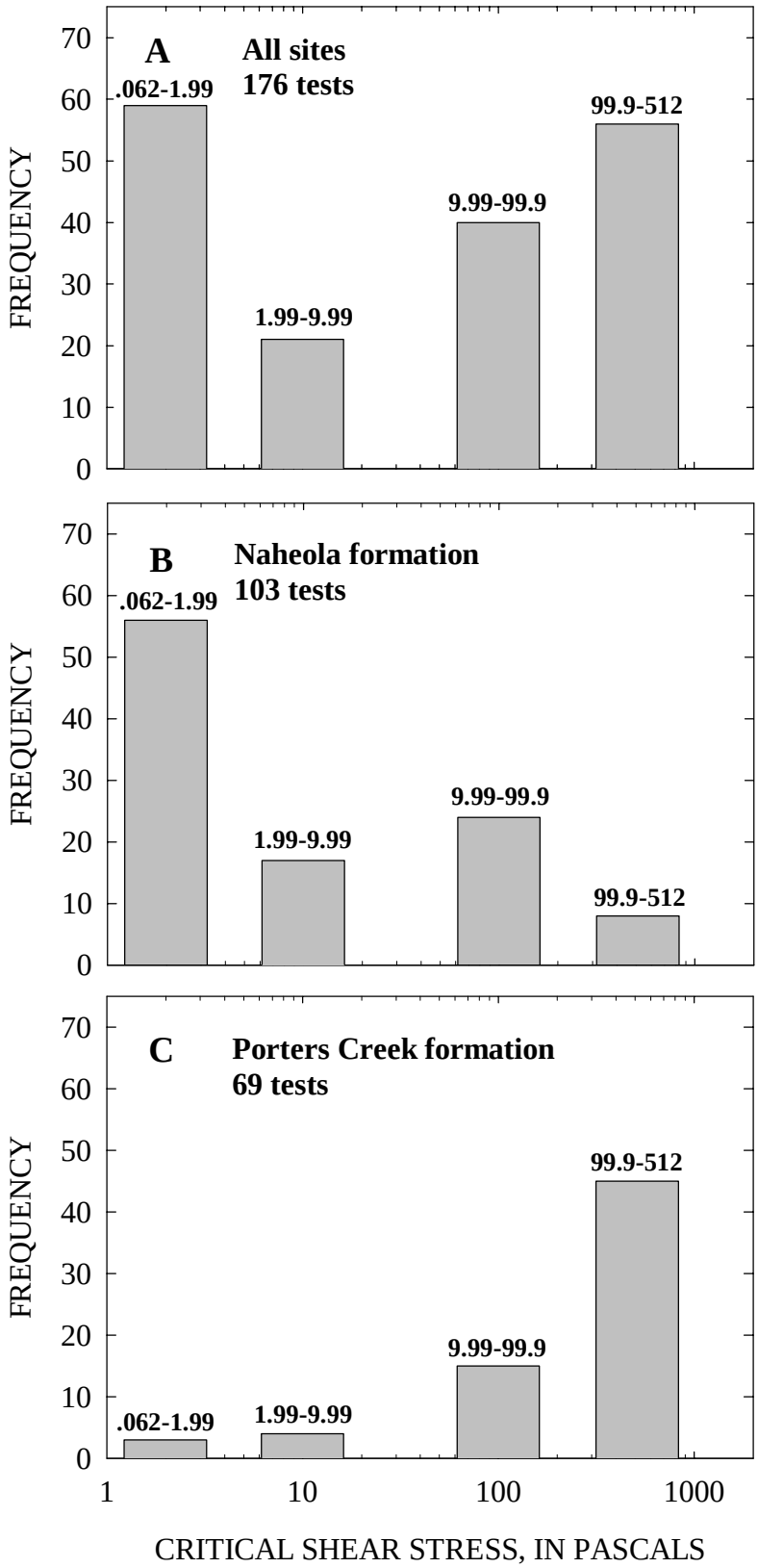

Figure 11 A - Histogram of critical shear stress (τ_c) from all jet-tests conducted in the Yalobusha River Basin,
B - Histogram of critical shear stress (τ_c) from jet-tests conducted on the Naheola formation and
C - Histogram of critical shear stress (τ_c) from jet-tests conducted on the Porters Creek Clay formation.

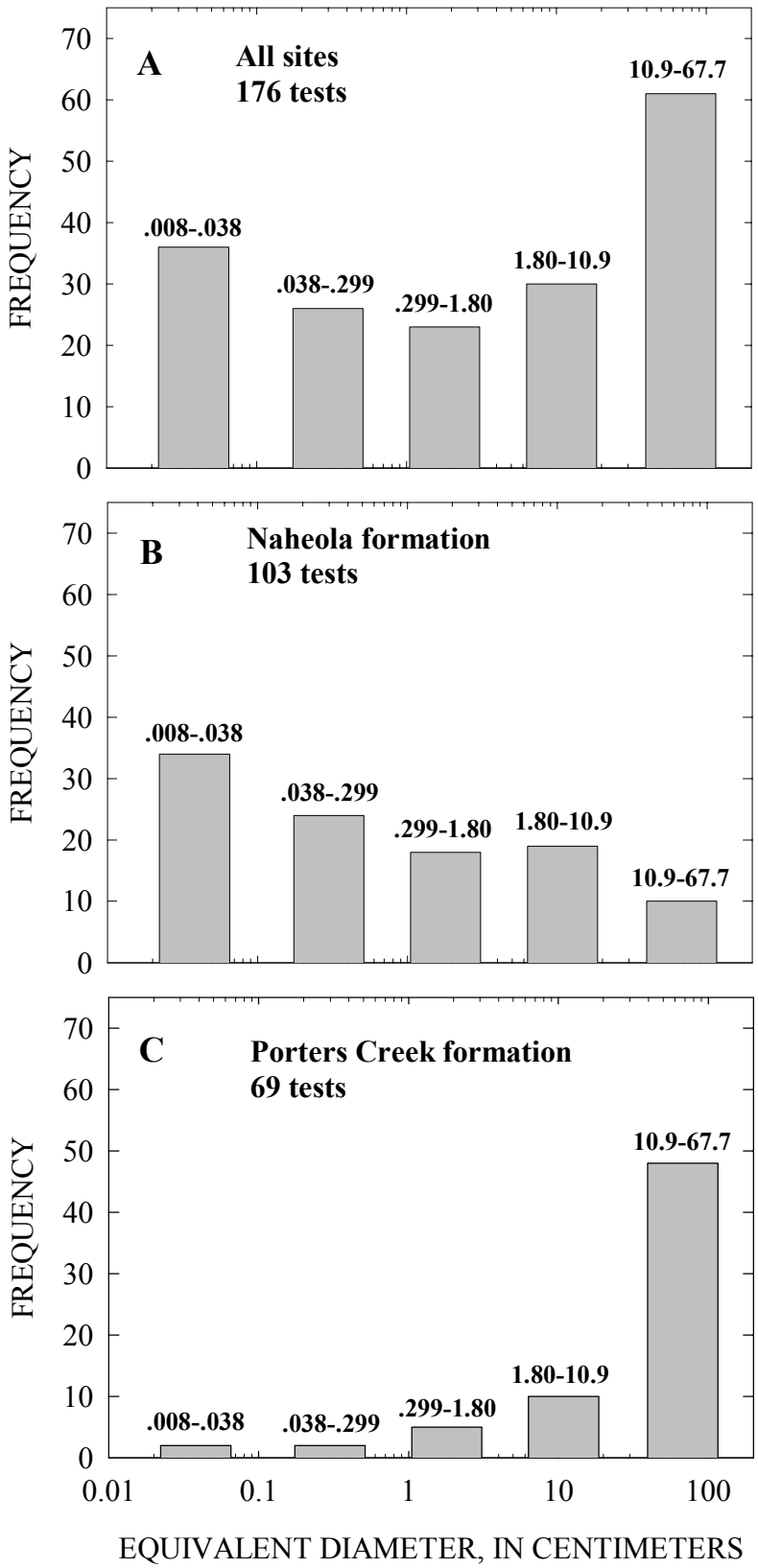

Figure 12 A - Histogram of equivalent particle diameters in the Yalobusha River Basin,
B - Histogram of equivalent particle diameters from the Naheola formation and
C - Histogram of equivalent particle diameters from the Porters Creek Clay formation.

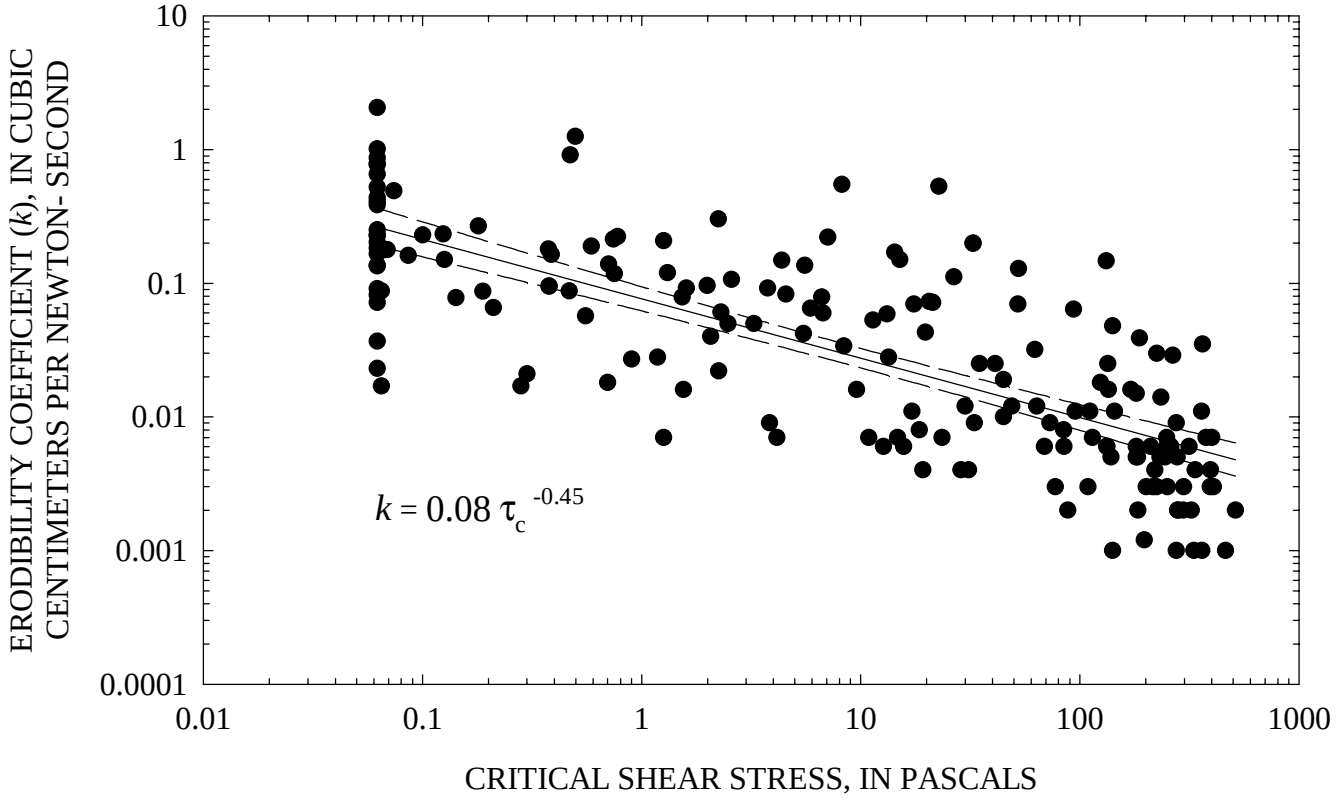

Figure 13 - Critical shear stress (τ_c) against erodibility coefficient (k).

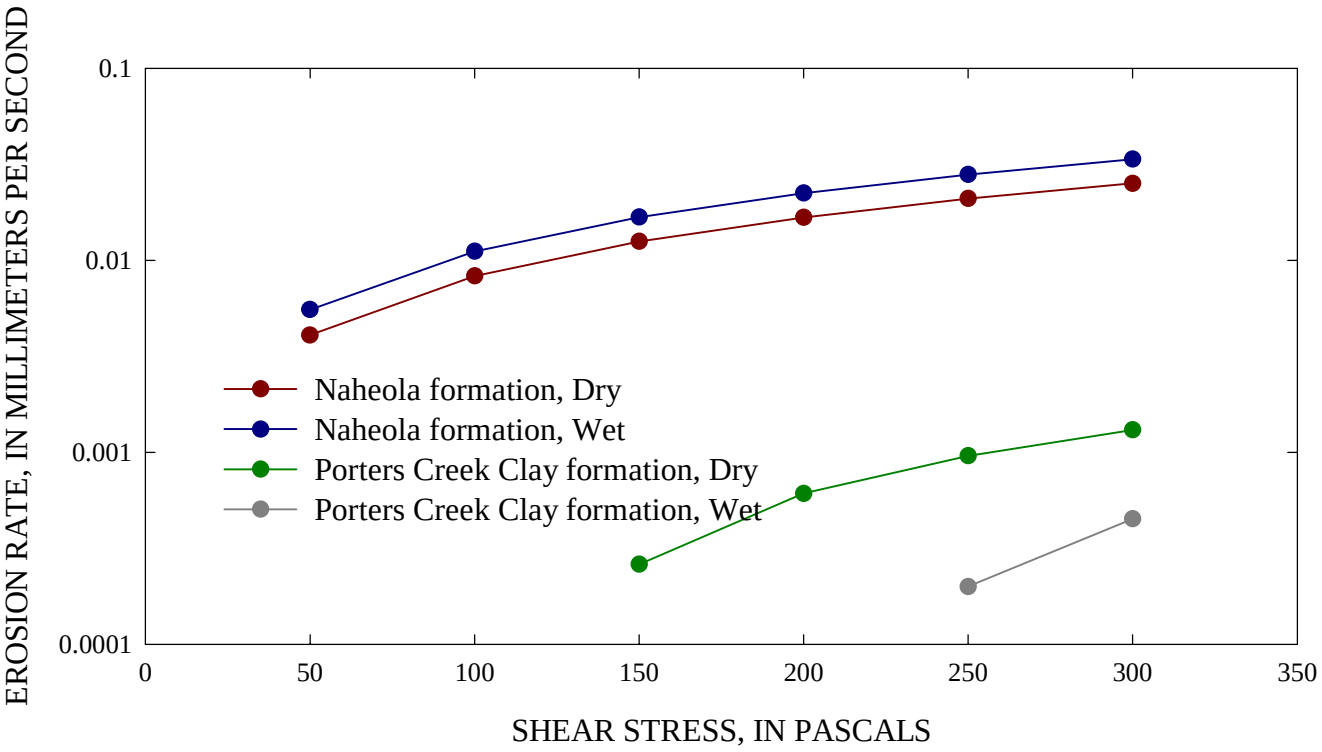

Figure 14 - Median erosion rate (ε) against critical shear stress (τ_c) by form and type of jet test.

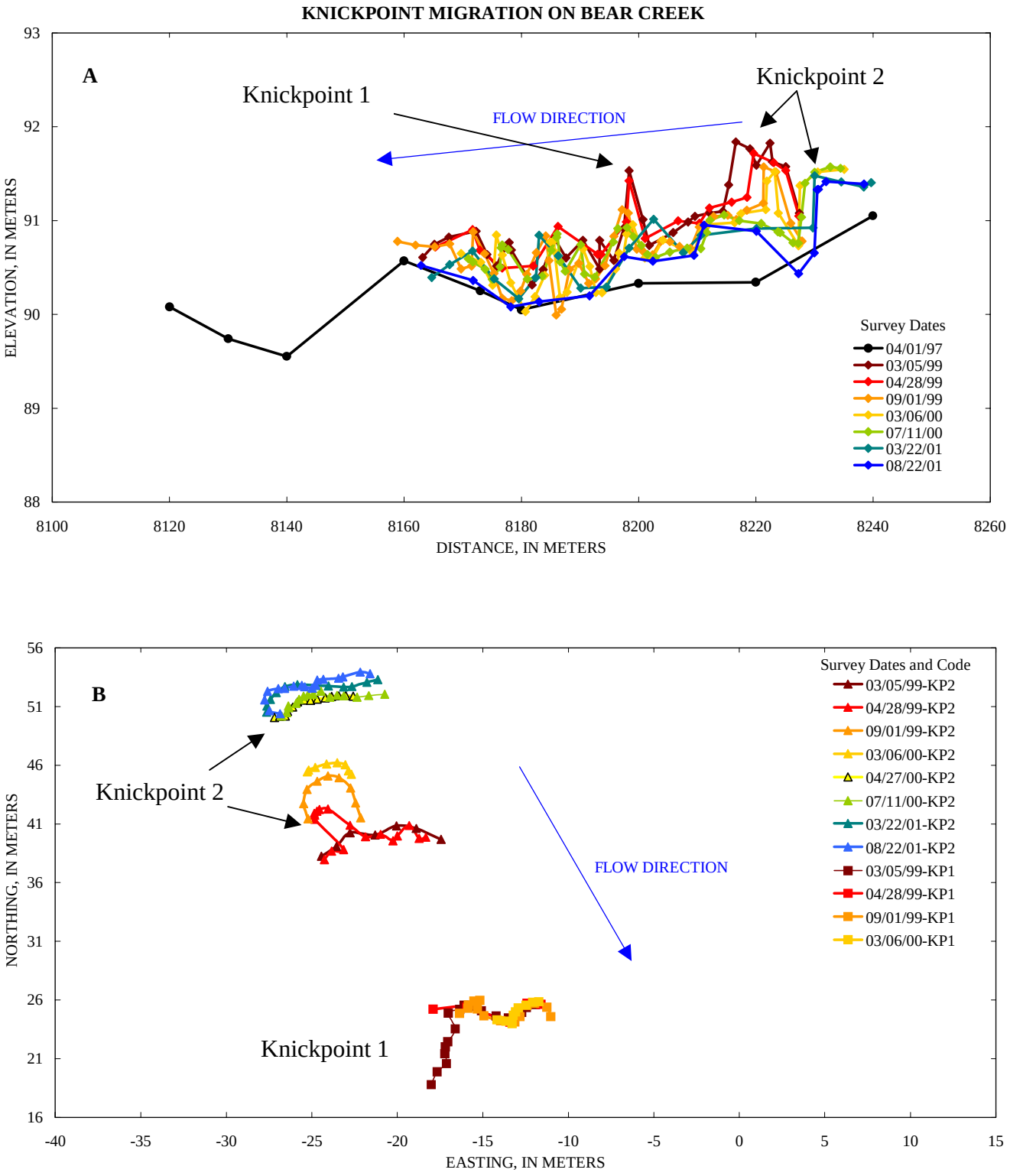

Figure 15 A - Bear Creek knickpoint thalweg profile and
B - Bear Creek knickpoint planimetric view.

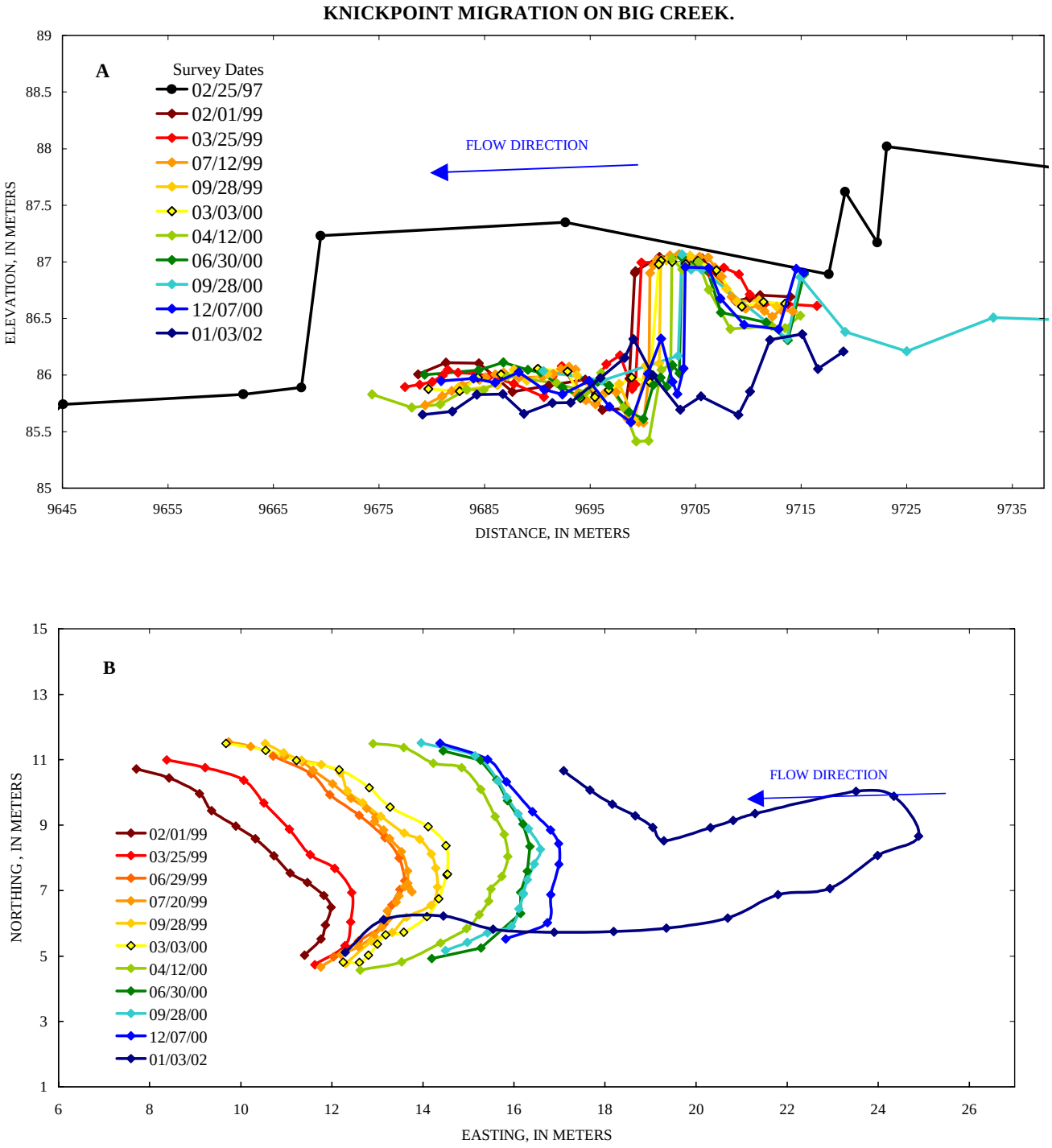

Figure 16 A - Big Creek knickpoint thalweg profile and
B - Big Creek knickpoint planimetric view.

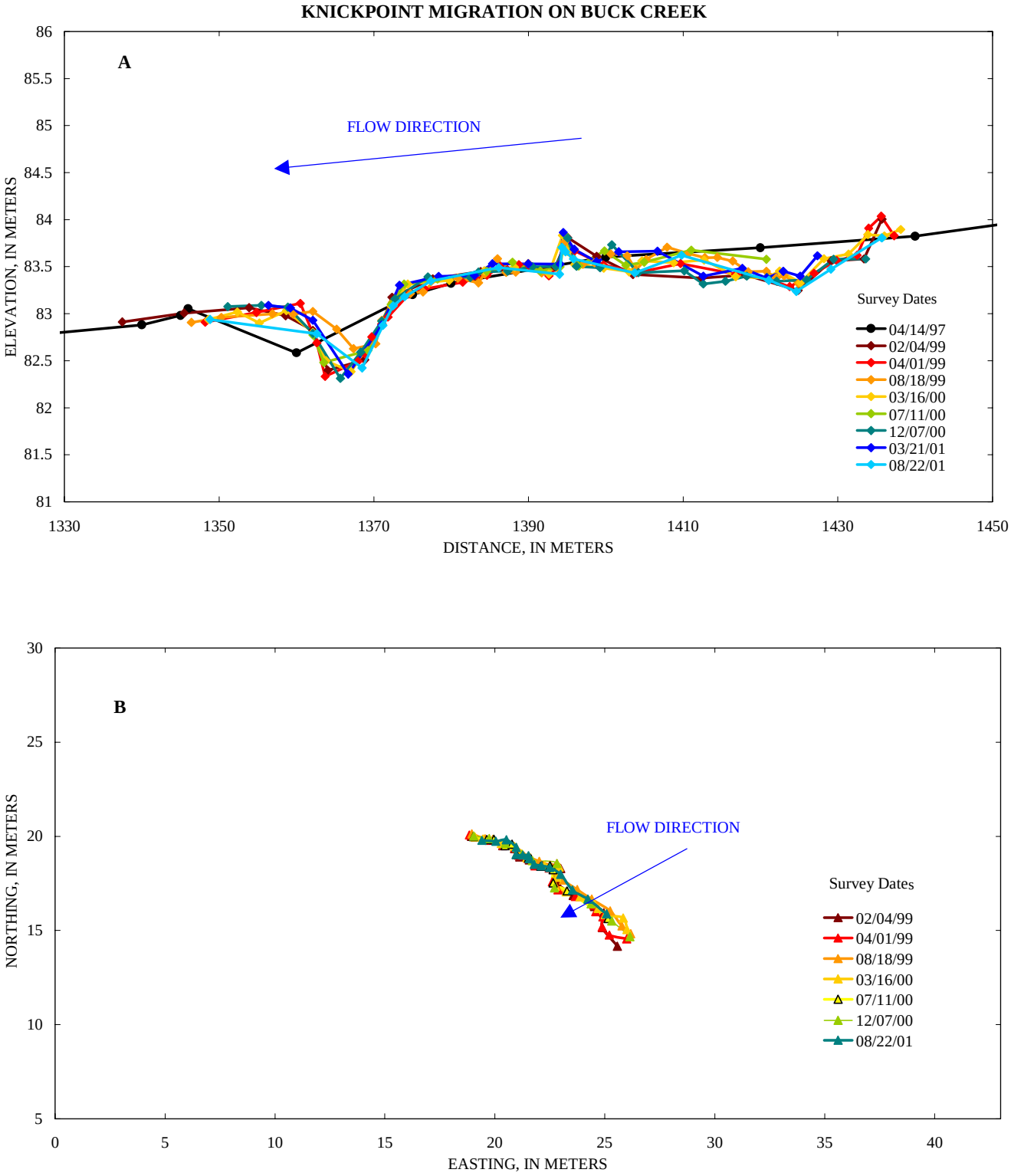

Figure 17 A - Buck Creek knickpoint thalweg profile and
B - Buck Creek knickpoint planimetric view.

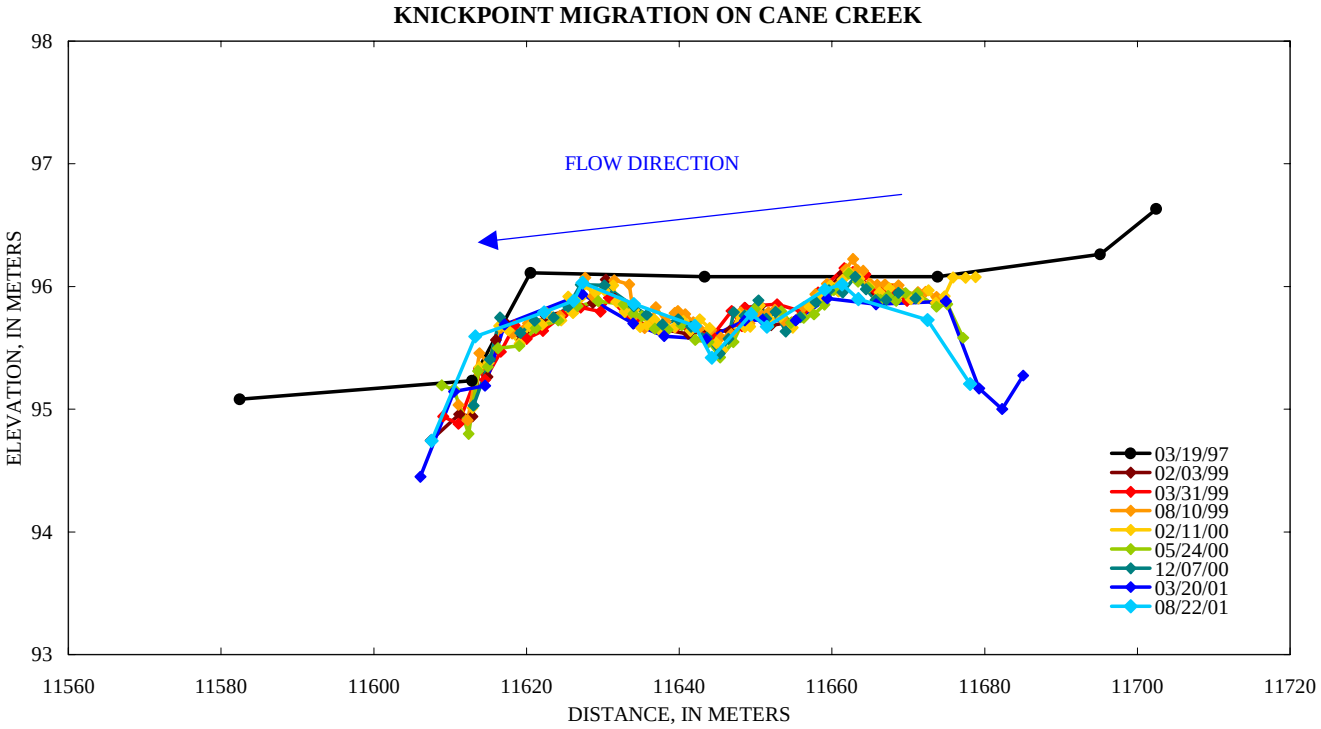

Figure 18 - Cane Creek knickpoint thalweg profile.

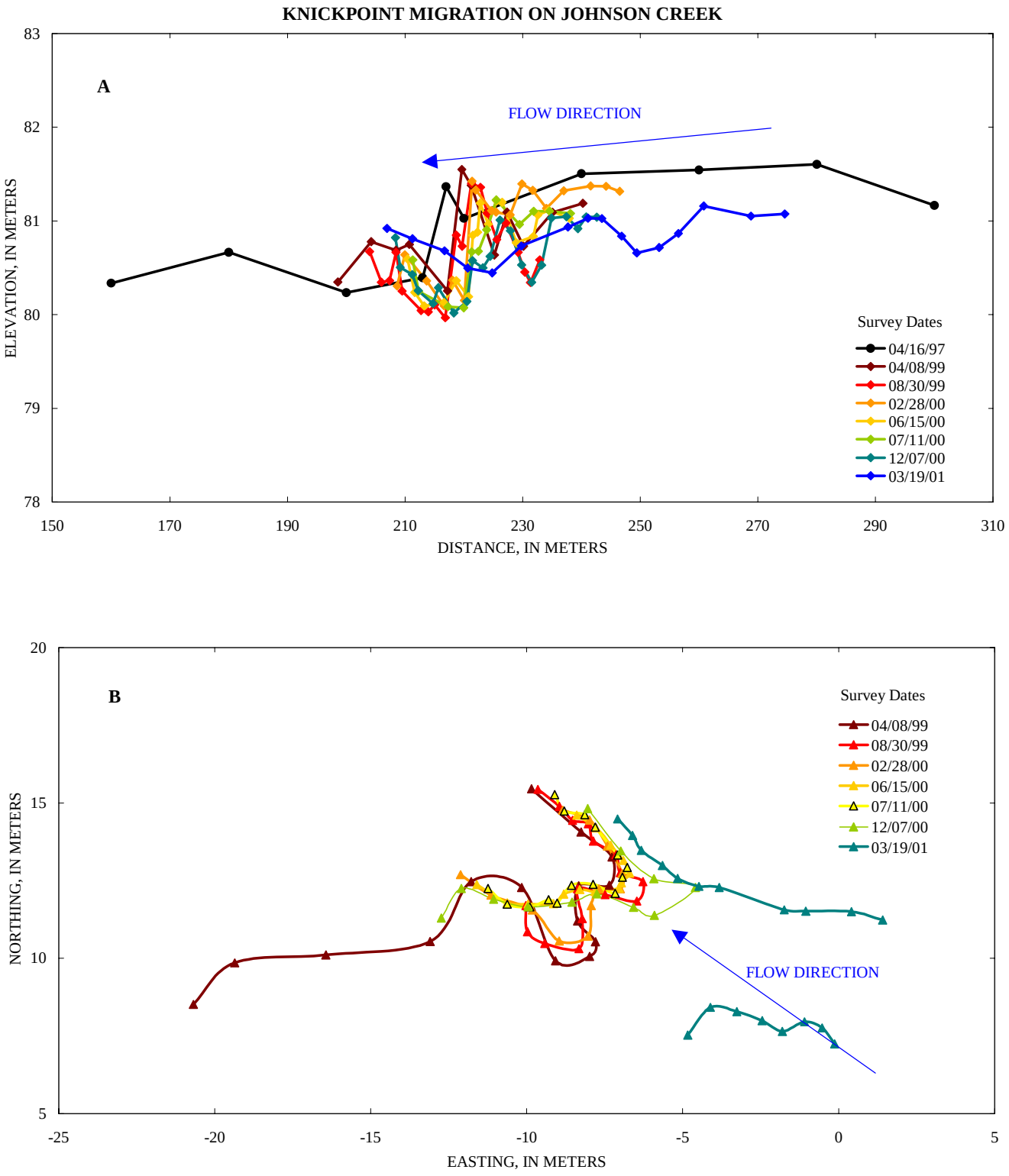

Figure 19 A - Johnson Creek knickpoint thalweg profile and
B - Johnson Creek knickpoint planimetric view.

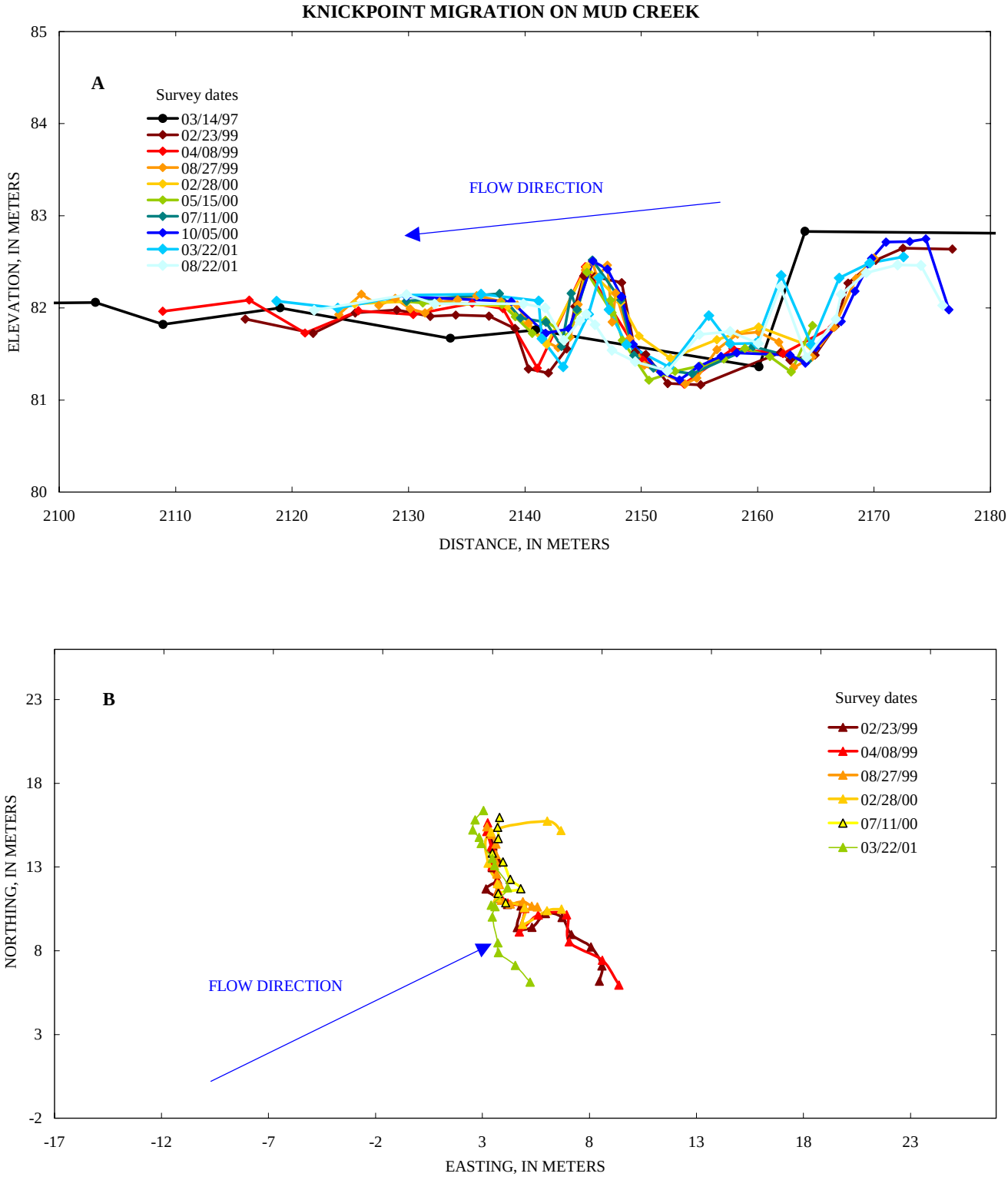

Figure 20 A - Mud Creek knickpoint thalweg profile and
B - Mud Creek knickpoint planimetric view.

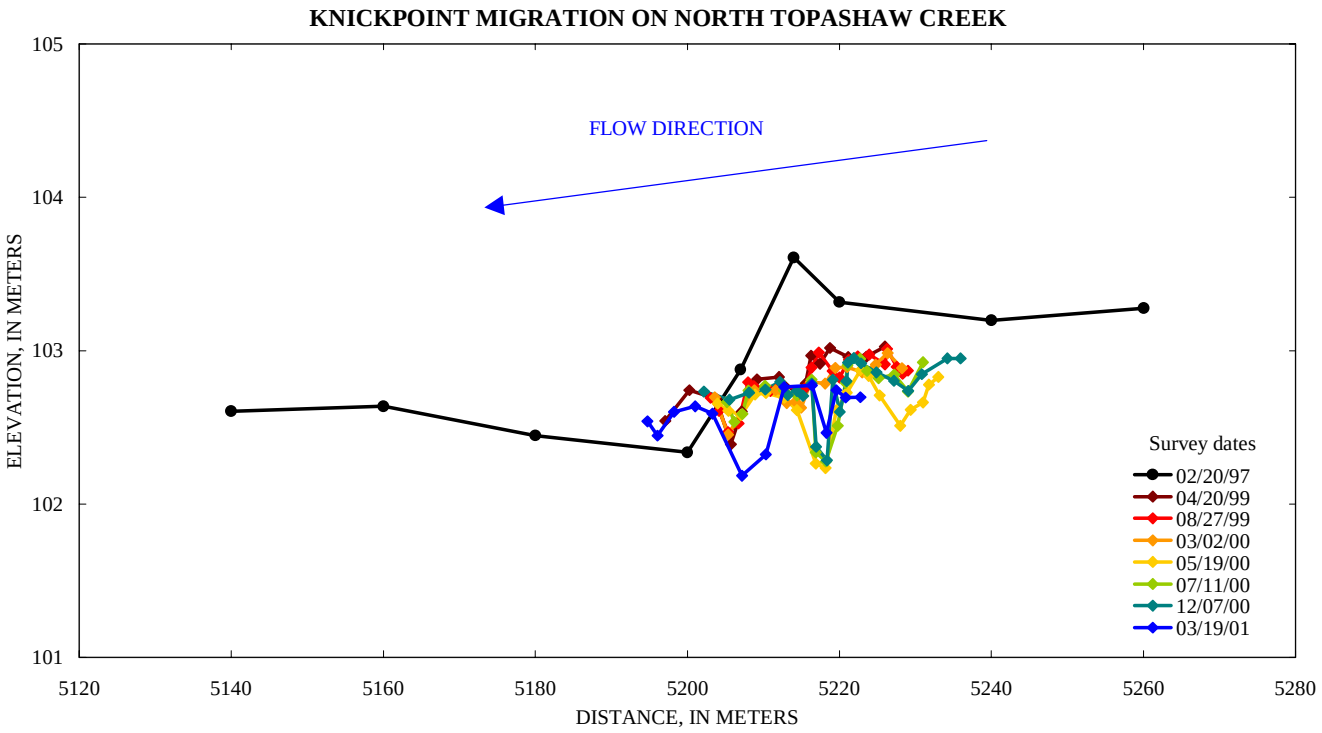

Figure 21 - North Topashaw Creek knickpoint thalweg profile.

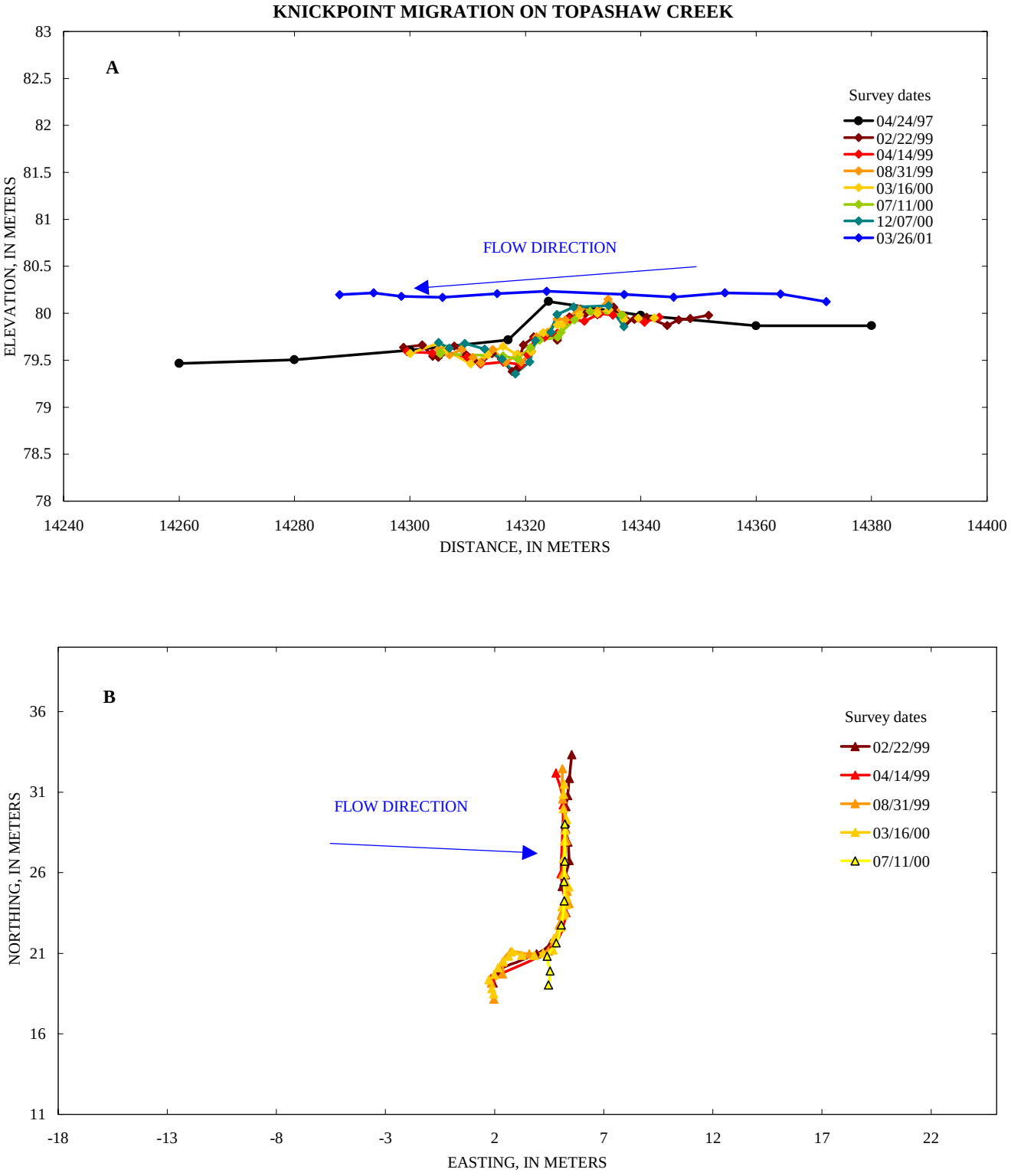

Figure 22 A - Topashaw Creek knickpoint thalweg profile and
B - Topashaw Creek knickpoint planimetric view.

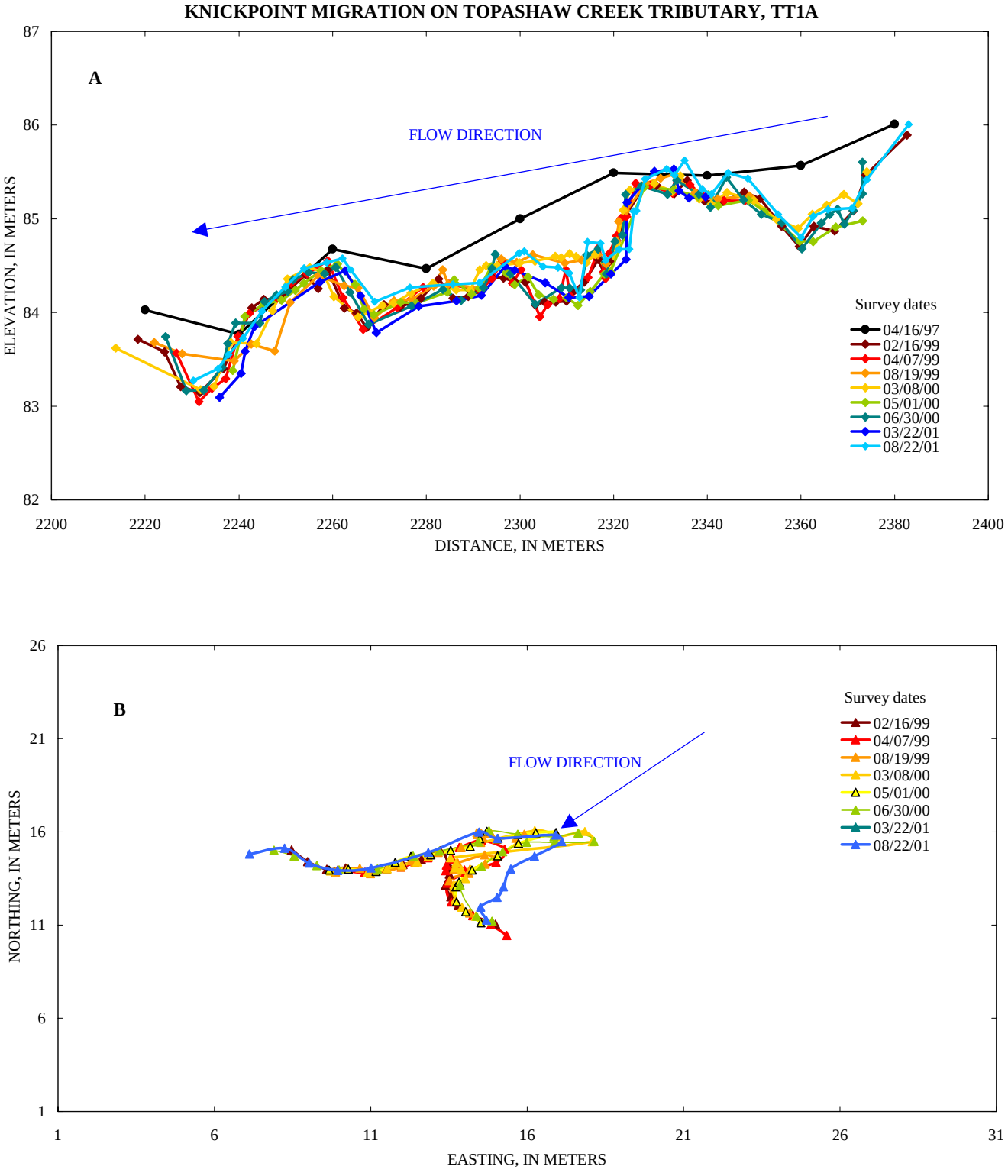

Figure 23 A - Topashaw Creek Tributary 1A knickpoint thalweg profile and
B - Topashaw Creek Tributary 1A knickpoint planimetric view.

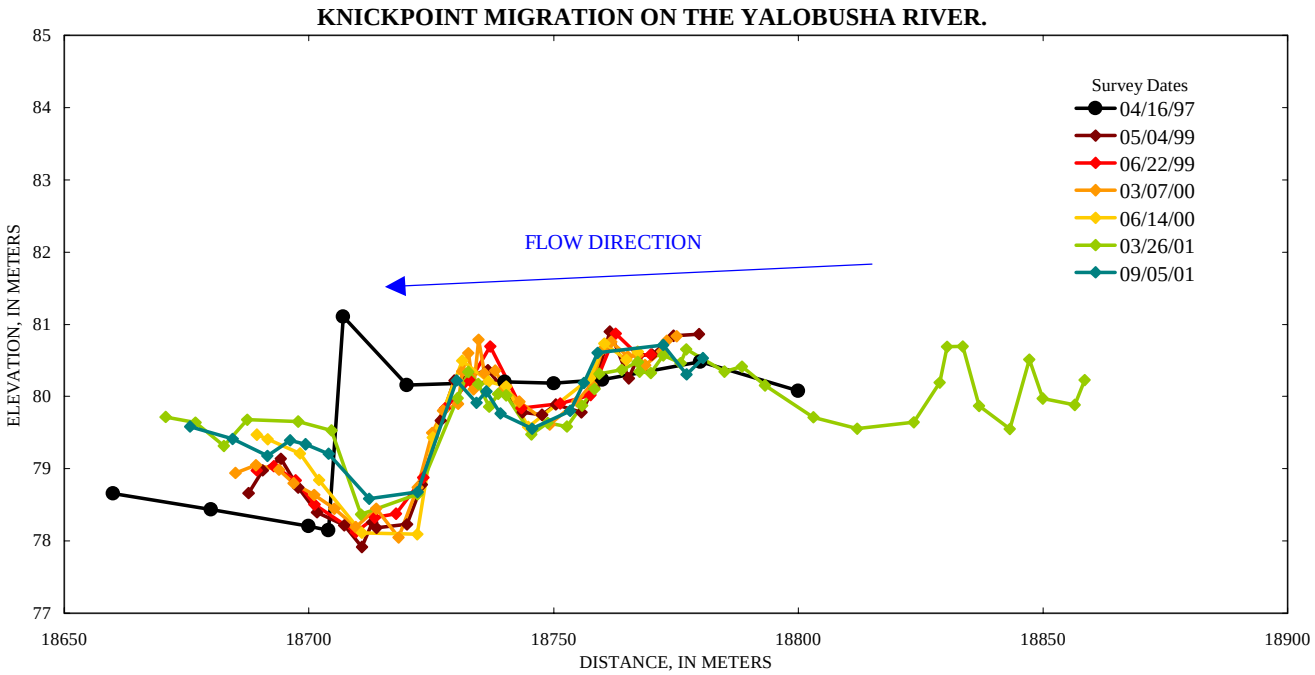

Figure 24 - Yalobusha River knickpoint thalweg profile.

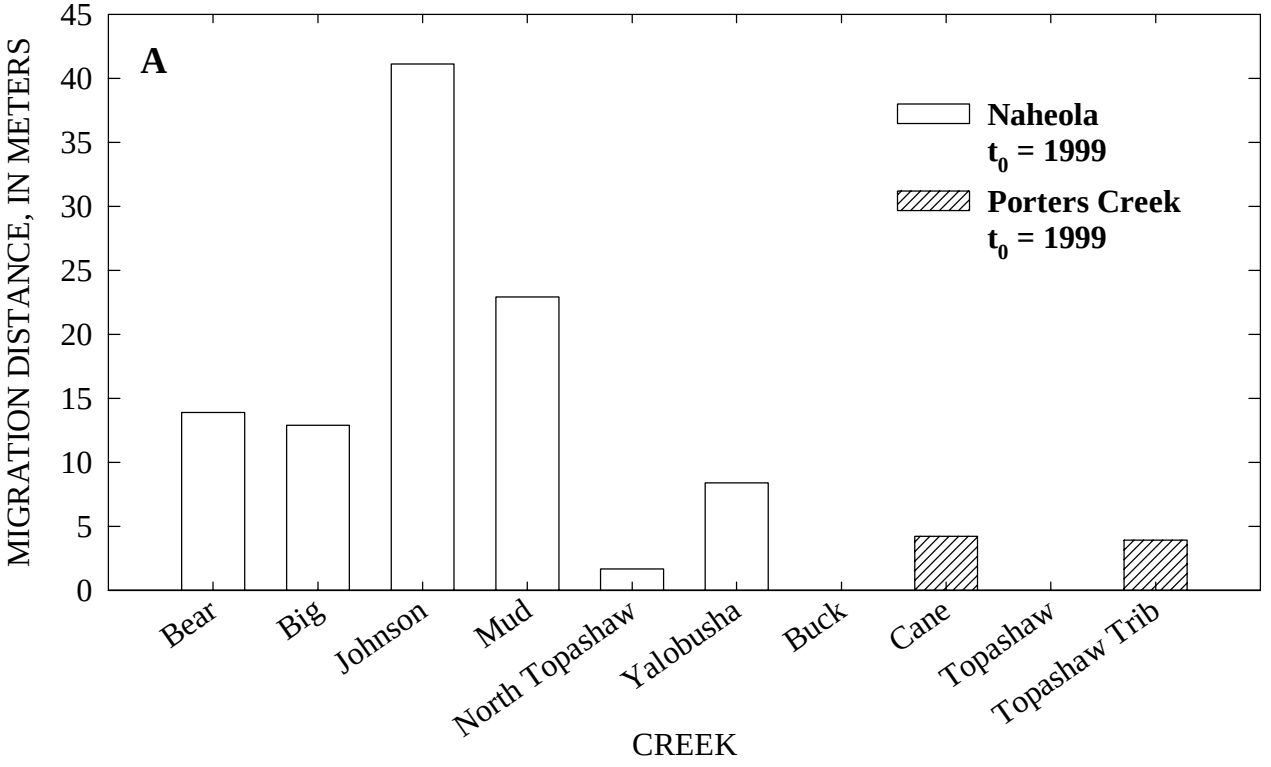

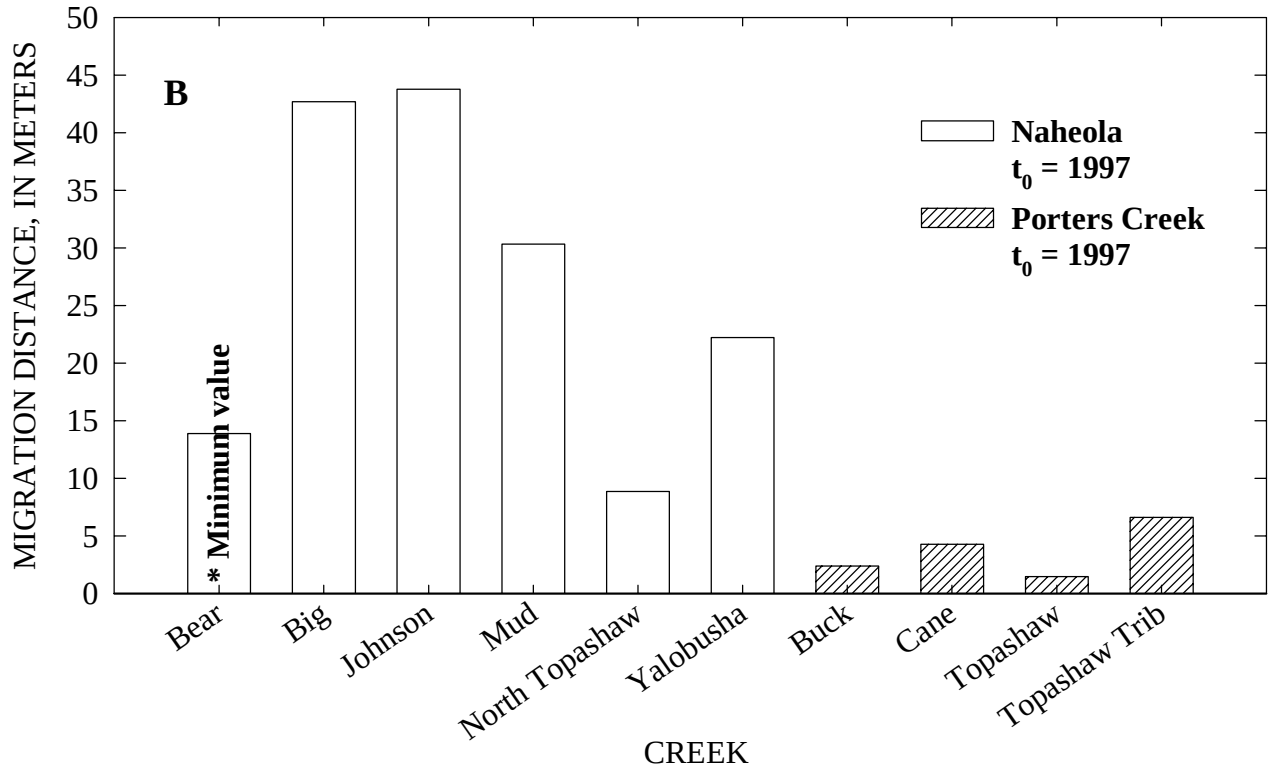

Figure 25 A - Comparison of migration rates since 1999 for the ten "intensive" sites showing the difference between Porters Creek Clay and Naheola formations and

Figure 25 B - Comparison of migration rates since 1997 for the ten "intensive" sites showing the difference between Porters Creek Clay and Naheola formations.

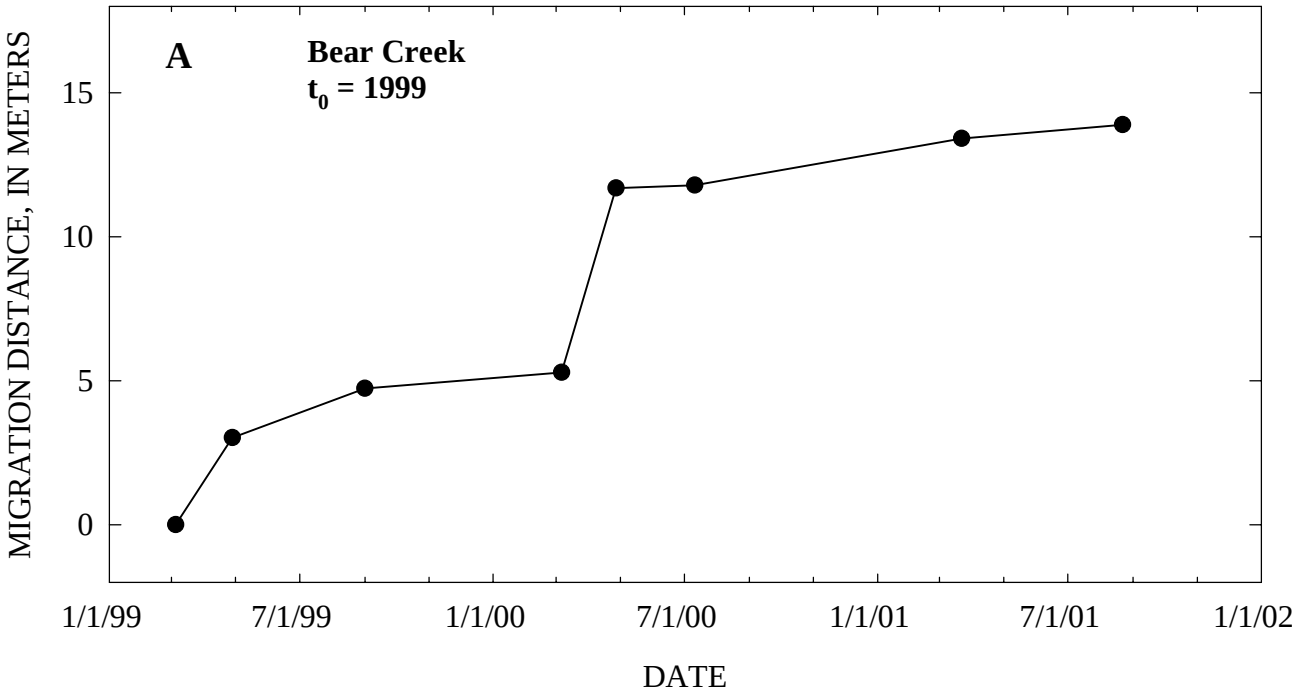

Figure 26 - Bear Creek knickpoint migration rates since 1999.

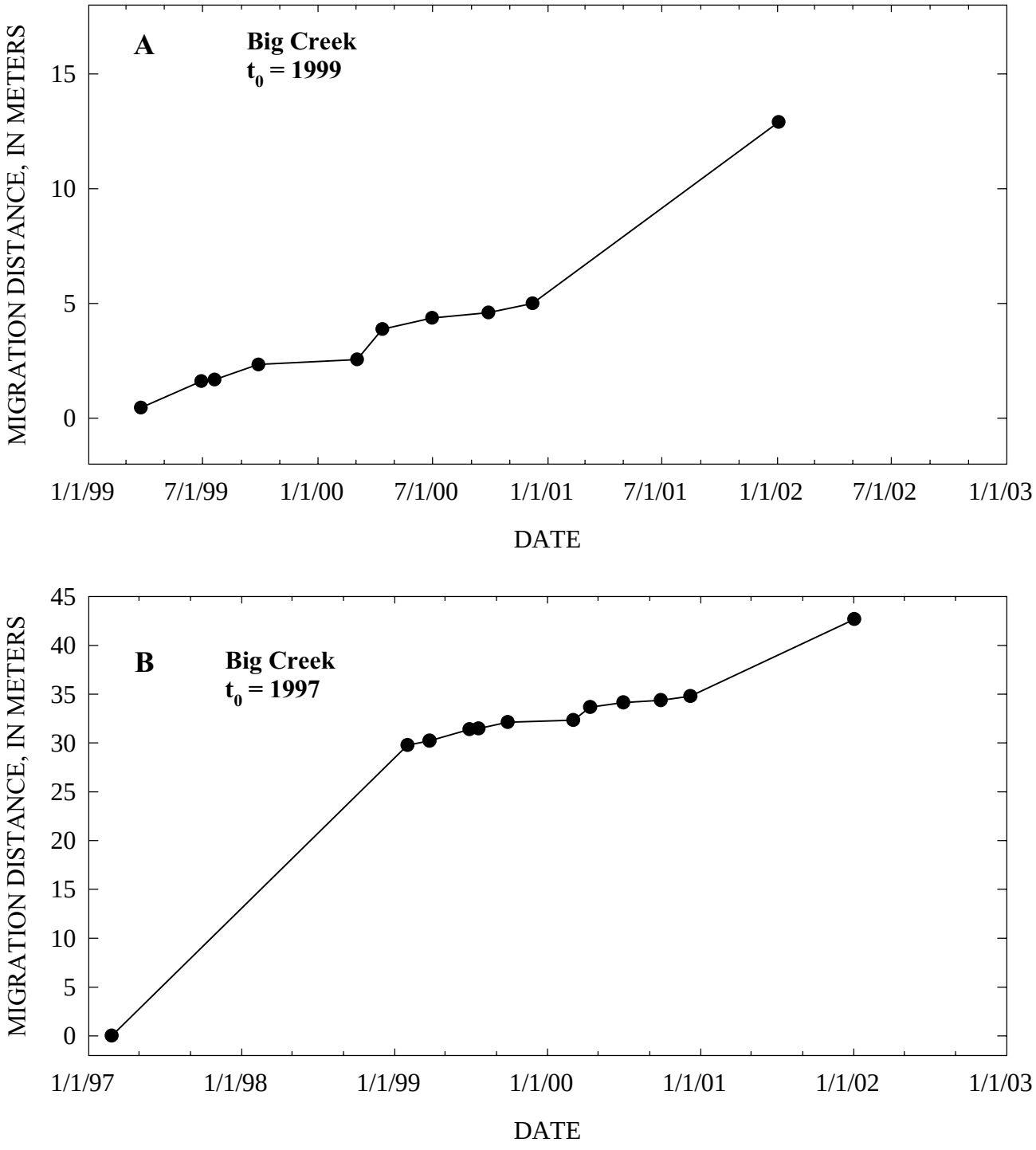

Figure 27 A - Big Creek knickpoint migration rates since 1999 and
B - Big Creek knickpoint migration rates since 1997.

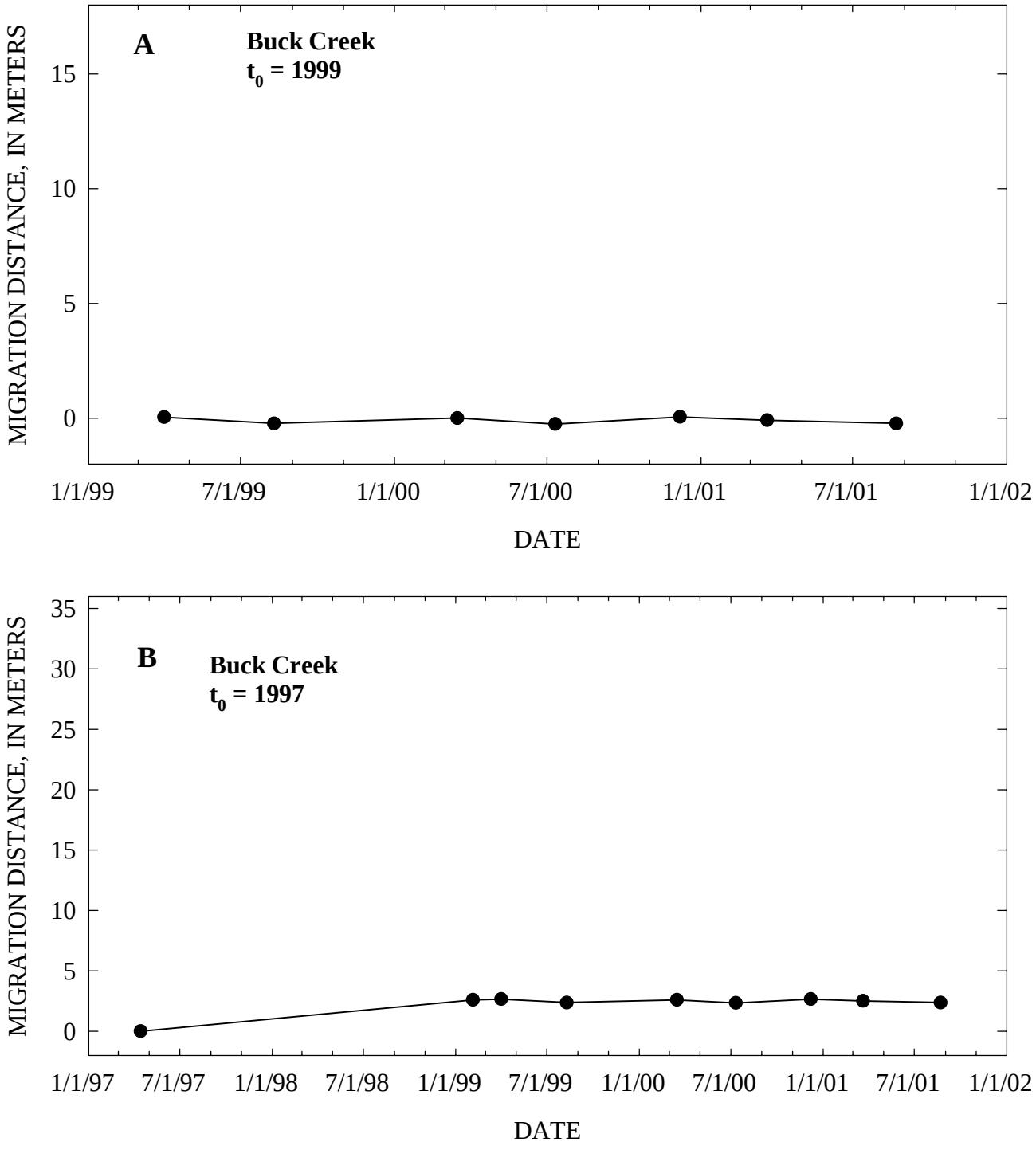

Figure 28 A - Buck Creek knickpoint migration rates since 1999 and
B - Buck Creek knickpoint migration rates since 1997.

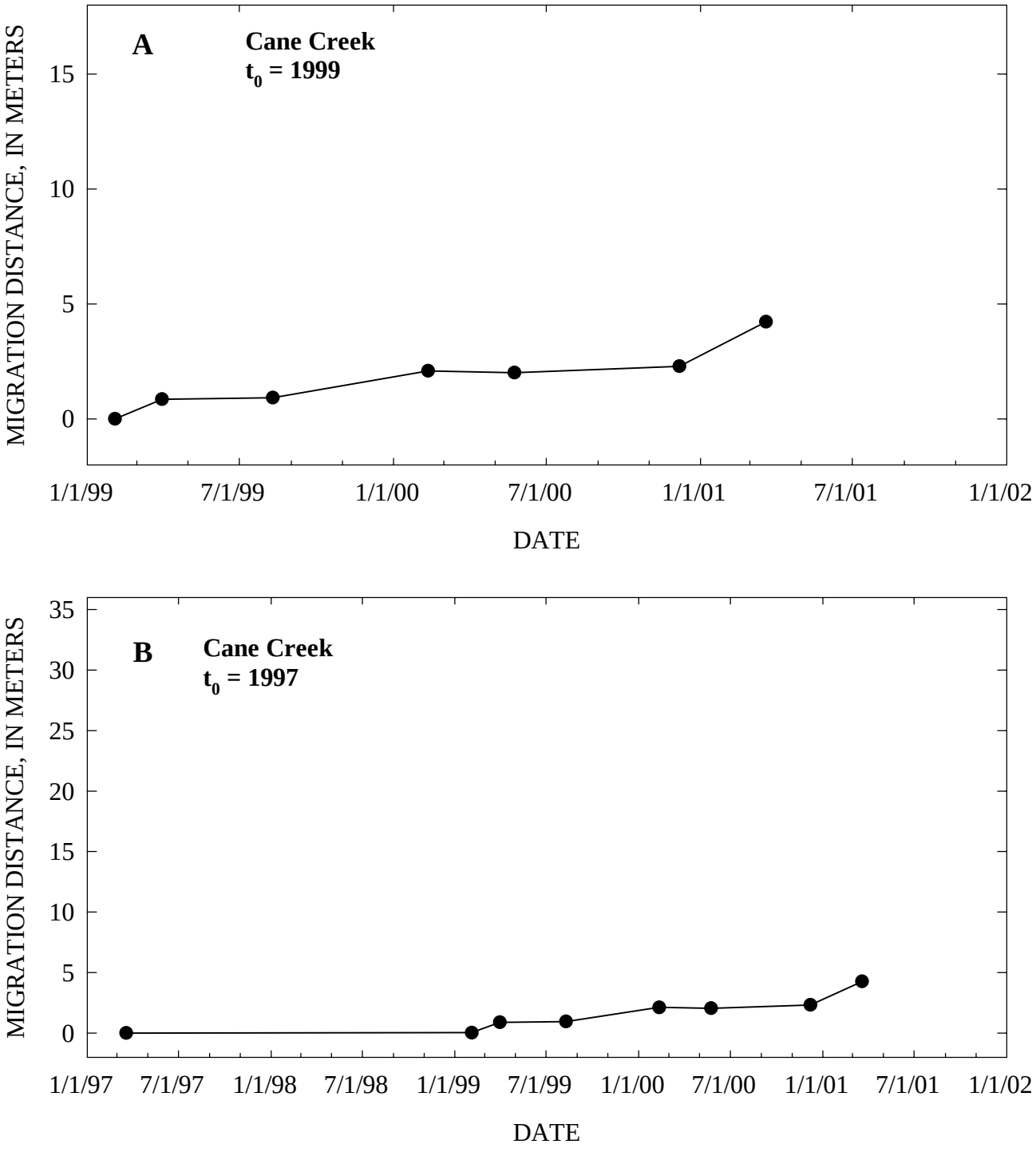

Figure 29 A - Cane Creek knickpoint migration rates since 1999 and
B - Cane Creek knickpoint migration rates since 1997.

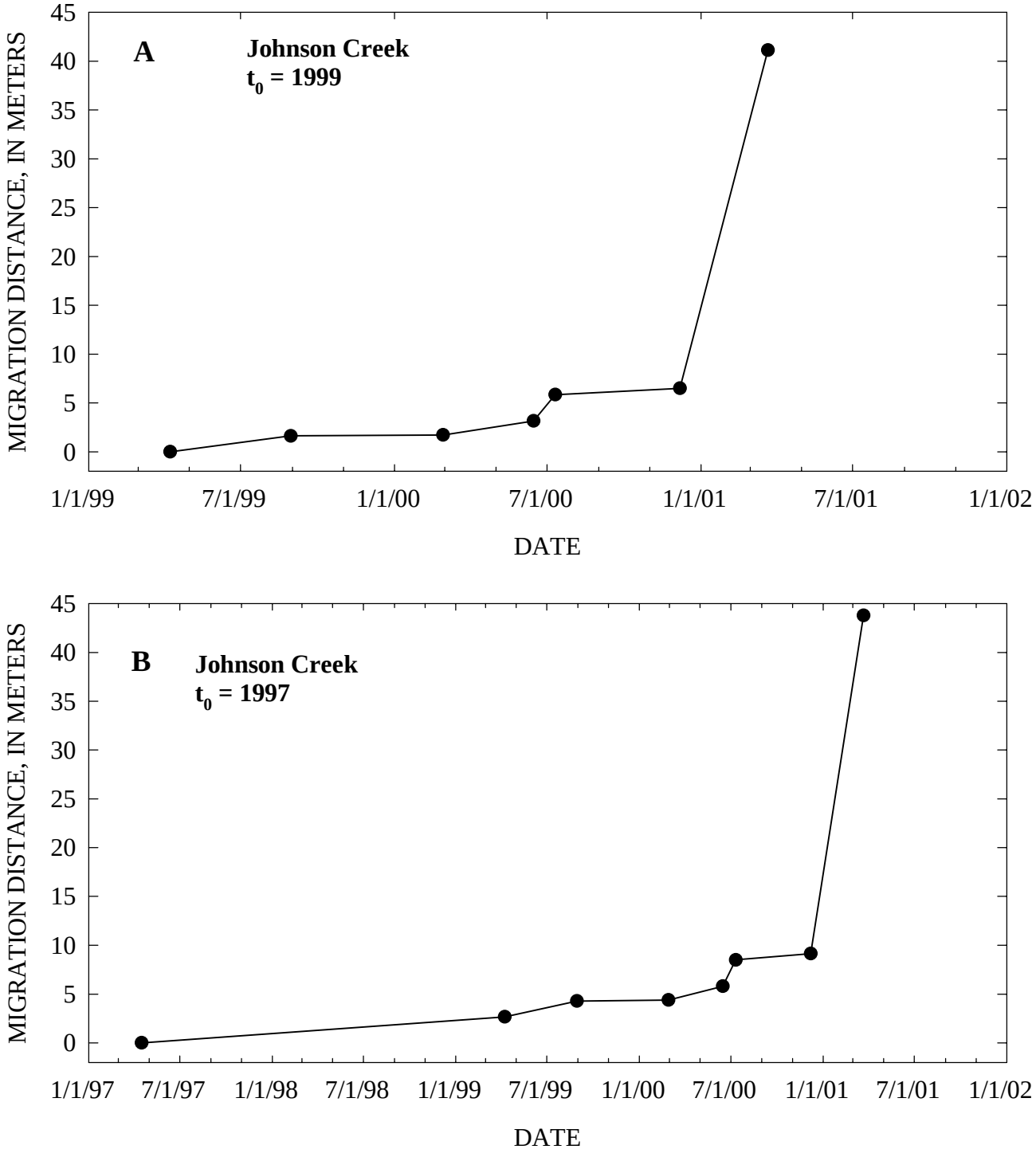

Figure 30 A - Johnson Creek knickpoint migration rates since 1999 and
B - Johnson Creek knickpoint migration rates since 1997.

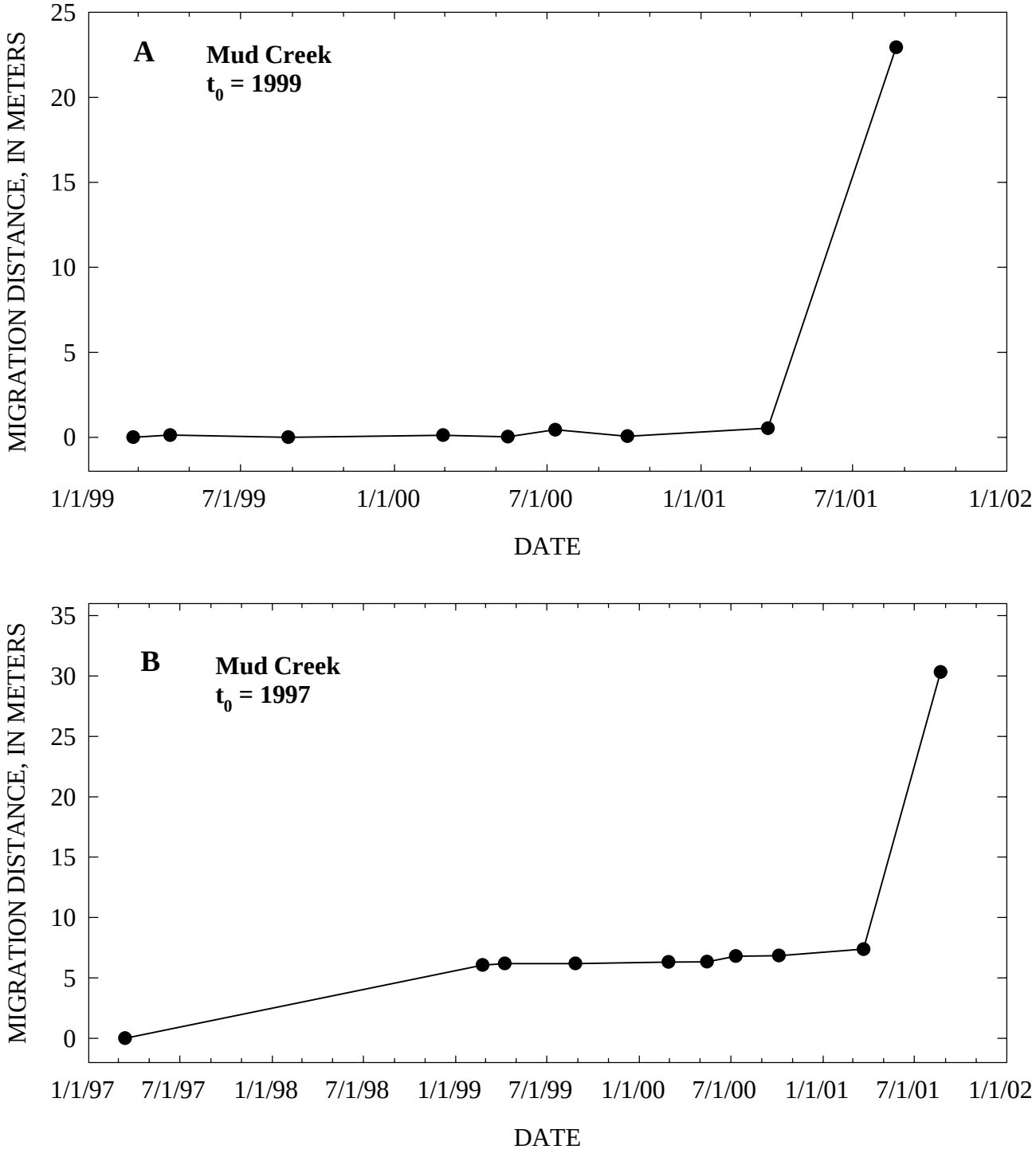

Figure 31 A - Mud Creek knickpoint migration rates since 1999 and
B - Mud Creek knickpoint migration rates since 1997.

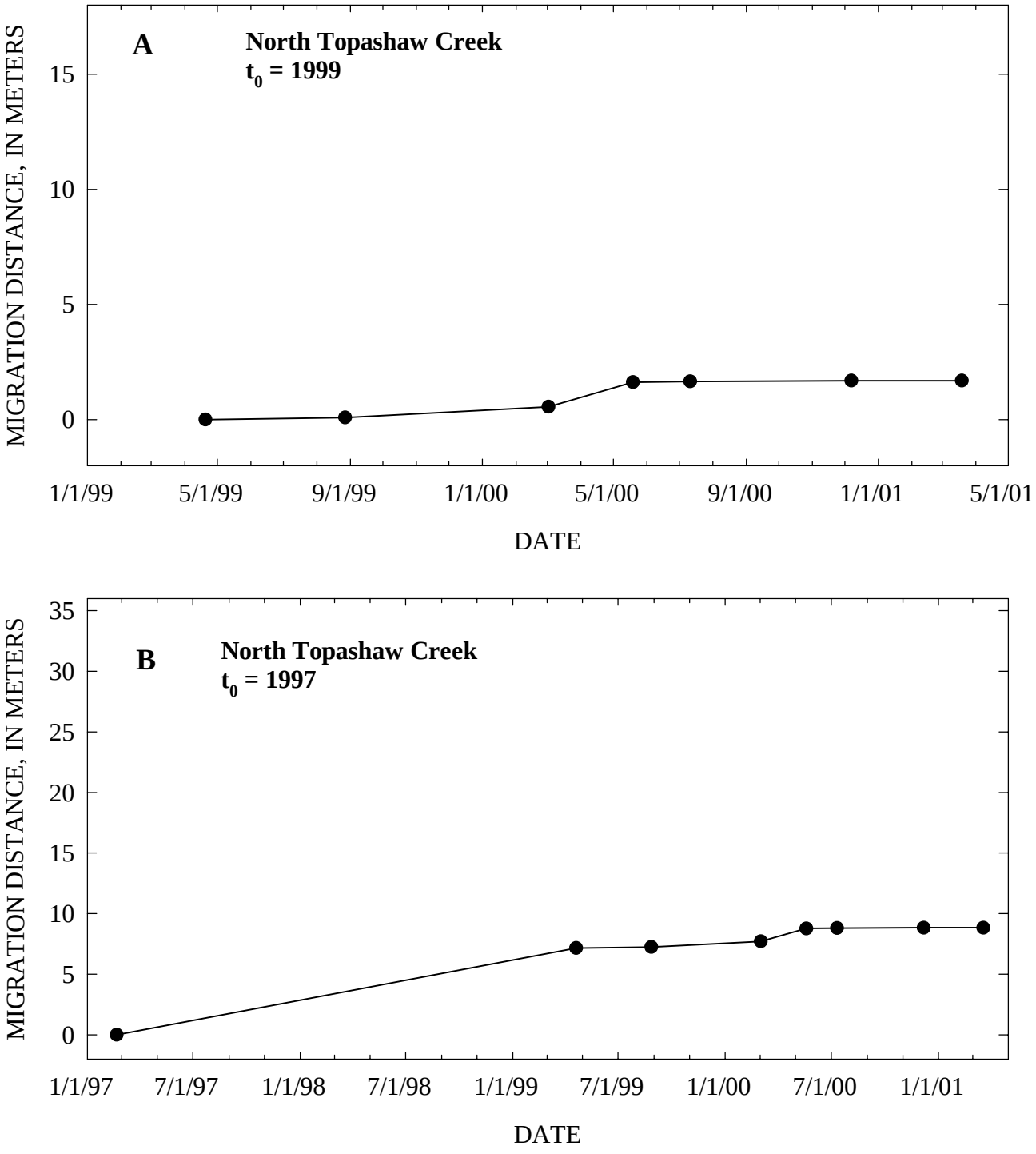

Figure 32 A - North Topashaw Creek knickpoint migration rates since 1999 and
B - North Topashaw Creek knickpoint migration rates since 1997.

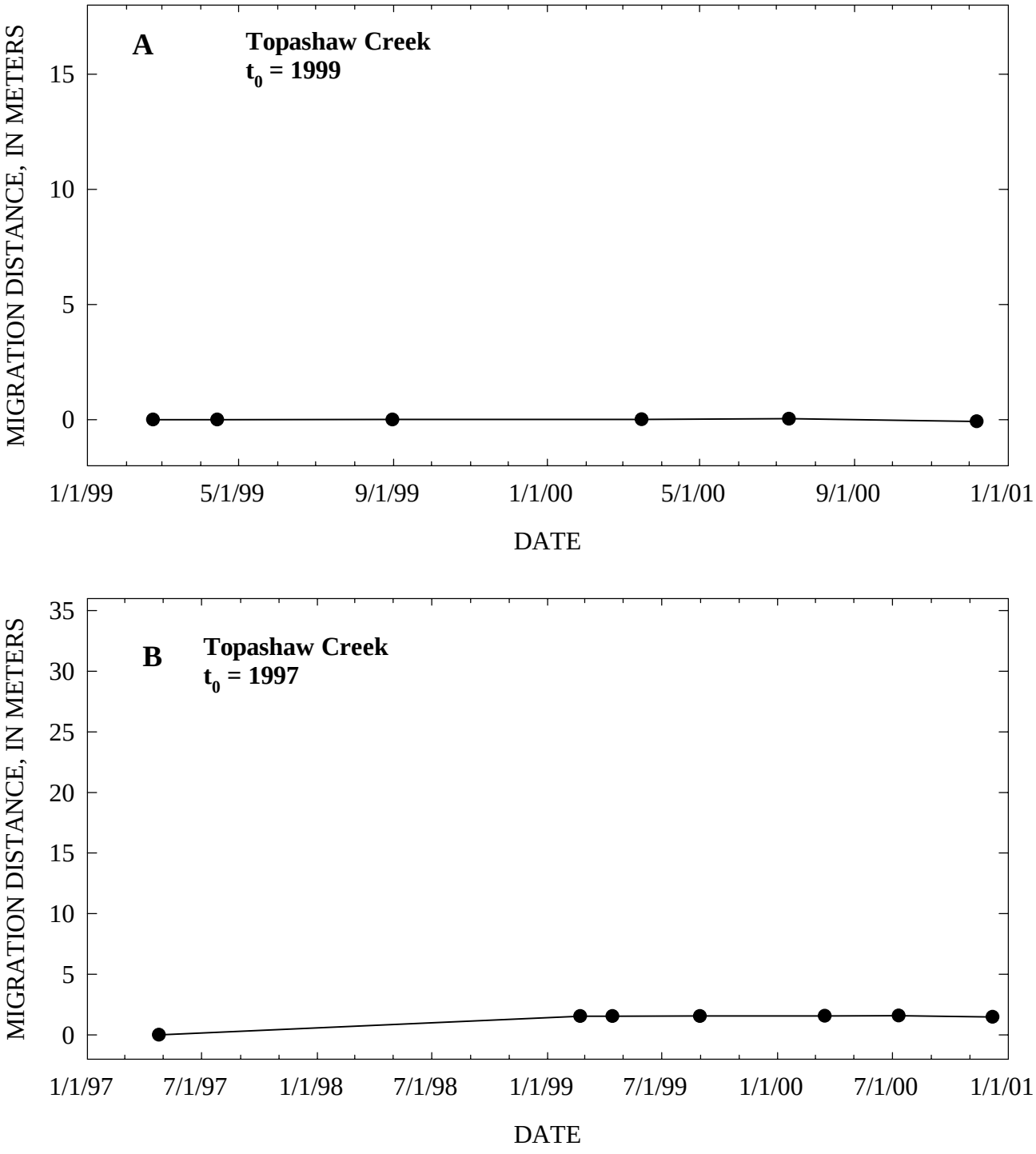

Figure 33 A - Topashaw Creek knickpoint migration rates since 1999 and
B - Topashaw Creek knickpoint migration rates since 1997.

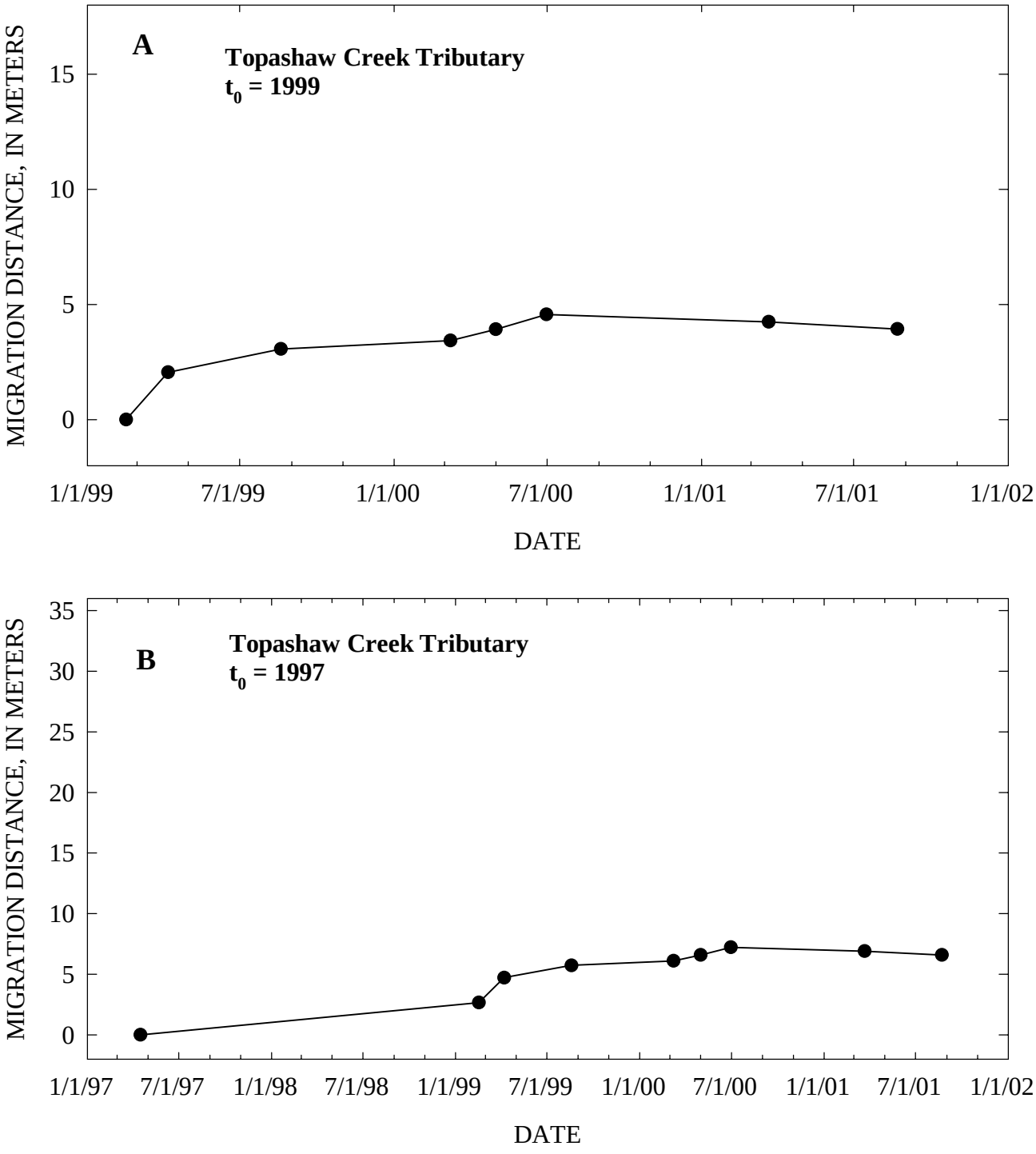

Figure 34 A - Topashaw Creek Tributary 1A knickpoint migration rates since 1999 and B - Topashaw Creek Tributary 1A knickpoint migration rates since 1997.

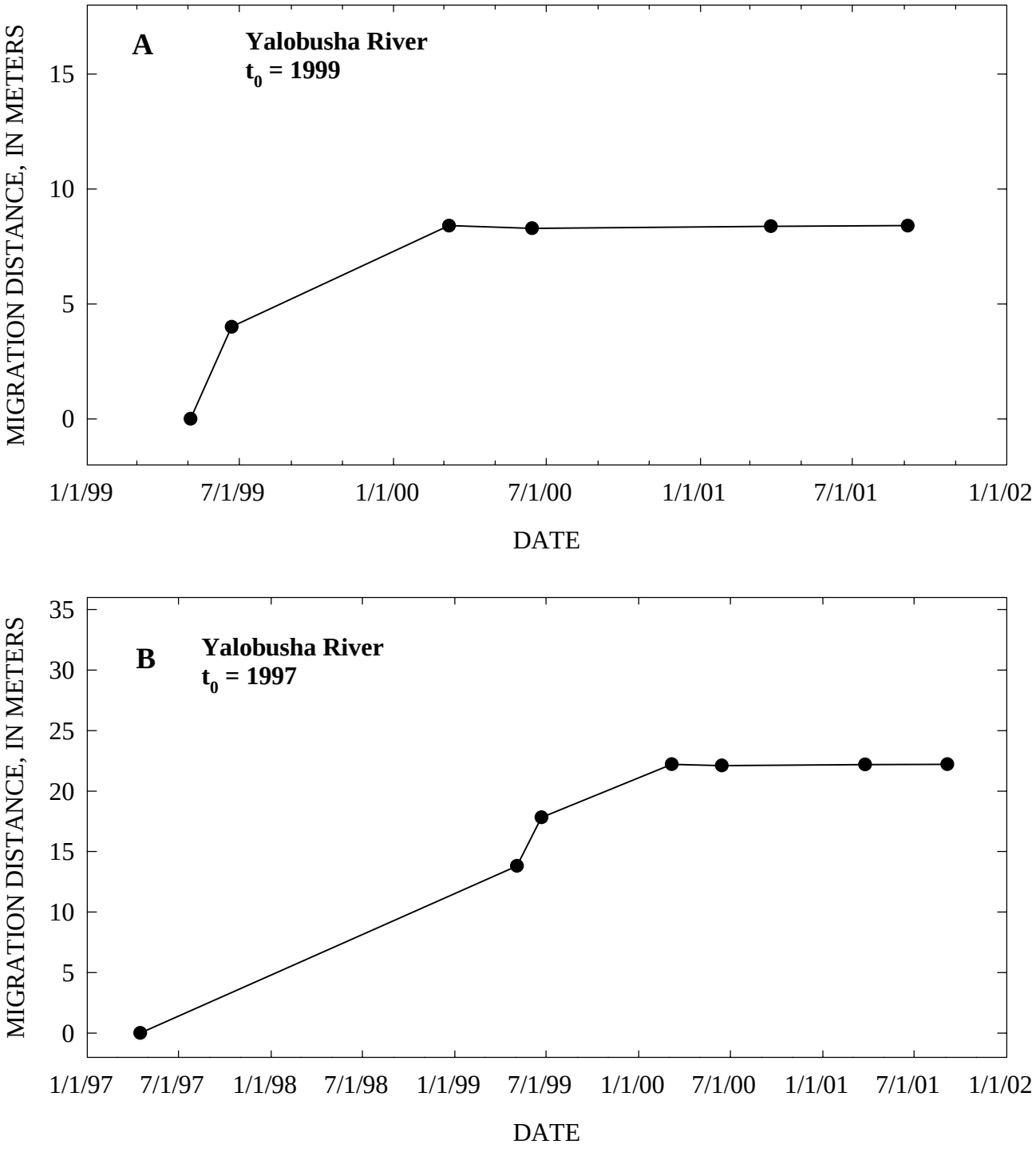

Figure 35 A - Yalobusha River knickpoint migration rates since 1999 and
B - Yalobusha River knickpoint migration rates since 1997.

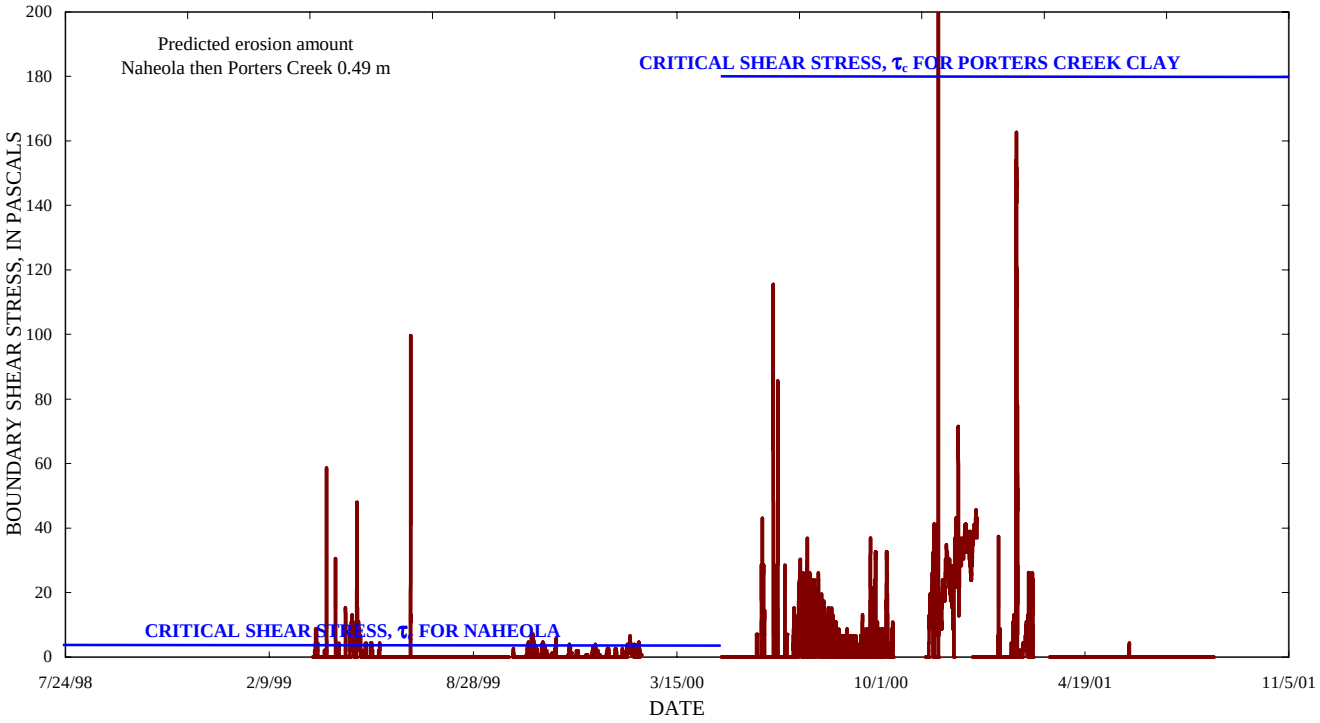

Figure 36 - Average boundary shear stress, τ_o against time and critical shear stress for Bear Creek, showing periods of exceedance and predicted erosion amount.

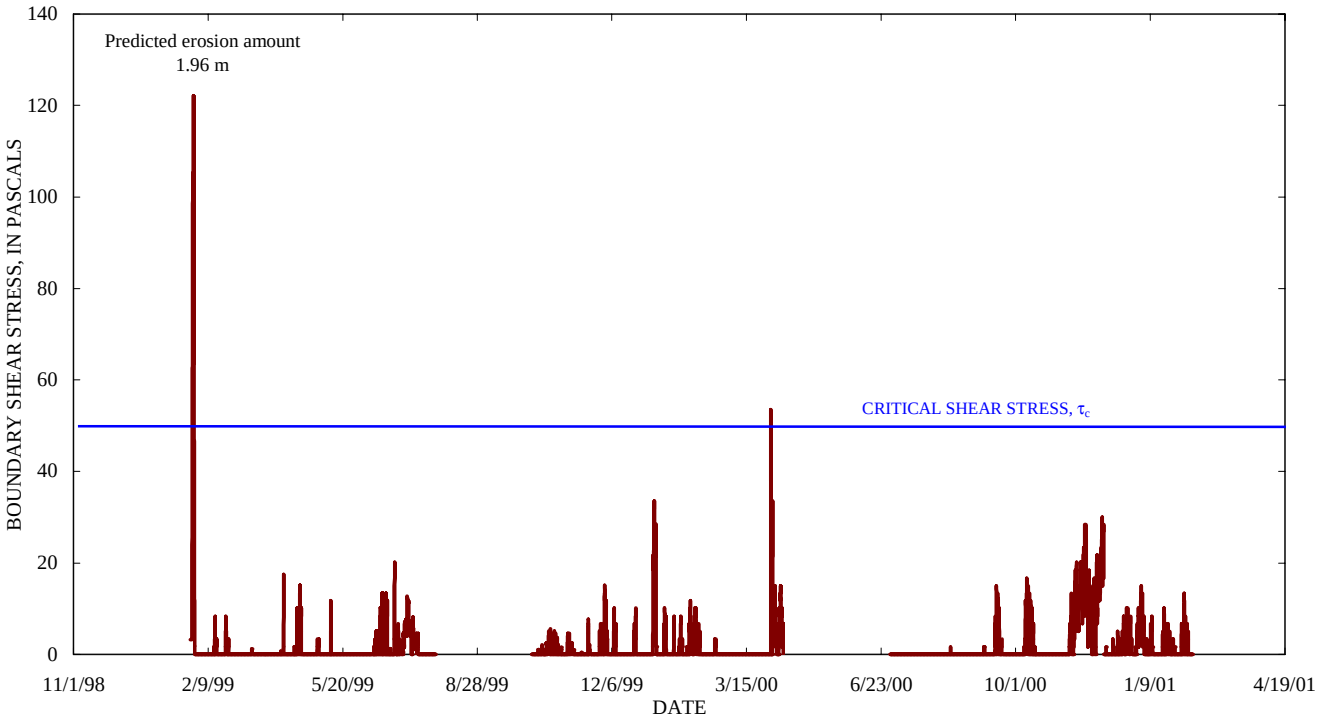

Figure 37 - Average boundary shear stress, τ_o against time and critical shear stress for Big Creek, showing periods of exceedance and predicted erosion amount.

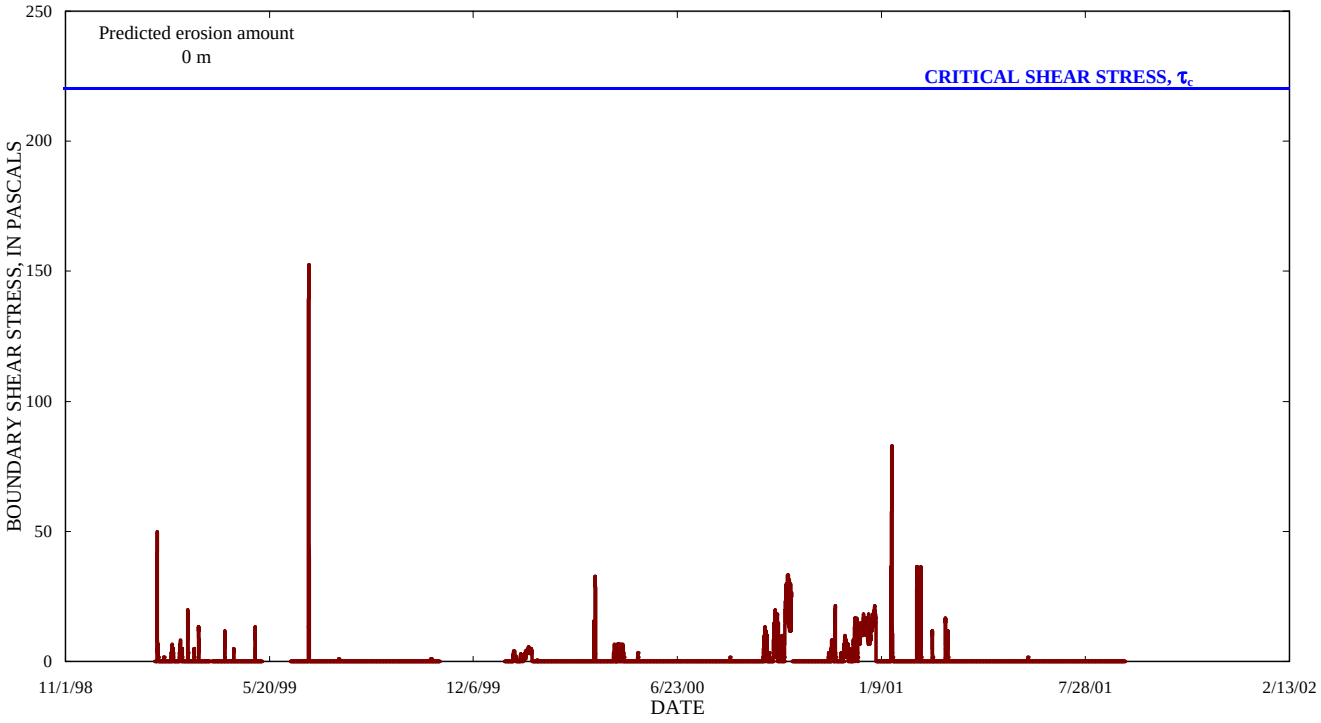

Figure 38 - Average boundary shear stress, τ_o against time and critical shear stress for Buck Creek, showing periods of exceedance and predicted erosion amount.

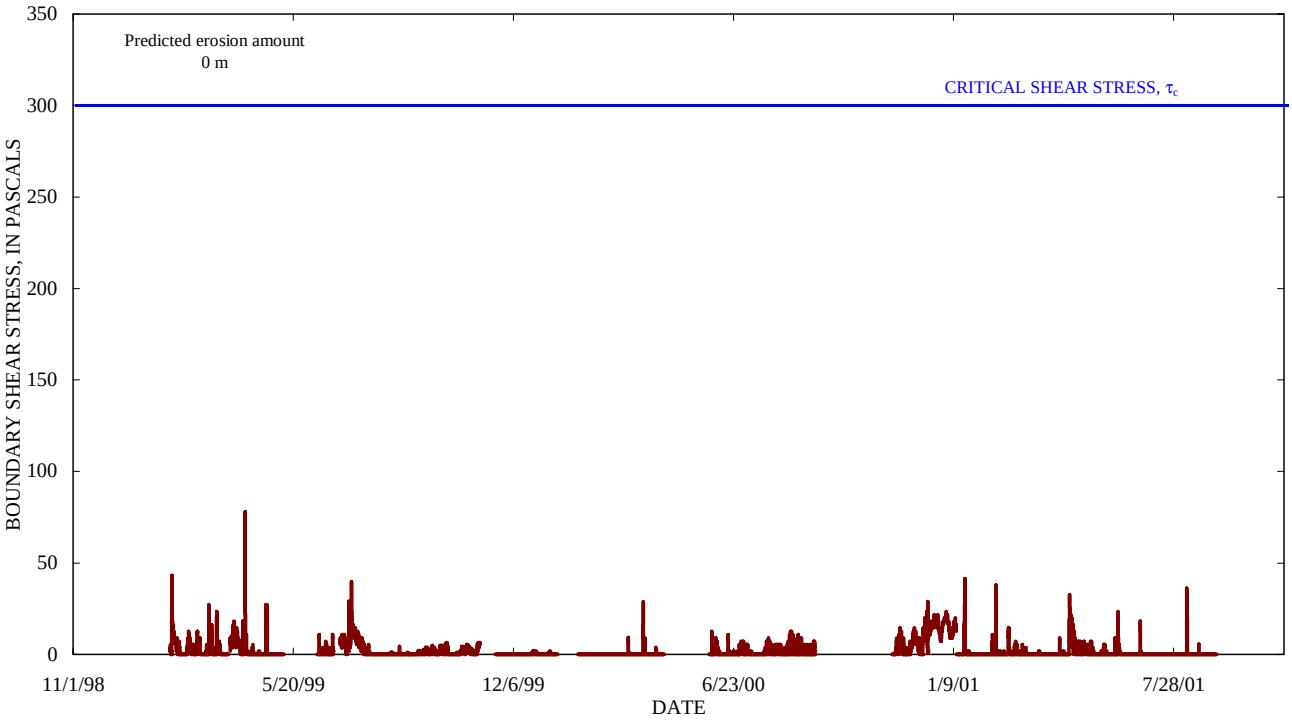

Figure 39 - Average boundary shear stress, τ_o against time and critical shear stress for Cane Creek, showing periods of exceedance and predicted erosion amount.

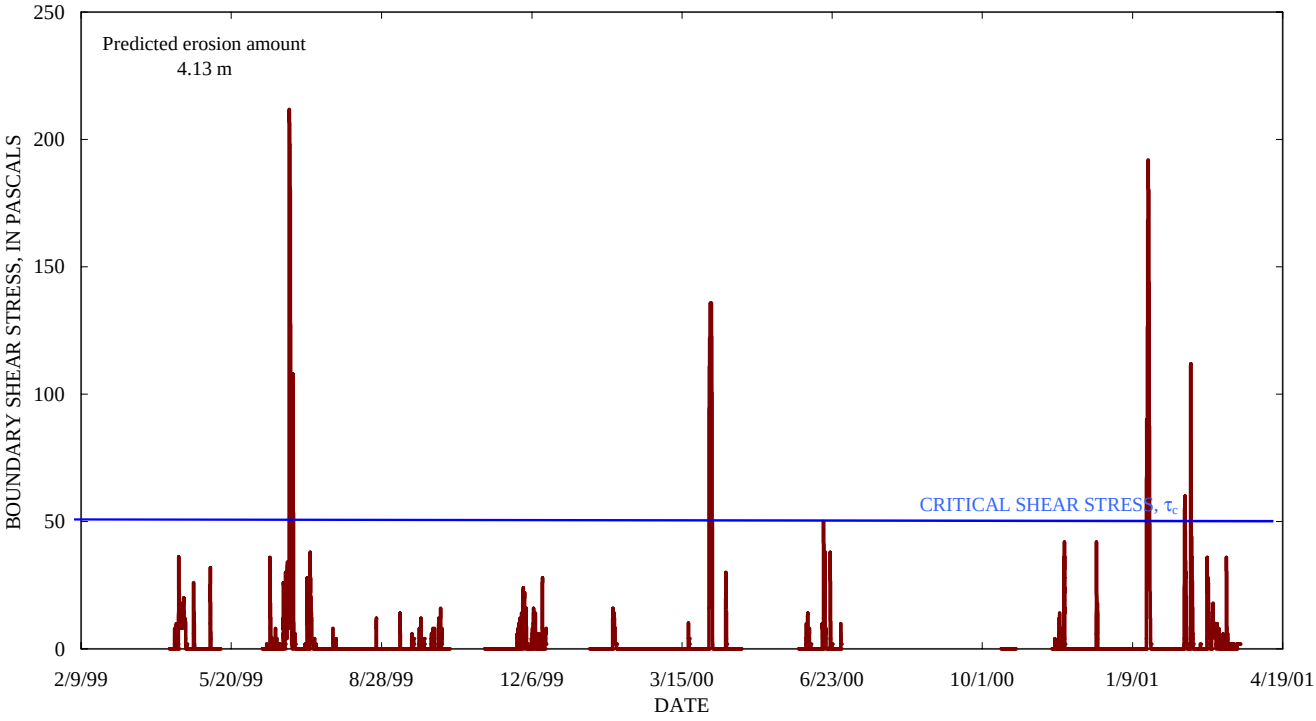

Figure 40 - Average boundary shear stress, τ_o against time and critical shear stress for Johnson Creek, showing periods of exceedance and predicted erosion amount.

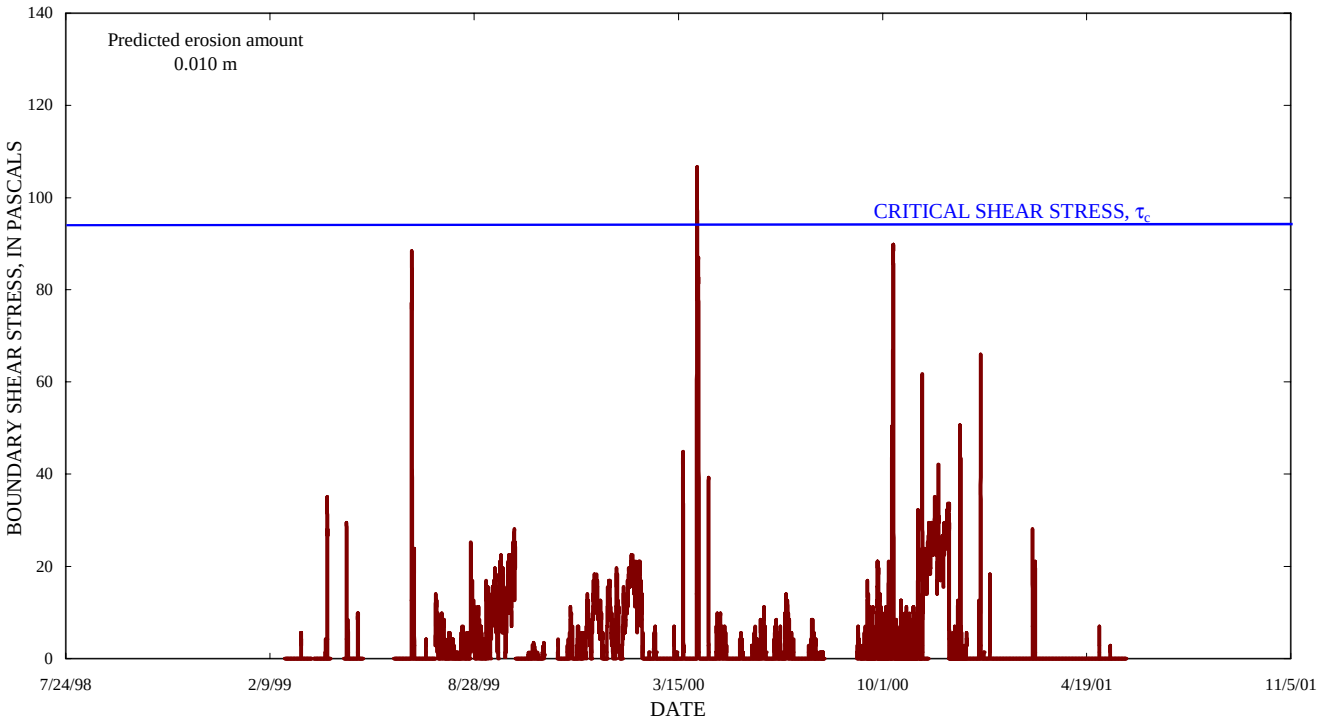

Figure 41 - Average boundary shear stress, τ_o against time and critical shear stress for Mud Creek, showing periods of exceedance and predicted erosion amount.

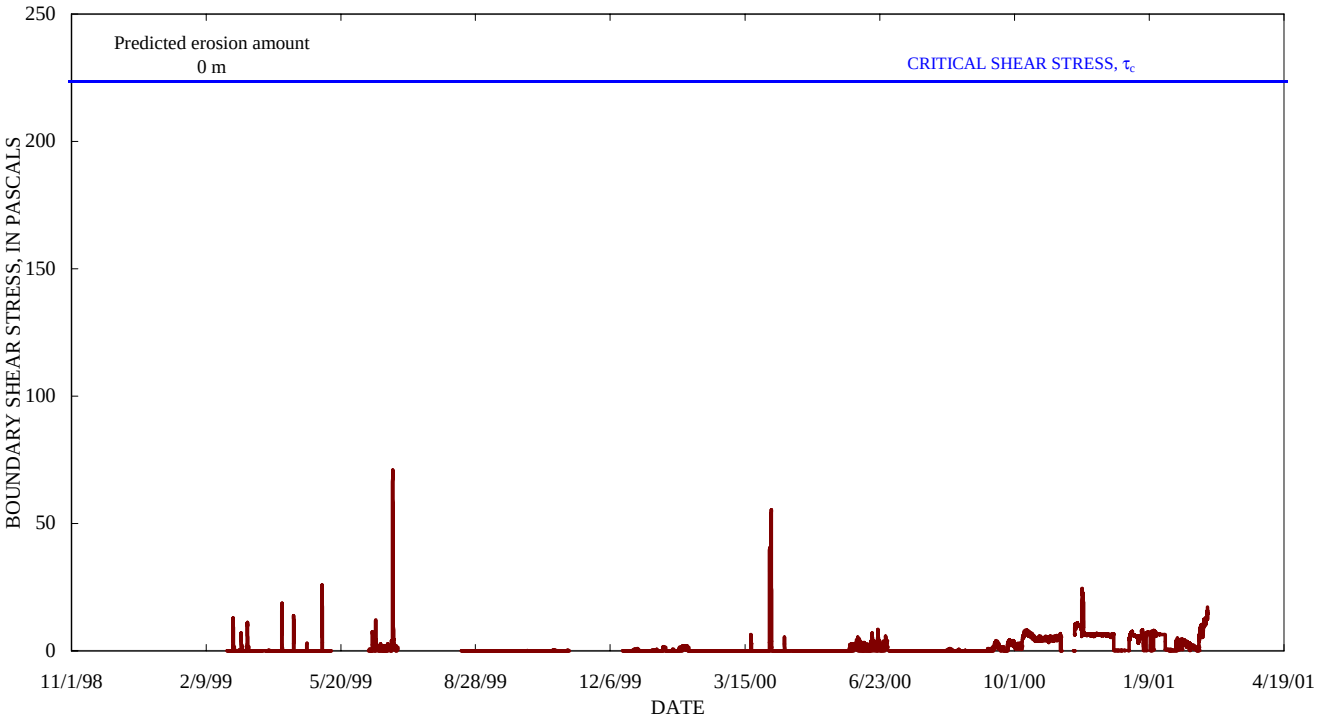

Figure 42 - Average boundary shear stress, τ_o against time and critical shear stress for Topashaw Creek, showing periods of exceedance and predicted erosion amount.

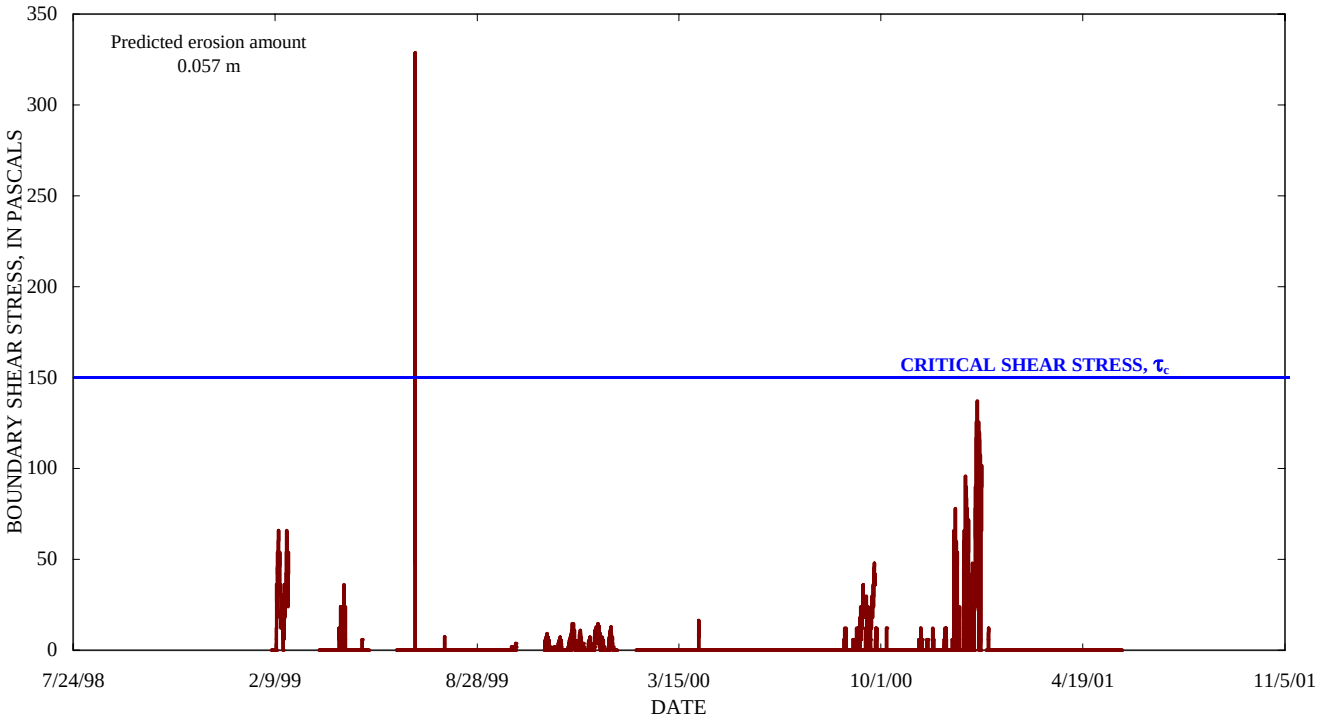

Figure 43 - Average boundary shear stress, τ_o against time and critical shear stress for Topashaw Creek Tributary 1A, showing periods of exceedance and predicted erosion amount.

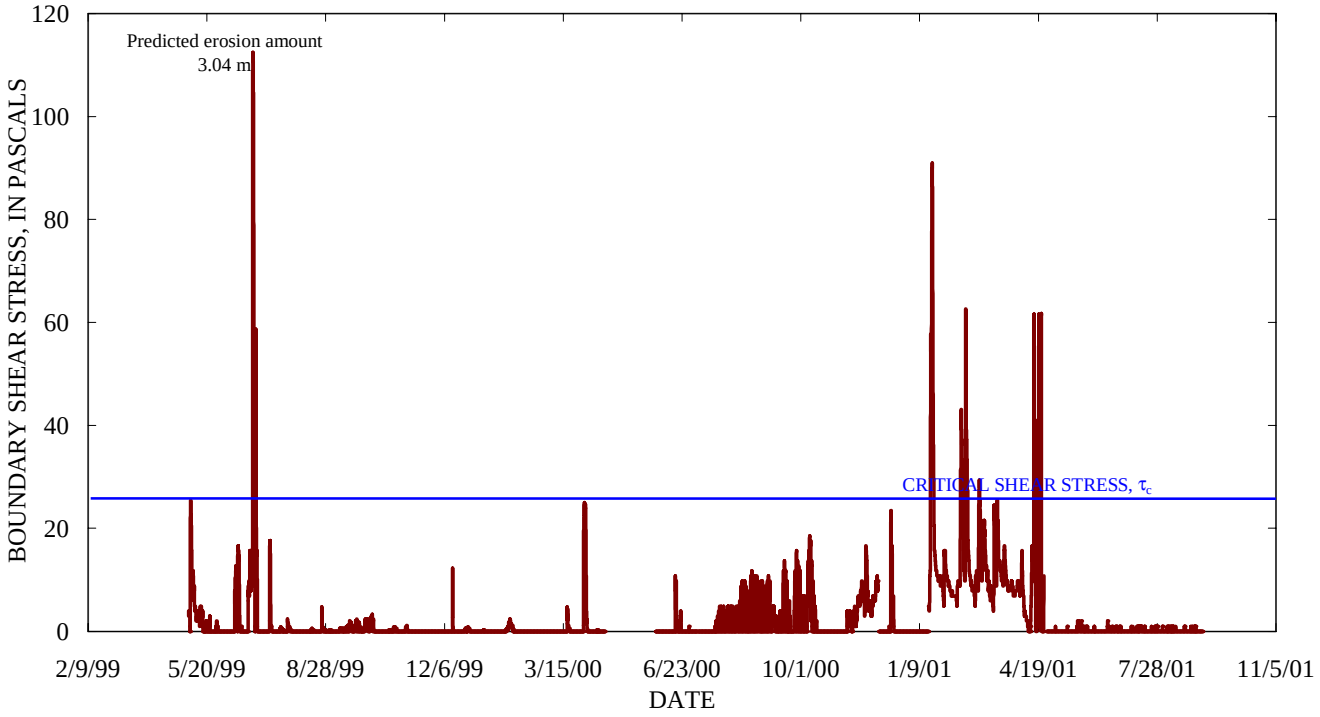

Figure 44 - Average boundary shear stress, τ_o against time and critical shear stress for the Yalobusha River, showing periods of exceedance and predicted erosion amount.

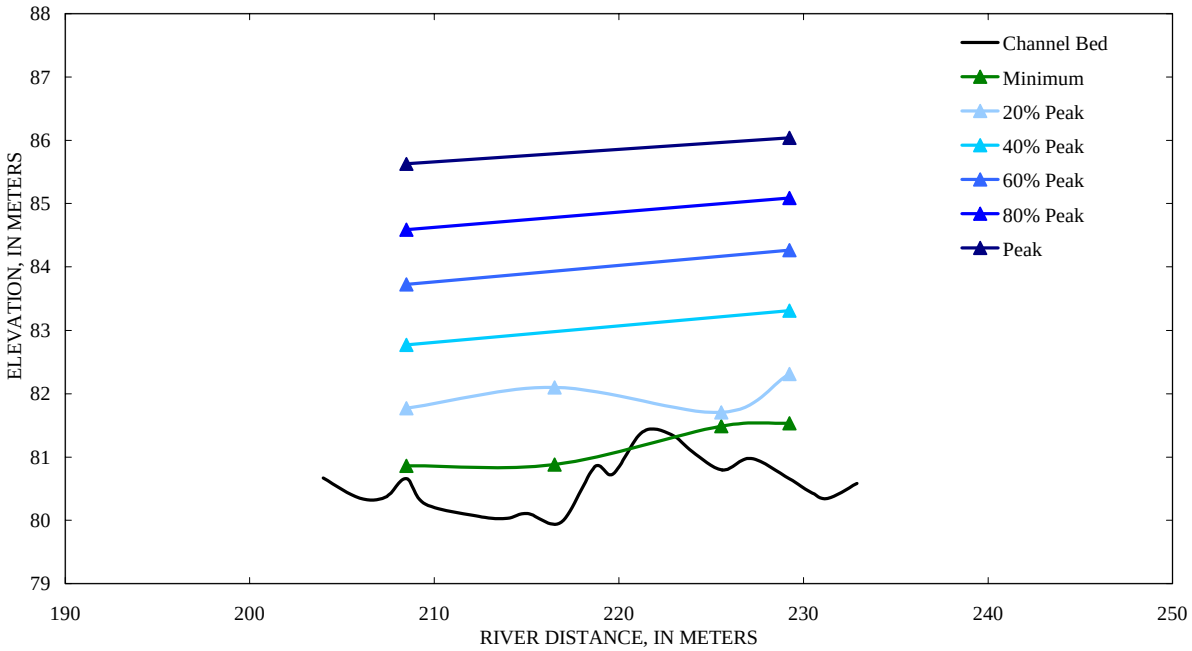

Figure 45 - Water surface profiles for Johnson Creek. Percentages represent the fraction of the upstream stage produced by the peak storm on record.

Figure 46 - Photograph of Bear Creek knickpoint taken 03/05/99 (by M. Griffith/ R. Neely). Note the active knickpoint in the foreground but also the dark ledge towards the center of the image. Since this time, the knickpoint in the foreground has washed through, and the upstream ledge is now actively migrating. This change was associated with a switch from the Naheola formation to the Porters Creek Clay Formation.

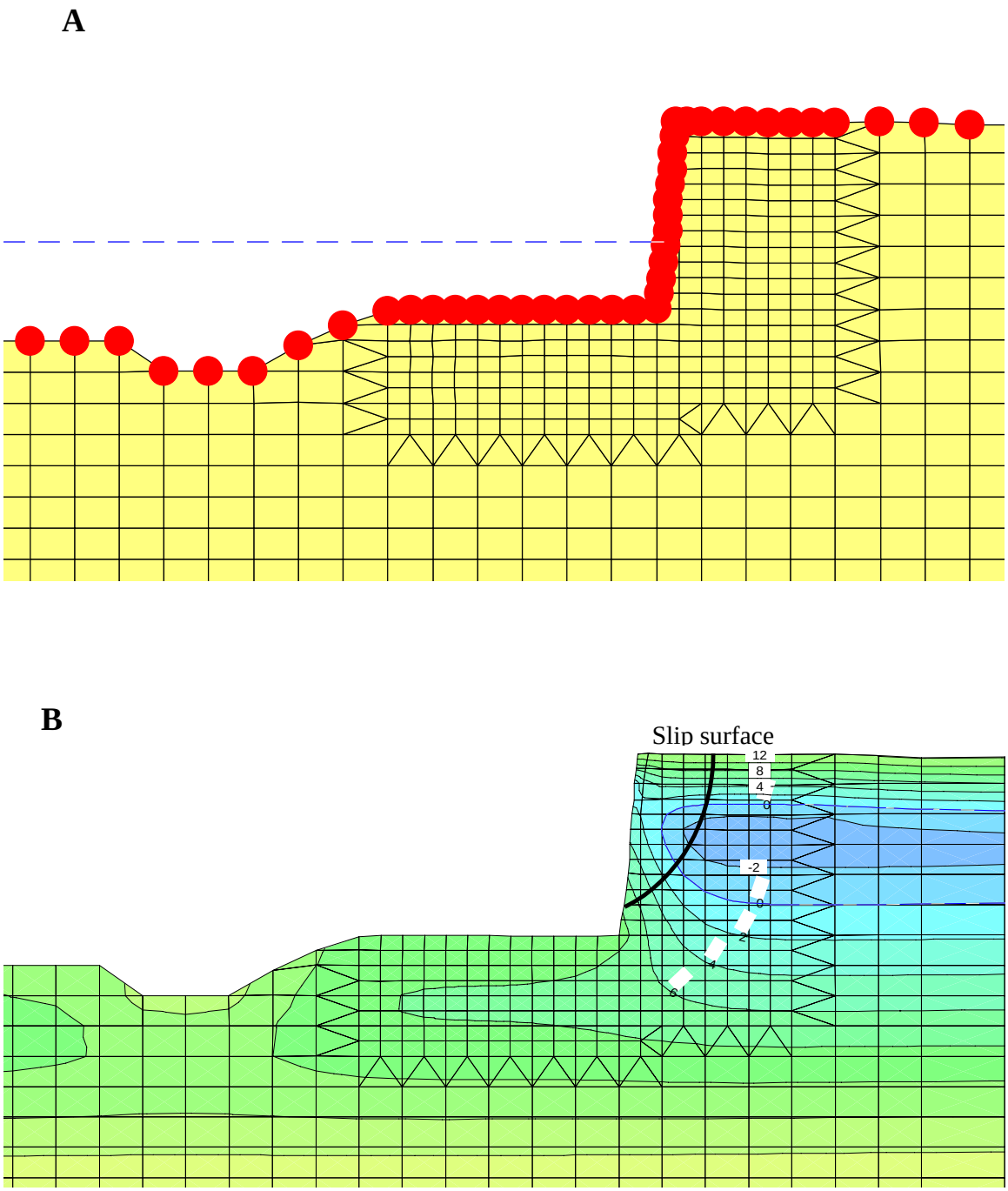

Figure 47 A - Typical finite-element modeling mesh for Big Creek and
B - Typical pore-water pressure output with predicted failure surface for Big Creek.

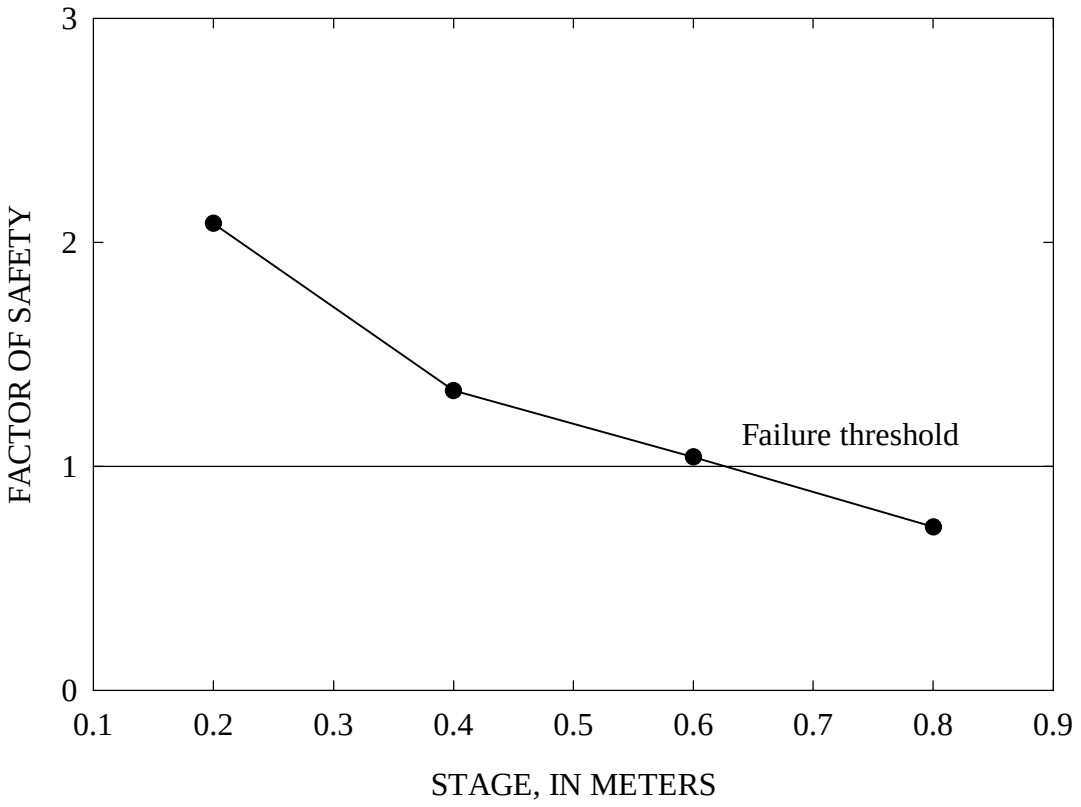

Figure 48 - Sensitivity analysis of the effect of stage height on factor of safety.

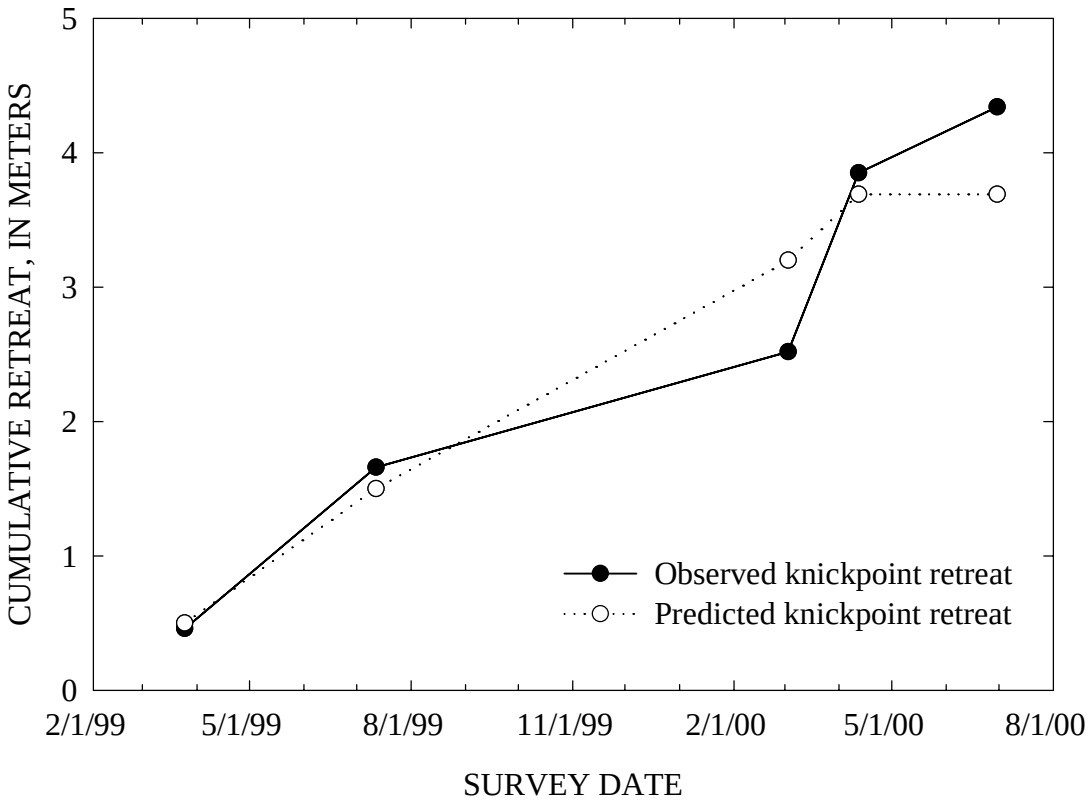

Figure 49 - Observed and predicted failures of knickpoint face on Big Creek.

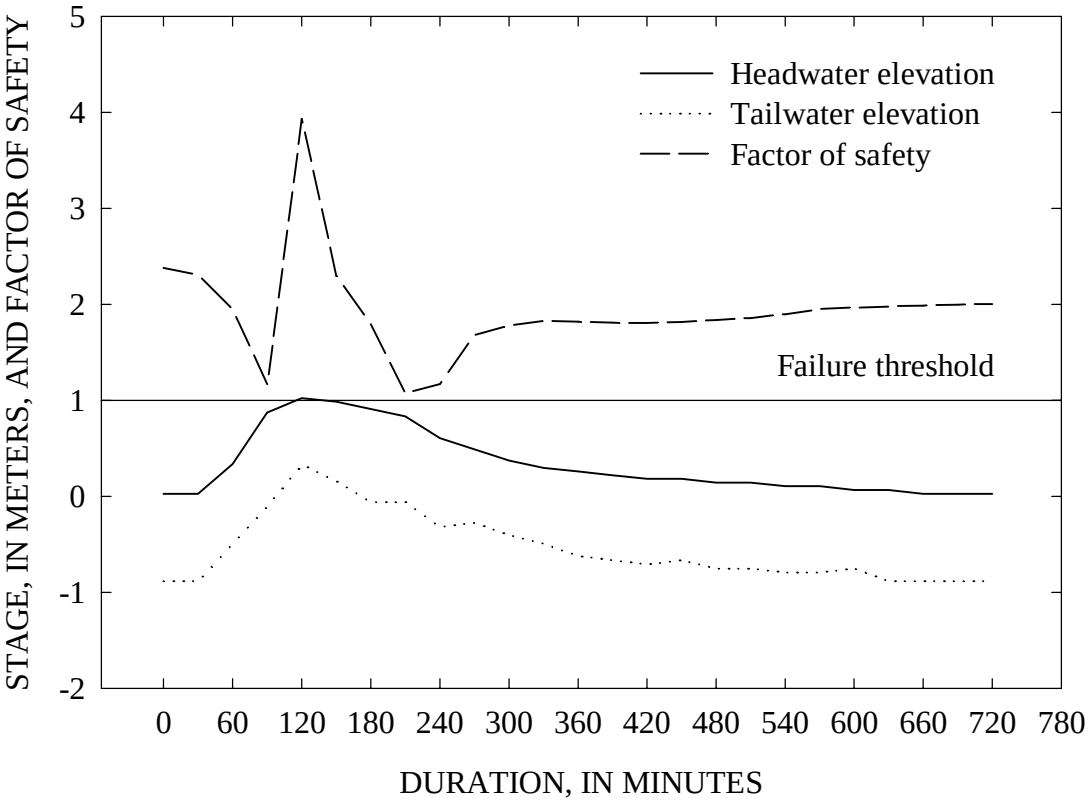

Figure 50 - Example factor of safety relation over the course of a modeled storm event on Big Creek.

TABLES

Table 1 - Numbered list of study sites corresponding to the site numbers shown on Figure 1.

Site	Creek Name	Station	Quad
1	Topashaw Trib 1	2+240	Atlanta
2	Bear	8+020	Atlanta
3	Cane	0+700	Atlanta
4	Bear	6+200	Atlanta
5	Bear	6+800	Atlanta
6	Bear	8+800	Atlanta
7	Bear	12+150	Atlanta
8	Bear Trib 2	0+640	Atlanta
9	Bear Trib 2	0+260	Atlanta
10	Bear Trib 2	1+000	Atlanta
11	Topashaw	14+000	Atlanta
12	Buck	2+740	Atlanta
13	Buck	3+000	Hohenlinden
14	Buck	3+820	Hohenlinden
15	Buck	4+200	Hohenlinden
16	Buck	5+800	Hohenlinden
17	Buck	10+720	Hohenlinden
18	Buck	11+580	Hohenlinden
19	Buck	12+460	Hohenlinden
20	Buck	12+980	Hohenlinden
21	Little Topashaw Trib 1	2+580	Hohenlinden
22	Little Topashaw Trib 1	2+260	Hohenlinden
23	Little Topashaw Trib 1	1+640	Hohenlinden
24	Little Topashaw	5+880	Hohenlinden
25	Little Topashaw	3+360	Hohenlinden
26	Big	9+600	Skuna
27	Little Topashaw	6+620	Hohenlinden
28	Little Topashaw	0+580	Hohenlinden
29	Dry	2+100	Hohenlinden
30	Dry	2+800	Hohenlinden
31	Dry	3+600	Hohenlinden
32	Dry	4+160	Hohenlinden
33	Dry	4+400	Hohenlinden
34	Dry	4+860	Hohenlinden
35	Little Topashaw Trib 1	0+160	Hohenlinden
36	Duncan	5+750	Bruce
37	Huffman	5+600	Bruce
38	Splunge	3+050	Bruce
39	Splunge	2+450	Calhoun
40	Bear	10+900	Atlanta
41	Little Topashaw	9+380	Hohenlinden
42	Little Topashaw	11+180	Hohenlinden
43	Little Topashaw	11+720	Hohenlinden

Table 1 (cont.) - Numbered list of study sites corresponding to the site numbers shown on Figure 1.

44	Topashaw	21+420	Hohenlinden
45	North Topashaw	1+520	Hohenlinden
46	North Topashaw	2+180	Hohenlinden
47	Meridian Trib 1	2+000	Vardaman
48	Meridian Trib 1	1+500	Vardaman
49	Meridian Trib 1	1+280	Vardaman
50	Meridian Trib 1	0+720	Vardaman
51	Meridian	11+740	Vardaman
52	Meridian	11+160	Vardaman
53	Meridian	8+380	Vardaman
54	Meridian	7+400	Vardaman
55	Hurricane	3+540	Vardaman
56	Walnut Trib 1	0+760	Vardaman
57	Walnut	5+060	Vardaman
58	Walnut	3+490	Vardaman
59	Walnut	2+900	Vardaman
60	Walnut	2+220	Vardaman
61	Topashaw	28+900	Mantee
63	Twin	0+200	Bruce
64	Huffman	5+600	Bruce
65	Huffman	6+200	Bruce
66	Huffman Trib 1	1+800	Bruce
67	Huffman	1+820	Bruce
68	Hurricane	5+620	Bruce
70	Hurricane	7+760	Bruce
74	Huffman	7+040	Bruce
75	Huffman	3+780	Bruce
77	Duncan	5+260	Bruce
80	Miles	3+320	Calhoun
100	Cane	11+615	Vardaman
101	Johnson	0+960	Atlanta
102	Topashaw	11+670	Calhoun
103	Topashaw	26+100	Mantee
104	Mud	2+150	Vardaman
105	Yalobusha	28+800	Atlanta
106	Johnson	0+150	Atlanta
107	Bear	8+500	Atlanta
108	Buck	1+310	Atlanta
109	Yalobusha	32+900	Woodland
110	Yalobusha	25+700	Atlanta
200	Topashaw	23+600	Hohenlinden
201	Cane	1+910	Atlanta
202	Big	6+700	Skuna
203	Bear	5+400	Atlanta

Table 2 - Number of "general" study sites sorted by stream where erodibility measurements were made.

Creek Name	Total Sites	Sites Tested	# Jet Tests	Untestable	Estimated	Low Values
Bear	8	8	16	0	0	0
Bear Trib 2	3	3	8	0	0	3
Big	2	2	7	0	0	0
Buck	10	7	19	3	0	1
Cane	3	2	4	1	0	0
Dry	6	3	10	1	2	3
Duncan	2	1	2	1	0	0
Huffman	6	5	10	0	1	3
Huffman Trib 1	1	1	2	0	0	1
Hurricane	3	3	6	0	0	2
Johnson	2	2	5	0	0	0
Little Topashaw	7	5	10	2	0	2
Little Topashaw Trib 1	4	4	7	0	0	3
Meridian	4	4	8	0	0	0
Meridian Trib 1	4	4	8	0	0	0
Miles	1	1	2	0	0	0
Mud	1	1	4	0	0	0
North Topashaw	2	1	2	1	0	0
Splunge	2	2	4	0	0	1
Topashaw	6	6	18	0	0	0
Topashaw Trib 1	1	1	4	0	0	0
Twin	1	1	4	0	0	1
Walnut	5	5	8	0	0	2
Walnut Trib 1	1	0	0	1	0	0
Yalobusha	3	3	8	0	0	0
Totals	**88**	**75**	**176**	**10**	**3**	**22**

Table 3 - Summary of all jet-test results.

Creek Name	Site/Station	Date	Formation	Test #	Material type	τ_c (Pa)	k (cm^3/N-s)	γ_{amb}	γ_{dry}	w (%)
Bear	08+020, 00-002	3/22/00	PC	1	Wet	135	0.016	16.2	11.9	36.1
Bear	08+020, 00-002	3/22/00	PC	2	Wet	223	0.003	16.1	12.4	29.3
Bear	06+200, 00-004	3/23/00	PC	1	Wet	28.7	0.004	15.6	11.8	31.9
Bear	06+200, 00-004	3/23/00	PC	2	Wet	360	0.001	15.4	11.8	30.6
Bear	06+800, 00-005	3/27/00	PC	1	Wet	278	0.005	15.4	10.9	42.2
Bear	06+800, 00-005	3/27/00	PC	2	Wet	187	0.039	15.4	11.3	36.6
Bear	08+800, 00-006	3/28/00	N	1	Wet	4.56	0.083	17.0	13.5	25.8
Bear	08+800, 00-006	3/28/00	N	2	Wet	0.705	0.139	18.0	14.1	27.7
Bear	08+800, 00-006	3/28/00	N	3	Dry	2.06	0.040	18.1	14.4	
Bear	12+150, 00-007	6/20/00	PC	1	Wet	171	0.016	-	-	-
Bear	12+150, 00-007	6/20/00	PC	2	Wet	228	0.007	15.6	11.0	42.1
Bear	10+900, 00-040	6/28/00	N	1	Dry	1.18	0.028	18.1	14.8	22.16
Bear	10+900, 00-040	6/28/00	N	2	Wet	134	0.025	16.6	11.9	39.49
Bear	05+400, 98-203, B3	4/23/98	N	1	Cum	260	0.006	17.1	13.5	26.7
Bear	05+400, 98-203, B3	4/23/98	N	2	Wet	-	-	17.0	13.3	27.9
Bear	08+500, 99-107, B3C	9/20/99	N	1	Dry	1.99	0.096	18.5	13.5	36.8
Bear	08+500, 99-107, B3C	9/21/99	N	2	Dry	5.48	0.042	19.6	15.3	28.2
Bear Trib 2	00+640, 00-008	4/7/00	N	1	Wet	7.07	0.221	16.7	13.3	25.2
Bear Trib 2	00+640, 00-008	4/7/00	N	2	Dry	44.9	0.010	16.8	13.2	27.4
Bear Trib 2	00+640, 00-008	4/7/00	N	3	Wet	0.062	0.774	17.8	14.0	27.1
Bear Trib 2	00+640, 00-008	4/7/00	N	4	Dry	0.062	0.184	18.0	14.7	22.6
Bear Trib 2	00+260, 00-009	4/12/00	N	1	Wet	0.21	0.066	18.6	14.9	24.5
Bear Trib 2	00+260, 00-009	4/12/00	N	2	Wet	8.38	0.034	17.3	13.8	25.4
Bear Trib 2	01+000, 00-010	4/17/00	N	1	Dry	0.553	0.057	17.5	14.1	24.3
Bear Trib 2	01+000, 00-010	4/17/00	N	2	Dry	0.062	0.072	17.7	14.5	21.8
Big	08+210, 00-026, Big6	1/12/99	N	1	Wet	8.2	0.549	-	-	-
Big	08+210, 00-026, Big6	1/12/99	N	2	Wet	0.497	1.26	-	-	-
Big	08+210, 00-026, Big6	1/12/99	N	3	Wet	2.57	0.107	-	-	-
Big	08+210, 00-026, Big6	1/12/99	Sh	4	Wet	224	0.030	17.3	14.1	22.8
Big	08+210, 00-026, Big6	1/12/99	Sh	5	Wet	18.5	0.008	17.3	14.2	21.8
Big	06+700, 98-202, 5C d/s	4/20/98	N	1	Wet	49	0.012	17.2	13.7	25.2
Big	06+700, 98-202, 5C d/s	4/20/98	N	1	Wet	133	0.006	-	-	-
Buck	02+740, 00-012	4/18/00	PC	1	Dry	144	0.011	19.0	10.7	77.9
Buck	02+740, 00-012	4/18/00	PC	2	Wet	19.2	0.004	14.4	9.7	47.9
Buck	03+000, 00-013, Bu2	9/21/99	N	2	Wet	3.26	0.050	19.6	15.3	28.2
Buck	03+000, 00-013, Bu2	9/21/99	N	1	Dry	13.4	0.028	20.5	16.3	25.9
Buck	03+820, 00-014	4/21/00	N	1	Dry	0.775	0.223	19.0	15.8	20.1
Buck	03+820, 00-014	4/21/00	N	2	Wet	0.376	0.18	18.7	15.6	19.7
Buck	03+820, 00-014	4/21/00	N	3	Dry	1.26	0.208	-	-	-
Buck	03+820, 00-014	4/21/00	N	4	Wet	0.062	0.866	-	-	-
Buck	04+200, 00-015	5/9/00	N	1	Wet	2.24	0.303	16.9	13.7	23.6
Buck	04+200, 00-015	5/9/00	N	2	Dry	17.5	0.07	16.2	13.5	20.3
Buck	05+800, 00-016	9/18/00	N	1	Wet	22.7	0.532	15.5	12.7	22.5
Buck	05+800, 00-016	9/18/00	N	2	Dry	1.6	0.092	16.5	13.7	21.1
Buck	10+720, 00-017	9/19/00	PC	1	Wet	33.0	0.009	13.7	9.8	39.2
Buck	10+720, 00-017	9/19/00	PC	2	Wet	10.9	0.007	14.0	10.4	34.4
Buck	11+580, 00-018	4/25/00	Dep	-	-	-	-	-	-	-
Buck	12+460, 00-019,	5/11/00	Dep	-	-	-	-	-	-	-
Buck	12+980, 00-020,	5/11/00	Dep	-	-	-	-	-	-	-
Buck	01+310, 99-108, Bu1	4/23/98	PC	1	Wet	111	0.011	16.9	12.8	32.2
Buck	01+310, 99-108, Bu1	1/13/99	PC	1	Wet	249	0.007	16.2	12.7	27.6
Buck	01+310, 99-108, Bu1	4/23/98	PC	2	Wet	-	-	16.5	12.5	31.8
Buck	01+310, 99-108, Bu1	1/13/99	PC	2	Wet	336	0.004	16.1	12.5	28.3
Buck	01+310, 99-108, Bu1	1/13/99	conglomerate	3	Wet	275	0.009	-	-	-
Buck	01+310, 99-108, Bu1	1/13/99	conglomerate	4	Wet	132	0.147	-	-	-
Cane	00+700, 00-003	2/10/00	Dep	-	-	-	-	-	-	-
Cane	01+910, 98-201, C-0	4/21/98	PC	1	Cum	95	0.011	17.0	13.1	29.9
Cane	01+910, 98-201, C-0	4/21/98	PC	2	-	73	0.009	17.3	13.8	32.5
Cane	11+615, 99-100, C4	1/11/99	PC	1	Wet	362	0.035	18.1	15.4	17.9
Cane	11+615, 99-100, C4	1/11/99	PC	2	Wet	234	0.014	18.1	15.2	18.6
Cane	11+615, 99-100, C4	1/11/99	PC	3	Wet	-	-	18.0	15.3	18.1
Dry	02+100, 00-029	5/25/00	N	1	Dry	0.062	1.014	15.9	12.1	31.8
Dry	02+100, 00-029	5/25/00	N	2	Wet	0.062	0.037	15.8	12.8	23.7
Dry	02+800, 00-030	6/7/00	N	1	Wet	3.76	0.092	16.2	12.3	32.1
Dry	02+800, 00-030	6/7/00	N	2	Dry	0.062	2.064	16.3	12.6	29.6
Dry	02+800, 00-030	6/7/00	N	3	Wet	0.124	0.234	-	-	-
Dry	02+800, 00-030	6/7/00	N	4	Dry	0.062	0.654	-	-	-
Dry	03+600, 00-031	5/23/00	N	-	-	* 2.53	* 0.091	-	-	-
Dry	04+160, 00-032	5/23/00	Concrete	-	-	-	-	-	-	-
Dry	04+400, 00-033	5/23/00	N	-	-	* 2.53	* 0.091	-	-	-
Dry	04+860, 00-034	6/8/00	N	1	Wet	0.086	0.162	17.0	13.6	24.6
Dry	04+860, 00-034	6/8/00	N	2	Dry	13.2	0.059	18.2	15.5	17.9
Dry	04+860, 00-034	6/8/00	N	3	Wet	0.126	0.150	-	-	-
Dry	04+860, 00-034	6/8/00	N	4	Dry	6.72	0.060	-	-	-
Duncan	05+750, 00-036	6/15/00	Dep	-	-	-	-	-	-	-
Duncan	05+260, 01-077	4/10/01	N	1	Dry	34.9	0.025	17.1	15	13.9
Duncan	05+260, 01-077	4/10/01	N	2	Wet	0.3	0.021	-	-	-
Huffman	04+700, 00-037	6/15/00	Dep	-	-	* 181	* 0.006	-	-	-
Huffman	05+600, 01-064	1/9/01	N	1	Dry	21.3	0.072	16.1	12.8	26.3

Huffman	05+600, 01-064	1/9/01	N	2	Wet	2.3	0.061	16.3	12.7	27.7
Huffman	02+600, 01-065	1/10/01	N	1	Dry	26.6	0.112	16.5	13.1	26.1
Huffman	02+600, 01-065	1/10/01	N	2	Wet	0.1	0.230	16.6	12.2	35.5
Huffman	01+820, 01-067	4/9/01	N	1	Dry	0.062	0.230	19.6	17.4	12.6
Huffman	01+820, 01-067	4/9/01	N	2	Wet	0.062	0.227	19.7	16.7	18.1
Huffman	07+040, 01-074	4/26/01	N	1	Dry	0.062	0.091	19.3	16.4	17.7
Huffman	07+040, 01-074	4/26/01	N	2	Dry	0.9	0.027	19.3	16.2	19.1
Huffman	03+780, 01-075	8/27/01	N	1	Wet	17.1	0.011	16.9	13.7	23.7
Huffman	03+780, 01-075	8/27/01	N	3	Dry	41.1	0.025	17.0	14.0	21.7
Huffman Trib 1	01+800, 01-066	1/16/01	N	1	Wet	0.062	0.136	16.1	12.0	33.5
Huffman Trib 1	01+800, 01-066	1/16/01	N	2	Dry	5.9	0.065	15.9	11.8	34.7
Hurricane	03+540, 00-055	8/14/00	N	1	Dry	6.65	0.079	24.7	14.4	18.0
Hurricane	03+540, 00-055	8/14/00	N	2	Dry	15.7	0.006	16.9	13.1	28.8
Hurricane	05+620, 01-068	1/24/01	PC	1	Dry	0.7	0.018	15.8	11.3	39.7
Hurricane	05+620, 01-068	1/24/01	PC	2	Wet	9.6	0.016	14.2	9.8	45.0
Hurricane	07+760, 01-070	1/25/01	N	1	Dry	0.062	0.411	13.9	13.9	0.0
Hurricane	07+760, 01-070	1/25/01	N	2	Wet	0.062	0.023	13.6	13.6	0.0
Johnson	00+150, 99-106, JM-A	5/17/99	N	1	Dry	0.378	0.095	17.9	15.1	18.7
Johnson	00+960, 99-101, JM-C, lower unit	9/22/99	N	1	Dry	1.55	0.016	-	-	-
Johnson	00+960, 99-101, JM-C, lower unit	9/22/99	N	2	Dry	69	0.006	-	-	-
Johnson	00+960, 99-101, JM-C, lower unit	9/22/99	N	1	Dry	0.387	0.164	-	-	-
Johnson	00+960, 99-101, JM-C, lower unit	9/22/99	N	2	Dry	1.31	0.120	-	-	-
Little Topashaw	05+880, 00-024	5/23/00	PC	1	Dry	31.1	0.004	15.9	11.5	37.8
Little Topashaw	05+880, 00-024	5/23/00	PC	2	Wet	2.25	0.022	15.7	11.4	37.8
Little Topashaw	03+360, 00-025, LT1	8/11/99	N	1	Wet	44.9	0.019	17.16	13.17	30.30
Little Topashaw	03+360, 00-025, LT1	8/11/99	N	2	Dry	63.6	0.012	16.46	12.70	29.60
Little Topashaw	03+360, 00-025, LT1	8/11/99	N	1	Dry	29.9	0.012	-	-	-
Little Topashaw	06+620, 00-027	5/23/00	Dep	-	-	-	-	-	-	-
Little Topashaw	00+580, 00-028	5/23/00	Dep	-	-	-	-	-	-	-
Little Topashaw	09+380, 00-041	7/12/00	PC	1	Dry	141	0.001	14.6	13.7	6.3
Little Topashaw	09+380, 00-041	7/12/00	PC	2	Wet	141	0.048	13.7	9.0	53.1
Little Topashaw	11+180, 00-042	7/7/00	N	1	Wet	11.38	0.053	18.3	15.1	21.3
Little Topashaw	11+180, 00-042	7/7/00	N	2	Dry	0.062	0.438	18.6	14.9	24.6
Little Topashaw	11+720, 00-043	7/10/00	N	1	Wet	0.062	0.786	18.4	14.8	24.7
Little Topashaw Trib 1	02+580, 00-021	5/16/00	PC	1	Dry	23.5	0.007	15.3	10.9	39.9
Little Topashaw Trib 1	02+580, 00-021	5/16/00	PC	2	Wet	Jet Failure	-	-	-	-
Little Topashaw Trib 1	02+260, 00-022	5/17/00	N	1	Dry	0.142	0.078	17.4	14.2	23.6
Little Topashaw Trib 1	02+260, 00-022	5/17/00	N	2	Wet	0.062	0.202	15.5	12.0	28.8
Little Topashaw Trib 1	01+640, 00-023	5/18/00	N	1	Dry	0.062	0.385	16.7	13.4	24.9
Little Topashaw Trib 1	01+640, 00-023	5/18/00	N	2	Wet	0.062	0.135	-	-	-
Little Topashaw Trib 1	00+160, 00-035	6/12/00	N	1	Wet	1.53	0.079	18.2	14.9	22.1
Little Topashaw Trib 1	00+160, 00-035	6/12/00	N	2	Dry	0.589	0.19	18.0	15.5	15.6
Meridian	11+740, 00-051	8/2/00	PC	1	Dry	14.7	0.007	14.9	11.2	33.1
Meridian	11+740, 00-051	8/2/00	PC	2	Wet	201	0.003	17.3	12.7	35.5
Meridian	11+160, 00-052	8/3/00	PC	1	Dry	3.84	0.009	16.0	12.0	33.4
Meridian	11+160, 00-052	8/3/00	PC	2	Wet	109	0.003	15.2	11.3	35.4
Meridian	08+380, 00-053	8/7/00	PC	1	Dry	407	0.003	15.9	11.7	36.1
Meridian	08+380, 00-053	8/7/00	PC	2	Wet	275	0.001	14.1	10.6	53.6
Meridian	07+400, 00-054	8/8/00	PC	1	Dry	181	0.006	16.9	13.1	29.0
Meridian	07+400, 00-054	8/8/00	PC	2	Wet	184	0.002	16.4	12.6	30.0
Meridian Trib 1	02+000, 00-047	7/25/00	N	1	Wet	296	0.002	18.3	16.0	14.0
Meridian Trib 1	02+000, 00-047	7/25/00	N	2	Dry	19.7	0.043	21.0	18.5	13.3
Meridian Trib 1	01+500, 00-048	7/26/00	N	1	Dry	114	0.007	16.9	12.7	33.5
Meridian Trib 1	01+500, 00-048	7/26/00	N	2	Wet	232	0.005	17.2	13.0	32.3
Meridian Trib 1	01+280, 00-049	7/27/00	PC	1	Wet	462	0.001	16.2	11.7	38.6
Meridian Trib 1	01+280, 00-049	7/27/00	PC	2	Dry	77.4	0.003	16.7	12.2	37.6
Meridian Trib 1	00+720, 00-050	8/1/00	PC	1	Wet	139	0.005	16.2	12.0	34.3
Meridian Trib 1	00+720, 00-050	8/1/00	PC	2	Dry	251	0.003	14.5	10.7	36.6
Miles	03+320, 01-080	5/2/01	N	1	Dry	0.741	0.214	20.7	17.9	16.1
Miles	03+320, 01-080	5/2/01	N	2	Wet	0.069	0.179	17.0	14.3	18.6
Mud	02+150, 99-104, Mu1-B	5/18/99	N	1	Wet	84.5	0.006	18.9	15.0	25.5
Mud	02+150, 99-104, Mu1-B	5/18/99	N	2	Wet	20.5	0.073	18.9	15.0	25.5
Mud	02+150, 99-104, Mu1-B	5/18/99	N	3	Dry	93.5	0.064	16.7	13.4	24.4
Mud	02+150, 99-104, Mu1-B	5/18/99	N	4	Dry	181	0.015	16.7	13.4	24.4
North Topashaw	01+520, 00-045	7/18/00	PC	1	Wet	210	0.006	15.2	11.2	36.1
North Topashaw	01+520, 00-045	7/18/00	PC	2	Dry	84.3	0.008	16.6	12.4	33.8
North Topashaw	02+180, 00-046	No H2O	PC		-	-	-	-	-	-
Splunge	03+050, 00-038	6/26/00	N	1	Dry	0.062	0.166	17.8	14.8	20.3
Splunge	03+050, 00-038	6/26/00	N	2	Dry	14.3	0.171	19.73	16.16	22.1
Splunge	02+450, 00-039	6/27/00	PC	1	Dry	0.065	0.017	16.1	12.0	34.2
Splunge	02+450, 00-039	6/27/00	PC	2	Wet	0.281	0.017	15.9	11.5	37.5
Topashaw	14+000, 00-011, T4	5/20/99	PC	1	Dry	265	0.029	16.2	11.8	37.0
Topashaw	14+000, 00-011, T4	5/20/99	PC	2	Wet	183	0.005	16.5	12.1	36.4
Topashaw	14+000, 00-011, T4	5/20/99	PC	3	Dry	359	0.011	-	-	-
Topashaw	14+000, 00-011, T4	5/20/99	PC	4	Wet	250	0.006	-	-	-
Topashaw	21+420, 00-044	7/13/00	PC	1	Dry	4.14	0.007	16.6	12.4	33.8
Topashaw	21+420, 00-044	7/13/00	PC	2	Wet	512	0.002	16.3	12.4	31.3
Topashaw	28+560, 00-061, T9	12/16/99	PC	1	Wet	323	0.002	14.6	10.8	38.6
Topashaw	28+560, 00-061, T9	12/16/99	PC	2	Wet	279	0.002	15.6	11.7	33.4
Topashaw	11+670, 99-102, T2-C1	7/14/99	PC	1	Wet	220	0.004	-	-	-
Topashaw	11+670, 99-102, T2-C1	8/10/99	PC	1	Wet	297	0.003	-	-	-
Topashaw	11+670, 99-102, T2-C1	8/10/99	PC	2	Wet	12.7	0.006	-	-	-
Topashaw	11+670, 99-102, T2-C1	8/10/99	PC	3	Dry	245	0.005	-	-	-
Topashaw	11+670, 99-102, T2-C1	8/10/99	PC	4	Dry	315	0.006	-	-	-

Topashaw	23+600, 98-200, T6	4/22/98	PC	1	Wet	88	0.002	16.6	13.1	27.9
Topashaw	23+600, 98-200, T6	4/22/98	PC	2	Wet	331	0.001	16.8	13.1	28.3
Topashaw	23+600, 98-200, T6	4/22/98	PC	2	Wet	393	0.003	16.8	13.1	28.3
Topashaw	26+100, 99-103, T7	9/23/99	PC	1	Dry	400	0.007	-	-	-
Topashaw	26+100, 99-103, T7	9/23/99	PC	2	Wet	281	0.002	-	-	-
Topashaw Trib 1	02+240, 00-001, TT1-1, d/s	1/14/99	PC	3	Dry	52.4	0.129	-	-	-
Topashaw Trib 1	02+240, 00-001, TT1-1, d/s	1/14/99	PC	4	Dry	52.1	0.070	-	-	-
Topashaw Trib 1	02+240, 00-001, TT1-1, u/s	1/14/99	PC	1	Wet	394	0.004	15.3	12.3	24.5
Topashaw Trib 1	02+240, 00-001, TT1-1, u/s	1/14/99	PC	2	Wet	181	0.005	15.2	12.2	24.3
Twin	00+200, 01-063	1/8/01	N	1	Wet	0.471	0.915	17.9	15.0	19.2
Twin	00+200, 01-063	1/8/01	N	2	Wet	0.18	0.269	18.5	15.6	18.4
Twin	00+200, 01-063	1/8/01	N	3	Dry	0.062	0.082	-	-	-
Twin	00+200, 01-063	1/8/01	N	4	Dry	0.188	0.087	-	-	-
Walnut	05+060, 00-057	8/16/00	N	2	Dry	5.56	0.136	17.1	14.2	20.7
Walnut	05+060, 00-057	8/16/00	N	1	Dry	0.062	0.523	18.2	15.5	16.9
Walnut	03+490, 00-058	9/6/00	N	1	Dry	4.37	0.149	13.0	11.0	18.1
Walnut	03+490, 00-058	9/6/00	N	2	Dry	0.065	0.088	17.5	15.3	14.4
Walnut	02+900, 00-059	9/5/00	N	1	Dry	124	0.018	16.1	13.0	23.9
Walnut	02+900, 00-059	9/5/00	N	2	Wet	0.074	0.493	16.8	13.5	24.4
Walnut	02+220, 00-060	9/7/00	N	1	Wet	62.2	0.032	16.0	13.2	21.4
Walnut	02+220, 00-060	9/7/00	N	2	Dry	0.062	0.251	15.3	14.0	9.2
Walnut Trib 1	00+760, 00-056	7/31/00	Dep	-	-	-	-	-	-	-
Yalobusha	25+700, 99-110, Y2-A	5/19/99	PC	1	Dry	215	0.003	16.5	11.9	38.4
Yalobusha	25+700, 99-110, Y2-A	5/19/99	PC	1	Wet	133	0.006	16.0	11.2	42.7
Yalobusha	25+700, 99-110, Y2-A	5/19/99	PC	2	Wet	376	0.007	16.0	11.2	42.7
Yalobusha	28+800, 99-105, Y3-E	5/17/99	N	1	Wet	0.749	0.118	17.6	14.3	23.0
Yalobusha	28+800, 99-105, Y3-E	5/17/99	N	2	Wet	0.467	0.088	17.6	14.3	23.0
Yalobusha	28+800, 99-105, Y3-E	5/17/99	N	3	Dry	0.378	0.095	-	-	-
Yalobusha	32+900, 99-109, Y3-F, D/S Pyland	9/23/99	N	1	Dry	15.1	0.150	-	-	-
Yalobusha	32+900, 99-109, Y3-F, D/S Pyland	9/23/99	N	2	Dry	2.48	0.050	-	-	-

0.062 = Exceptionally low test values assigned a constant value.
PC = Porters Creek clay formation.
N = Naheola formation.
Sh = shale.
SC = sandy clay
BD-SP = beaver dam, sand.
Dep = depositional.
* = Assigned value based on an average for the material type.

Table 4 - Jet-test results averaged for each site.

Creek Name	Site/Station	Formation	τ_c (Pa)	k (cm^3/N-s)
Bear	08+020, 00-002	PC	179	0.010
Bear	06+200, 00-004	PC	194	0.003
Bear	06+800, 00-005	PC	233	0.022
Bear	08+800, 00-006	N	2.44	0.087
Bear	12+150, 00-007	PC	199	0.012
Bear	05+400, 98-203, B3	N	260	0.006
Bear	08+500, 99-107, B3C	N	3.74	0.069
Bear	10+900, 00-040	N	67.6	0.027
Bear Trib 2	00+640, 00-008	N	13.0	0.300
Bear Trib 2	00+260, 00-009	N	4.30	0.050
Bear Trib 2	01+000, 00-010	N	0.308	0.065
Big	09+600, 00-026, Big6	N	3.76	0.639
Big	09+600, 00-026, Big6	Sh	121	0.019
Big	06+700, 98-202, 5C d/s	N	91.0	0.009
Buck	02+740, 00-012	PC	227	0.014
Buck	03+000, 00-013, Bu2	N	8.33	0.039
Buck	03+820, 00-014	N	0.618	0.369
Buck	04+200, 00-015	N	9.87	0.187
Buck	05+800, 00-016	N	12.2	0.312
Buck	10+720, 00-017	PC	22.0	0.008
Buck	11+580, 00-018	SC	-	-
Buck	12+460, 00-019	BD-SP	-	-
Buck	12+980, 00-020	BD-SP	-	-
Buck	01+310, 99-108, Bu1	PC	221	0.036
Cane	00+700, 00-003	Dep	-	-
Cane	01+910, 98-201, C-0	PC	84.0	0.010
Cane	11+615, 99-100, C4	PC	298	0.025
Dry	02+100, 00-029	N	0.062	0.526
Dry	02+800, 00-030	N	1.00	0.761
Dry	03+600, 00-031	N	1.53	0.088
Dry	04+160, 00-032	Concrete	-	-
Dry	04+400, 00-033	N	1.53	0.088
Dry	04+860, 00-034	N	5.03	0.108
Duncan	05+750, 00-036	SC	-	-
Duncan	05+260, 01-077	N	17.6	0.023
Huffman	04+700, 00-037	PC	183	0.006
Huffman	05+600, 01-064	N	11.8	0.067
Huffman	02+600, 01-065	N	13.3	0.171
Huffman	01+820, 01-067	N	0.062	0.229
Huffman	07+040, 01-074	N	0.486	0.059
Huffman	03+780, 01-075	N	29.1	0.018
Huffman Trib 1	01+800, 01-066	N	3.00	0.101
Hurricane	03+540, 00-055	N	11.2	0.043
Hurricane	05+620, 01-068	PC	5.1	0.017
Hurricane	07+760, 01-070	N	0.062	0.217
Johnson	00+150, 99-106, JM-A	N	0.378	0.095
Johnson	00+960, 99-101, JM-C	N	1.08	0.100

Little Topashaw	05+880, 00-024	PC	16.7	0.013
Little Topashaw	03+360, 00-025, LT1	N	46.1	0.014
Little Topashaw	06+620, 00-027	BD-SP	-	-
Little Topashaw	00+580, 00-028	Dep	-	-
Little Topashaw	09+380, 00-041	PC	141	0.025
Little Topashaw	11+180, 00-042	N	11.4	0.246
Little Topashaw	11+720, 00-043	N	0.062	0.786
Little Topashaw Trib 1	02+580, 00-021	PC	23.5	0.007
Little Topashaw Trib 1	02+260, 00-022	N	0.102	0.140
Little Topashaw Trib 1	01+640, 00-023	N	0.062	0.260
Little Topashaw Trib 1	00+160, 00-035	N	1.06	0.135
Meridian	11+740, 00-051	PC	130	0.009
Meridian	11+160, 00-052	PC	140	0.012
Meridian	08+380, 00-053	PC	380	0.003
Meridian	07+400, 00-054	PC	183	0.004
Meridian Trib 1	02+000, 00-047	N	158	0.023
Meridian Trib 1	01+500, 00-048	N	173	0.006
Meridian Trib 1	01+280, 00-049	PC	334	0.004
Meridian Trib 1	00+720, 00-050	PC	195	0.004
Miles	03+320, 01-080	N	0.405	0.197
Mud	02+150, 99-104, Mu1-B	N	94.9	0.040
North Topashaw	01+520, 00-045	PC	147	0.007
Splunge	03+050, 00-038	N	7.18	0.169
Splunge	02+450, 00-039	PC	0.173	0.017
Topashaw	14+000, 00-011, T4	PC	264	0.013
Topashaw	21+420, 00-044	PC	256	0.005
Topashaw	28+900, 00-061, T9	PC	301	0.002
Topashaw	11+670, 99-102, T2-C1	PC	281	0.005
Topashaw	23+600, 98-200, T6	PC	271	0.002
Topashaw	26+100, 99-103, T7	PC	341	0.005
Topashaw Trib 1	02+240, 00-001, TT1-1, u/s	PC	170	0.052
Twin	00+200, 01-063	N	0.210	0.193
Walnut	05+060, 00-057	N	2.81	0.330
Walnut	03+490, 00-058	N	4.37	0.149
Walnut	02+900, 00-059	N	63.3	0.169
Walnut	02+220, 00-060	N	31.1	0.142
Walnut Trib 1	00+760, 00-056	BD-SP	-	-
Yalobusha	25+700, 99-110, Y3-A at Bull	PC	241	0.005
Yalobusha	28+800, 99-105, Y3-E, at Johnson	N	0.531	0.100
Yalobusha	32+900, 99-109, Y3-F, D/S Pyland	N	24.8	0.122

PC = Porters Creek clay formation.
N = Naheola formation.
Sh = shale.
SC = sandy clay
BD-SP = beaver dam, sand.
Dep = depositional.

Color Key	τ_c (Pa)	k (cm^3/N-s)
Red	0.062 < 1.99	> 0.199
Yellow	2.00 < 9.99	0.090 < 0.199
Blue	10 < 99.9	0.011 < 0.090
Gray	> 99.9	< 0.011
Green	Predicted value for material	Predicted value for material

Table 5 - Mean and median values of τ_c and k for the Porters Creek Clay and Naheola formations.

Formation	**Statistic**	**Critical shear stress (τ_c), in Pa**		**Erodibility coefficient (k), in cm^3/N-s**	
		All values	Average values	All values	Average values
Naheola	Mean	23.1	25.4	0.191	0.172
	Median	1.53	4.30	0.088	0.108
Porters Creek Clay	Mean	185	189	0.011	0.012
	Median	183	195	0.006	0.009

Table 6 - Average boundary shear stress values for a range of flow depths and bed slopes.

Depth, in m	**Bed slope, in m/m**		
	0.001	0.002	0.004
1	9.81	19.6	39.2
2	19.6	39.2	78.5
4	39.2	78.5	157
8	78.5	157	314

Table 7 - Mean and median values of τ_c and k for the Porters Creek Clay and Naheola formations showing the differences caused by perennially wet and intermittently dry conditions.

Formation	**Statistic**	**Critical shear stress (τ_c), in Pa**	**Erodibility coefficient (k), in cm^3/N-s**	**n**
Naheola-dry	Mean	17.4	0.172	58
	Median	1.58	0.085	58
Naheola-wet	Mean	25.1	0.218	46
	Median	0.727	0.113	46
PC-dry	Mean	149	0.017	22
	Median	113	0.007	22
PC-wet	Mean	208	0.009	43
	Median	210	0.005	43

Table 8 - Calculated potential rates of erosion in mm/s due to hydraulic stresses for all sites and for median values of the Porters Creek Clay and Naheola formations using Equation (5).

Creek Name	Site/Station	Formation	Shear stress, in Pa					
			50	100	150	200	250	300
Bear	05+400, 98-203, B3	N	0.0	0.0	0.0	0.0	0.0	0.0002
Bear	06+200, 00-004	PC	0.0	0.0	0.0	0.0	0.0001	0.0003
Bear	06+800, 00-005	PC	0.0	0.0	0.0	0.0	0.0004	0.0015
Bear	08+020, 00-002	PC	0.0	0.0	0.0	0.0002	0.0007	0.0011
Bear	08+500, 99-107, B3C	N	0.0032	0.0066	0.010	0.014	0.017	0.020
Bear	08+800, 00-006	N	0.0042	0.0085	0.013	0.017	0.022	0.026
Bear	10+900, 00-040	N	0.0	0.0009	0.0022	0.0035	0.0048	0.0062
Bear	12+150, 00-007	PC	0.0	0.0	0.0	0.0	0.0006	0.0012
Bear Trib 2	00+260, 00-009	N	0.0023	0.0048	0.0073	0.0098	0.012	0.015
Bear Trib 2	00+640, 00-008	N	0.011	0.026	0.041	0.056	0.071	0.086
Bear Trib 2	01+000, 00-010	N	0.0032	0.0064	0.0097	0.013	0.016	0.019
Big	06+700, 98-202, 5C d/s	N	0.0	0.0001	0.0005	0.0010	0.0014	0.0019
Big	09+600, 00-026, Big6	N	0.030	0.061	0.093	0.125	0.157	0.189
Big	09+600, 00-026, Big6	Sh	0.0	0.0	0.0006	0.0015	0.0025	0.0034
Buck	01+310, 99-108, Bu1	PC	0.0	0.0	0.0	0.0	0.0010	0.0028
Buck	02+740, 00-012	PC	0.0	0.0	0.0	0.0	0.0003	0.0010
Buck	03+000, 00-013, Bu2	N	0.0016	0.0036	0.0055	0.0075	0.0094	0.011
Buck	03+820, 00-014	N	0.018	0.037	0.055	0.074	0.092	0.110
Buck	04+200, 00-015	N	0.0075	0.017	0.026	0.036	0.045	0.054
Buck	05+800, 00-016	N	0.012	0.027	0.043	0.059	0.074	0.090
Buck	10+720, 00-017	PC	0.0002	0.0006	0.0010	0.0014	0.0018	0.0022
Buck	11+580, 00-018	SC	0.0	0.0	0.0	0.0	0.0	0.0
Buck	12+460, 00-019	BD-SP	0.0	0.0	0.0	0.0	0.0	0.0
Buck	12+980, 00-020	BD-SP	0.0	0.0	0.0	0.0	0.0	0.0
Cane	00+700, 00-003	Dep	0.0	0.0	0.0	0.0	0.0	0.0
Cane	01+910, 98-201, C-0	PC	0.0	0.0002	0.0007	0.0012	0.0017	0.0022
Cane	11+615, 99-100, C4	PC	0.0	0.0	0.0	0.0	0.0	0.0
Dry	02+100, 00-029	N	0.026	0.053	0.079	0.105	0.131	0.158
Dry	02+800, 00-030	N	0.037	0.075	0.113	0.151	0.189	0.228
Dry	03+600, 00-031	N	0.0043	0.0087	0.013	0.017	0.022	0.026
Dry	04+160, 00-032	Concrete	0.0	0.0	0.0	0.0	0.0	0.0
Dry	04+400, 00-033	N	0.0043	0.0087	0.013	0.017	0.022	0.026
Dry	04+860, 00-034	N	0.0049	0.010	0.016	0.021	0.026	0.032
Duncan	05+260, 01-077	N	0.0007	0.0019	0.0030	0.0042	0.0053	0.0065
Duncan	05+750, 00-036	SC	0.0	0.0	0.0	0.0	0.0	0.0
Huffman	01+820, 01-067	N	0.011	0.023	0.034	0.046	0.057	0.069
Huffman	02+600, 01-065	N	0.0063	0.015	0.023	0.032	0.040	0.049
Huffman	03+780, 01-075	N	0.0004	0.0013	0.0022	0.0031	0.0040	0.0049
Huffman	04+700, 00-037	PC	0.0	0.0	0.0	0.0001	0.0004	0.0007
Huffman	05+600, 01-064	N	0.0025	0.0059	0.0092	0.013	0.016	0.019
Huffman	07+040, 01-074	N	0.0029	0.0059	0.0088	0.012	0.015	0.018
Huffman Trib 1	01+800, 01-066	N	0.0047	0.0097	0.015	0.020	0.025	0.030
Hurricane	03+540, 00-055	N	0.0017	0.0038	0.0060	0.0081	0.010	0.012
Hurricane	05+620, 01-068	PC	0.0008	0.0016	0.0025	0.0033	0.0042	0.0050
Hurricane	07+760, 01-070	N	0.011	0.022	0.033	0.043	0.054	0.065
Johnson	00+150, 99-106, JM-A	N	0.0047	0.0095	0.014	0.019	0.024	0.028
Johnson	00+960, 99-101, JM-C	N	0.0049	0.0099	0.015	0.020	0.025	0.030
Little Topashaw	00+580, 00-028	Dep	0.0	0.0	0.0	0.0	0.0	0.0
Little Topashaw	03+360, 00-025, LT1	N	0.0001	0.0008	0.0015	0.0022	0.0029	0.0036
Little Topashaw	05+880, 00-024	PC	0.0004	0.0011	0.0017	0.0024	0.0030	0.0037
Little Topashaw	06+620, 00-027	BD-SP	0.0	0.0	0.0	0.0	0.0	0.0
Little Topashaw	09+380, 00-041	PC	0.0	0.0	0.0002	0.0015	0.0027	0.0040
Little Topashaw	11+180, 00-042	N	0.0095	0.022	0.034	0.046	0.059	0.071
Little Topashaw	11+720, 00-043	N	0.039	0.079	0.118	0.157	0.196	0.236

Little Topashaw Trib 1	00+160, 00-035	N	0.0066	0.013	0.020	0.027	0.034	0.040
Little Topashaw Trib 1	01+640, 00-023	N	0.013	0.026	0.039	0.052	0.065	0.078
Little Topashaw Trib 1	02+260, 00-022	N	0.0070	0.014	0.021	0.028	0.035	0.042
Little Topashaw Trib 1	02+580, 00-021	PC	0.0002	0.0005	0.0009	0.0012	0.0016	0.0019
Meridian	07+400, 00-054	PC	0.0	0.0	0.0	0.0001	0.0003	0.0005
Meridian	08+380, 00-053	PC	0.0	0.0	0.0	0.0	0.0	0.0
Meridian	11+160, 00-052	PC	0.0	0.0	0.0001	0.0007	0.0013	0.0019
Meridian	11+740, 00-051	PC	0.0	0.0	0.0002	0.0006	0.0011	0.0015
Meridian Trib 1	00+720, 00-050	PC	0.0	0.0	0.0	0.0	0.0002	0.0004
Meridian Trib 1	01+280, 00-049	PC	0.0	0.0	0.0	0.0	0.0	0.0
Meridian Trib 1	01+500, 00-048	N	0.0	0.0	0.0	0.0002	0.0005	0.0008
Meridian Trib 1	02+000, 00-047	N	0.0	0.0	0.0	0.0010	0.0021	0.0033
Miles	03+320, 01-080	N	0.0097	0.020	0.029	0.039	0.049	0.059
Mud	02+150, 99-104, Mu1-B	N	0.0	0.0002	0.0022	0.0042	0.0061	0.0081
North Topashaw	01+520, 00-045	PC	0.0	0.0	0.0	0.0004	0.0007	0.0011
Splunge	02+450, 00-039	PC	0.0008	0.0017	0.0025	0.0034	0.0042	0.0051
Splunge	03+050, 00-038	N	0.0072	0.016	0.024	0.033	0.041	0.049
Topashaw	11+670, 99-102, T2-C1	PC	0.0	0.0	0.0	0.0	0.0	0.0001
Topashaw	14+000, 00-011, T4	PC	0.0	0.0	0.0	0.0	0.0	0.0005
Topashaw	21+420, 00-044	PC	0.0	0.0	0.0	0.0	0.0	0.0002
Topashaw	23+600, 98-200, T6	PC	0.0	0.0	0.0	0.0	0.0	0.0001
Topashaw	26+100, 99-103, T7	PC	0.0	0.0	0.0	0.0	0.0	0.0
Topashaw	28+900, 00-061, T9	PC	0.0	0.0	0.0	0.0	0.0	0.0
Topashaw Trib 1	02+240, 00-001, TT1-1, u/s	PC	0.0	0.0	0.0	0.0016	0.0042	0.0068
Twin	00+200, 01-063	N	0.0096	0.019	0.029	0.039	0.048	0.058
Walnut	02+220, 00-060	N	0.0027	0.0098	0.017	0.024	0.031	0.038
Walnut	02+900, 00-059	N	0.0	0.0062	0.015	0.023	0.032	0.040
Walnut	03+490, 00-058	N	0.0068	0.014	0.022	0.029	0.037	0.044
Walnut	05+060, 00-057	N	0.016	0.032	0.048	0.065	0.081	0.098
Walnut Trib 1	00+760, 00-056	BD-SP	0.0	0.0	0.0	0.0	0.0	0.0
Yalobusha	25+700, 99-110, Y3-A at Bull	PC	0.0	0.0	0.0	0.0	0.0	0.0003
Yalobusha	28+800, 99-105, Y3-E, at Johnson	N	0.0049	0.0099	0.015	0.020	0.025	0.030
Yalobusha	32+900, 99-109, Y3-F, D/S Pyland	N	0.0031	0.0092	0.015	0.021	0.027	0.034

PC = Porters Creek clay formation.
N = Naheola formatior
Sh = shale.
SC = sandy clay
BD-SP = beaver dam, sand.
Dep = depositional.

Naheola	**Mean**	**0.0076**	**0.016**	**0.025**	**0.033**	**0.042**	**0.050**
	Median	**0.0047**	**0.010**	**0.015**	**0.021**	**0.026**	**0.032**
Porters Creek	**Mean**	**0.0001**	**0.0002**	**0.0003**	**0.0006**	**0.0010**	**0.0015**
	Median	**0.0**	**0.0**	**0.0**	**0.0**	**0.0004**	**0.0010**

Table 9 - Calculated potential erosion amounts in m for a storm of one-day duration at the specified shear stresses for all sites and for median values of the Porters Creek Clay and Naheola formations using Equation (5).

Creek Name	Site/Station	Formation	Shear stress, in Pa					
			50	100	150	200	250	300
Bear	05+400, 98-203, B3	N	0.00	0.00	0.00	0.00	0.00	0.02
Bear	06+200, 00-004	PC	0.00	0.00	0.00	0.00	0.01	0.02
Bear	06+800, 00-005	PC	0.00	0.00	0.00	0.00	0.03	0.13
Bear	08+020, 00-002	PC	0.00	0.00	0.00	0.02	0.06	0.10
Bear	08+500, 99-107, B3C	N	0.28	0.57	0.87	1.17	1.47	1.77
Bear	08+800, 00-006	N	0.36	0.74	1.11	1.49	1.87	2.25
Bear	10+900, 00-040	N	0.00	0.07	0.19	0.30	0.42	0.53
Bear	12+150, 00-007	PC	0.00	0.00	0.00	0.00	0.05	0.10
Bear Trib 2	00+260, 00-009	N	0.20	0.41	0.63	0.85	1.06	1.28
Bear Trib 2	00+640, 00-008	N	0.96	2.26	3.55	4.85	6.14	7.44
Bear Trib 2	01+000, 00-010	N	0.28	0.56	0.83	1.11	1.39	1.67
Big	06+700, 98-202, 5C d/s	N	0.00	0.01	0.05	0.08	0.12	0.16
Big	09+600, 00-026, Big6	N	2.55	5.31	8.07	10.8	13.6	16.4
Big	09+600, 00-026, Big6	Sh	0.00	0.00	0.05	0.13	0.21	0.29
Buck	01+310, 99-108, Bu1	PC	0.00	0.00	0.00	0.00	0.09	0.24
Buck	02+740, 00-012	PC	0.00	0.00	0.00	0.00	0.03	0.09
Buck	03+000, 00-013, Bu2	N	0.14	0.31	0.48	0.65	0.81	0.98
Buck	03+820, 00-014	N	1.57	3.17	4.76	6.36	7.95	9.54
Buck	04+200, 00-015	N	0.65	1.46	2.26	3.07	3.88	4.69
Buck	05+800, 00-016	N	1.02	2.37	3.71	5.06	6.41	7.76
Buck	10+720, 00-017	PC	0.02	0.05	0.09	0.12	0.16	0.19
Buck	11+580, 00-018	SC	0.00	0.00	0.00	0.00	0.00	0.00
Buck	12+460, 00-019	BD-SP	0.00	0.00	0.00	0.00	0.00	0.00
Buck	12+980, 00-020	BD-SP	0.00	0.00	0.00	0.00	0.00	0.00
Cane	00+700, 00-003	Dep	0.00	0.00	0.00	0.00	0.00	0.00
Cane	01+910, 98-201, C-0	PC	0.00	0.01	0.06	0.10	0.14	0.19
Cane	11+615, 99-100, C4	PC	0.00	0.00	0.00	0.00	0.00	0.00
Dry	02+100, 00-029	N	2.27	4.54	6.81	9.08	11.3	13.6
Dry	02+800, 00-030	N	3.22	6.51	9.80	13.1	16.4	19.7
Dry	03+600, 00-031	N	0.37	0.75	1.13	1.51	1.89	2.27
Dry	04+160, 00-032	Concrete	0.00	0.00	0.00	0.00	0.00	0.00
Dry	04+400, 00-033	N	0.37	0.75	1.13	1.51	1.89	2.27
Dry	04+860, 00-034	N	0.42	0.89	1.35	1.82	2.29	2.75
Duncan	05+260, 01-077	N	0.06	0.16	0.26	0.36	0.46	0.56
Duncan	05+750, 00-036	SC	0.00	0.00	0.00	0.00	0.00	0.00
Huffman	01+820, 01-067	N	0.99	1.97	2.96	3.95	4.93	5.92
Huffman	02+600, 01-065	N	0.54	1.28	2.02	2.76	3.50	4.24
Huffman	03+780, 01-075	N	0.03	0.11	0.19	0.27	0.34	0.42
Huffman	04+700, 00-037	PC	0.00	0.00	0.00	0.01	0.03	0.06
Huffman	05+600, 01-064	N	0.22	0.51	0.79	1.08	1.37	1.66
Huffman	07+040, 01-074	N	0.25	0.51	0.76	1.02	1.27	1.53
Huffman Trib 1	01+800, 01-066	N	0.41	0.84	1.28	1.71	2.14	2.58
Hurricane	03+540, 00-055	N	0.14	0.33	0.52	0.70	0.89	1.07
Hurricane	05+620, 01-068	PC	0.07	0.14	0.21	0.29	0.36	0.43
Hurricane	07+760, 01-070	N	0.94	1.87	2.81	3.75	4.69	5.62
Johnson	00+150, 99-106, JM-A	N	0.41	0.82	1.23	1.64	2.05	2.46
Johnson	00+960, 99-101, JM-C	N	0.42	0.85	1.29	1.72	2.15	2.58
Little Topashaw	00+580, 00-028	Dep	0.00	0.00	0.00	0.00	0.00	0.00
Little Topashaw	03+360, 00-025, LT1	N	0.00	0.07	0.13	0.19	0.25	0.31
Little Topashaw	05+880, 00-024	PC	0.04	0.09	0.15	0.21	0.26	0.32
Little Topashaw	06+620, 00-027	BD-SP	0.00	0.00	0.00	0.00	0.00	0.00
Little Topashaw	09+380, 00-041	PC	0.00	0.00	0.02	0.13	0.24	0.34
Little Topashaw	11+180, 00-042	N	0.82	1.88	2.94	4.00	5.06	6.12
Little Topashaw	11+720, 00-043	N	3.391	6.79	10.2	13.6	17.0	20.4

Little Topashaw Trib 1	00+160, 00-035	N	0.57	1.15	1.74	2.32	2.90	3.49
Little Topashaw Trib 1	01+640, 00-023	N	1.12	2.25	3.37	4.49	5.61	6.74
Little Topashaw Trib 1	02+260, 00-022	N	0.60	1.21	1.81	2.42	3.02	3.63
Little Topashaw Trib 1	02+580, 00-021	PC	0.02	0.05	0.08	0.11	0.14	0.17
Meridian	07+400, 00-054	PC	0.00	0.00	0.00	0.01	0.02	0.04
Meridian	08+380, 00-053	PC	0.00	0.00	0.00	0.00	0.00	0.00
Meridian	11+160, 00-052	PC	0.00	0.00	0.01	0.06	0.11	0.16
Meridian	11+740, 00-051	PC	0.00	0.00	0.02	0.05	0.09	0.13
Meridian Trib 1	00+720, 00-050	PC	0.00	0.00	0.00	0.00	0.02	0.04
Meridian Trib 1	01+280, 00-049	PC	0.00	0.00	0.00	0.00	0.00	0.00
Meridian Trib 1	01+500, 00-048	N	0.00	0.00	0.00	0.01	0.04	0.07
Meridian Trib 1	02+000, 00-047	N	0.00	0.00	0.00	0.08	0.18	0.28
Miles	03+320, 01-080	N	0.84	1.69	2.54	3.39	4.24	5.09
Mud	02+150, 99-104, Mu1-B	N	0.00	0.02	0.19	0.36	0.53	0.70
North Topashaw	01+520, 00-045	PC	0.00	0.00	0.00	0.03	0.06	0.09
Splunge	02+450, 00-039	PC	0.07	0.15	0.22	0.29	0.37	0.44
Splunge	03+050, 00-038	N	0.63	1.36	2.09	2.82	3.55	4.28
Topashaw	11+670, 99-102, T2-C1	PC	0.00	0.00	0.00	0.00	0.00	0.01
Topashaw	14+000, 00-011, T4	PC	0.00	0.00	0.00	0.00	0.00	0.04
Topashaw	21+420, 00-044	PC	0.00	0.00	0.00	0.00	0.00	0.02
Topashaw	23+600, 98-200, T6	PC	0.00	0.00	0.00	0.00	0.00	0.01
Topashaw	26+100, 99-103, T7	PC	0.00	0.00	0.00	0.00	0.00	0.00
Topashaw	28+900, 00-061, T9	PC	0.00	0.00	0.00	0.00	0.00	0.00
Topashaw Trib 1	02+240, 00-001, TT1-1, u/s	PC	0.00	0.00	0.00	0.13	0.36	0.58
Twin	00+200, 01-063	N	0.83	1.67	2.50	3.34	4.17	5.01
Walnut	02+220, 00-060	N	0.23	0.85	1.46	2.07	2.69	3.30
Walnut	02+900, 00-059	N	0.00	0.54	1.27	2.00	2.73	3.46
Walnut	03+490, 00-058	N	0.59	1.23	1.87	2.52	3.16	3.81
Walnut	05+060, 00-057	N	1.34	2.77	4.19	5.61	7.04	8.46
Walnut Trib 1	00+760, 00-056	BD-SP	0.00	0.00	0.00	0.00	0.00	0.00
Yalobusha	25+700, 99-110, Y3-A at Bull	PC	0.00	0.00	0.00	0.00	0.00	0.02
Yalobusha	28+800, 99-105, Y3-E, at Johnson	N	0.43	0.86	1.29	1.72	2.16	2.59
Yalobusha	32+900, 99-109, Y3-F, D/S Pyland	N	0.27	0.79	1.32	1.85	2.37	2.90

PC = Porters Creek clay formation.
N = Naheola formation
Sh = shale.
SC = sandy clay
BD-SP = beaver dam, sand.
Dep = depositional.

	Naheola	**Mean**	**0.654**	**1.38**	**2.12**	**2.86**	**3.60**	**4.35**
		Median	**0.408**	**0.845**	**1.29**	**1.82**	**2.29**	**2.75**
	Porters Creek	**Mean**	**0.007**	**0.016**	**0.028**	**0.052**	**0.088**	**0.132**
		Median	**0.000**	**0.000**	**0.000**	**0.001**	**0.034**	**0.090**

Table 10 - Rates of knickpoint migration at the ten “intensive” sites and average values for the Porters Creek Clay and Naheola formations.

Name	Formation	Date of earliest survey	Number of surveys	Date of most recent survey	Migration distance, in m	Migration rate, in m/y
Bear	Naheola	03/05/99	8	08/22/01	13.9	5.6
Big	Naheola	02/25/97	12	01/03/02	42.6	8.8
Buck	Conglomerate	04/14/97	9	08/22/01	2.4	0.5
Cane	Porters Creek	03/13/97	8	08/22/01	4.3	1.0
Johnson	Naheola	04/16/97	8	03/22/01	43.8	11.1
Mud	Naheola	03/14/97	10	08/22/01	30.3	6.8
Topashaw	Porters Creek	04/24/97	7	12/07/00	1.5	0.4
Topashaw Trib.	Porters Creek	04/16/97	9	08/22/01	6.6	1.5
Yalobusha	Naheola	04/16/97	7	09/05/01	22.2	5.1
N. Topashaw	Naheola	02/20/97	8	03/19/01	8.8	2.2
Mean	**Naheola**					**6.6**
Mean	**Porters**					**1.0**

Table 11 - Geotechnical strength parameters for the Naheola and Porters Creek Clay formations showing the generally greater strengths of the Naheola formation.

Formation		**ϕ', in degrees**	**c_a, in kPa**	**c_u, in kPa**	**ψ, in kPa**	**γ_{amb}, in kN/m^3**	**w (%), by weight**
Naheola		18.3	6.84	21.0	7.02	17.5	23.2
Porters Creek Clay		14.0	5.28	19.8	13.9	16.0	34.9
Naheola	Dry	18.7	5.02	18.0	8.17	17.7	21.9
	Wet	17.9	9.45	22.0	5.71	17.3	24.6
Porters Creek Clay	Dry	12.5	2.78	17.2	4.85	16.1	36.5
	Wet	14.8	6.62	22.4	20.3	15.8	34.4

Table 12 - Summary of all BST data.

Creek Name	Site/Station	Date	Formation	Test #	Type	ϕ (degrees)	c_a (kPa)	c_u (kPa)	ψ (kPa)
Bear	8+020, 00-002	3/22/00	PC	1	D	7.4	2.3	-	1.00
Bear	8+020, 00-002	3/22/00	PC	2	W	19.3	8.8	-	2.90
Bear	6+200, 00-004	3/23/00	PC	1	D	8.5	7.8	-	0.13
Bear	6+200, 00-004	3/23/00	PC	2	W	15.6	1.2	-	1.10
Bear	6+800, 00-005	3/27/00	PC	1	D	11.8	1.2	-	-6.70
Bear	6+800, 00-005	3/27/00	PC	2	W	9.6	4.4	-	12.6
Bear	8+800, 00-006	3/28/00	N	1	W	13.0	6.3	-	15.4
Bear	8+800, 00-006	3/28/00	N	2	D	0.0		18.0	13.8
Bear	12+150, 00-007	6/20/00	PC	1	D	13.0	0.8	-	3.05
Bear	12+150, 00-007	6/20/00	PC	2	W	13.5	13.8	-	-
Bear	10+900, 00-040	6/28/00	N	2	W	5.7	22.0	-	5.78
Bear	5+400, 98-203, B3	4/23/98	N	1	-	12.7	1.8	14.6	17.0
Bear	5+400, 98-203, B3	4/23/98	N	2	-	-	-	-	16.2
Bear	8+500, 99-107, B3C	9/20/99	N	1	D	19.8	4.7	-	13.2
Bear	8+500, 99-107, B3C	9/21/99	N	2	D	17.2	6.8	-	8.72
Bear Trib 2	0+640, 00-008	4/7/00	N	1	D	16.7	14.0	-	0.36
Bear Trib 2	0+640, 00-008	4/7/00	N	2	W	13.5	11.6	-	0.10
Bear Trib 2	0+260, 00-009	4/12/00	N	1	D	11.3	12.0	-	-
Bear Trib 2	0+260, 00-009	4/12/00	N	2	W	26.6	16.0	-	-
Bear Trib 2	1+000, 00-010	4/17/00	N	1	D	12.4	1.0	-	4.56
Bear Trib 2	1+000, 00-010	4/17/00	N	2	W	21.3	6.4	-	0.05
Big	9+600, 00-026, Big6	1/12/99	N	4	-	21.4	13.3	-	5.00
Big	9+600, 00-026, Big6	1/12/99	N	5	-	15.2	4.7	-	7.00
Big	6+700, 98-202, 5C d/s	4/20/98	N	1	-	6.9	16.9	-	26.2
Big	6+700, 98-202, 5C d/s	4/20/98	N	2	-	-	-	-	21.0
Buck	2+740, 00-012	4/18/00	PC	1	D	0.0	-	14.4	0.09
Buck	2+740, 00-012	4/18/00	PC	2	W	14.6	7.2	-	-
Buck	3+000, 00-013, Bu2	9/21/99	N	1	D	33.4	4.6	-	14.0
Buck	3+000, 00-013, Bu2	9/21/99	N	1	W	30.9	0.6	-	14.0
Buck	3+820, 00-014	4/21/00	N	1	W	-	-	-	0.38
Buck	3+820, 00-014	4/21/00	N	2	D	20.3	9.2	-	2.23
Buck	4+200, 00-015	5/9/00	N	1	W	24.2	4.3	-	4.93
Buck	4+200, 00-015	5/9/00	N	2	D	18.8	1.8	-	2.23
Buck	5+800, 00-016	9/18/00	N	1	D	26.6	4.0	-	16.6
Buck	5+800, 00-016	9/18/00	N	2	W	29.4	0.0	-	3.06
Buck	10+720, 00-017	9/19/00	PC	1	W	26.1	0.0	-	1.98
Buck	10+720, 00-017	9/19/00	PC	-	-	-	-	-	0.96
Buck	11+580, 00-018	4/25/00	SC	-	-	-	-	-	-
Buck	12+460, 00-019	5/11/00	BD-SP	-	-	-	-	-	-
Buck	12+980, 00-020	5/11/00	BD-SP	-	-	-	-	-	-
Buck	1+310, 99-108, Bu1	4/23/98	PC	1	-	-	-	-	52.0
Buck	1+310, 99-108, Bu1	1/13/99	PC	1	-	13.4	6.3	-	15.0
Buck	1+310, 99-108, Bu1	4/23/98	PC	2	-	-	-	-	52.0
Buck	1+310, 99-108, Bu1	1/13/99	PC	2	-	15.3	7.5	-	5.50
Buck	1+310, 99-108, Bu1	1/13/99	conglomerate	3	-	-	-	-	-
Buck	1+310, 99-108, Bu1	1/13/99	conglomerate	4	-	-	-	-	14.0
Cane	0+700, 00-003	2/10/00	Dep	-	-	-	-	-	-
Cane	1+910, 98-201, C-0	4/21/98	PC	1	-	7.3	10.5	-	4.97
Cane	1+910, 98-201, C-0	4/21/98	PC	2	-	6.2	3.5	-	11.74
Cane	11+615, 99-100, C4	1/11/99	PC	1	-	24.2	6.5	-	55.0
Cane	11+615, 99-100, C4	1/11/99	PC	2	-	17.3	6.6	-	30.0
Dry	2+100, 00-029	5/25/00	N	1	D	11.3	12.0	-	31.0
Dry	2+100, 00-029	5/25/00	N	2	W	14.0	23.2	-	4.35
Dry	2+800, 00-030	6/7/00	N	1	D	21.8	1.0	-	4.35
Dry	2+800, 00-030	6/7/00	N	2	W	21.8	21.7	-	-
Dry	3+600, 00-031	5/23/00	N	-	-	-	-	-	-
Dry	4+160, 00-032	5/23/00	Concrete	-	-	-	-	-	-
Dry	4+400, 00-033	5/23/00	N	-	-	-	-	-	-
Dry	4+860, 00-034	6/8/00	N	1	D	14.0	4.2	-	3.10
Dry	4+860, 00-034	6/8/00	N	2	W	0.0	-	24.6	2.17
Duncan	5+750, 00-036	6/15/00	SC	-	-	-	-	-	-
Duncan	5+260, 01-077	4/10/01	PC/N	1	D	0.0	-	7.6	-
Duncan	5+260, 01-077	4/25/01	PC/N	1	W	8.5	10.8	-	-
Duncan	5+260, 01-077	4/25/01	PC/N	2	D	28.4	0.0	-	-

Huffman	5+600, 00-037	6/15/00	PC	-	-	-	-	-	-
Huffman	5+600, 01-064	1/9/01	N	1	D	21.3	0.0	-	-20.1
Huffman	5+600, 01-064	1/9/01	N	2	W	-	-	-	-32.9
Huffman	02+600, 01-065	1/10/01	N	1	D	16.7	4.0	-	-1.29
Huffman	02+600, 01-065	1/10/01	N	2	W	11.3	0.0	-	-8.18
Huffman	01+820, 01-067	4/9/01	N	1	D	18.8	2.3	-	25.3
Huffman	01+820, 01-067	4/9/01	N	2	W	-	-	-	-48.0
Huffman	07+040, 01-074	4/26/01	N	1	D	10.8	0.0	-	7.98
Huffman	07+040, 01-074	4/26/01	N	2	W	12.4	0.0	-	12.9
Huffman	03+780, 01-075	8/27/01	N	1	W	7.8	9.6	-	56.6
Huffman	03+780, 01-075	8/27/01	N	2	D	23.3	2.9	-	46.6
Huffman Trib 1	01+800, 01-066	1/16/01	N	1	D	13.0	10.1	-	5.21
Huffman Trib 1	01+800, 01-066	1/16/01	N	2	W	15.1	9.6	-	1.34
Hurricane	3+540, 00-055	8/14/00	N	1	D	27.0	4.2	-	12.1
Hurricane	3+540, 00-055	8/14/00	N	2	W	21.8	5.2	-	33.8
Hurricane	5+620, 01-068	1/24/01	PC	1	D	5.7	10.0	-	-11.0
Hurricane	5+620, 01-068	1/24/01	PC	2	W	18.9	0.0	-	5.91
Hurricane	7+760, 01-070	1/25/01	N	1	D	15.6	0.0	-	-19.9
Hurricane	7+760, 01-070	1/25/01	N	2	W	31.5	0.0	-	-23.8
Johnson	0+960, 99-101, JM-C, lower unit	9/22/99	N	1	D	17.3	6.6	-	8.70
Johnson	0+960, 99-101, JM-C, lower unit	9/22/99	N	2	D	17.3	6.6	-	13.1
Johnson	0+960, 99-101, JM-C, lower unit	9/22/99	N	1	D	14.9	5.6	-	1.65
Johnson	0+960, 99-101, JM-C, lower unit	9/22/99	N	2	D	16.4	8.1	-	9.47
Little Topashaw	5+880, 00-024	5/23/00	PC	1	D	10.8	3.9	-	-2.49
Little Topashaw	5+880, 00-024	5/23/00	PC	2	W	22.8	4.4	-	-
Little Topashaw	3+360, 00-025, LT1	8/11/99	N	1	D	24.2	4.0	-	-
Little Topashaw	3+360, 00-025, LT1	8/11/99	N	1	W	23.3	6.8	-	-
Little Topashaw	6+620, 00-027	5/23/00	BD-SP	-	-	-	-	-	-
Little Topashaw	0+580, 00-028	5/23/00	Dep	-	-	-	-	-	-
Little Topashaw	9+380, 00-041	7/12/00	PC	2	D	21.8	5.2	-	-0.95
Little Topashaw	11+180, 00-042	7/7/00	N	2	D	29.7	4.9	-	2.24
Little Topashaw	11+720, 00-043	7/10/00	N	2	D	14.0	10.2	-	2.75
Little Topashaw Trib 1	2+580, 00-021	5/16/00	PC	1	D	14.3	0.0	-	47.9
Little Topashaw Trib 1	2+580, 00-021	5/16/00	PC	2	W	0.0	-	6.5	0.20
Little Topashaw Trib 1	2+260, 00-022	5/17/00	N	1	D	15.1	8.2	-	-0.01
Little Topashaw Trib 1	2+260, 00-022	5/17/00	N	2	W	-	-	-	0.13
Little Topashaw Trib 1	1+640, 00-023	5/18/00	N	1	D	5.7	8.3	-	0.16
Little Topashaw Trib 1	1+640, 00-023	5/18/00	N	2	W	14.0	17.8	-	-4.24
Little Topashaw Trib 1	0+160, 00-035	6/12/00	N	1	D	19.5	0.0	-	15.7
Little Topashaw Trib 1	0+160, 00-035	6/12/00	N	2	W	0.0	-	26.8	17.4
Meridian	11+740, 00-051	8/2/00	PC	1	D	0.0	-	20.0	3.17
Meridian	11+740, 00-051	8/2/00	PC	2	W	16.7	6.0	-	2.63
Meridian	11+160, 00-052	8/3/00	PC	1	D	15.6	1.0	-	8.23
Meridian	11+160, 00-052	8/3/00	PC	2	W	17.2	5.2	-	-6.77
Meridian	8+380, 00-053	8/7/00	PC	1	D	-	-	-	8.47
Meridian	8+380, 00-053	8/7/00	PC	2	W	12.4	8.9	-	17.1
Meridian	7+400, 00-054	8/8/00	PC	1	W	12.7	0.0	-	13.9
Meridian	7+400, 00-054	8/8/00	PC	2	D	21.7	0.0	-	10.5
Meridian Trib 1	2+000, 00-047	7/25/00	N	1	D	26.6	9.3	-	5.70
Meridian Trib 1	2+000, 00-047	7/25/00	N	2	W	21.3	15.6	-	13.1
Meridian Trib 1	1+500, 00-048	7/26/00	N	1	D	8.0	11.6	-	7.86
Meridian Trib 1	1+500, 00-048	7/26/00	N	2	W	9.1	31.1	-	10.9
Meridian Trib 1	1+280, 00-049	7/27/00	PC	1	D	12.8	0.0	-	11.5
Meridian Trib 1	1+280, 00-049	7/27/00	PC	2	W	14.0	7.8	-	5.72
Meridian Trib 1	0+720, 00-050	8/1/00	PC	1	D	19.1	0.0	-	-5.66
Meridian Trib 1	0+720, 00-050	8/1/00	PC	2	W	23.6	0.0	-	0.66
Miles	03+320, 01-080	5/2/01	N	1	D	11.3	4.0	-	31.7
Miles	03+320, 01-080	5/2/01	N	2	W	24.7	0.0	-	-
North Topashaw	1+520, 00-045	7/18/00	PC	2	D	14.0	4.5	-	4.87
North Topashaw	2+180, 00-046	No H2O	PC	-	-	-	-	-	-
Splunge	3+050, 00-038	6/26/00	N	1	D	-	-	-	-0.14
Splunge	3+050, 00-038	6/26/00	N	2	W	24.7	15.2	-	0.92
Splunge	2+450, 00-039	6/27/00	PC	1	D	-	-	-	2.12
Splunge	2+450, 00-039	6/27/00	PC	2	W	11.3	16.0	-	1.44
Topashaw	21+420, 00-044	7/13/00	PC	2	D	24.2	2.2	-	19.5
Topashaw	28+900, 00-061, T9	12/16/99	PC	1	-	-	-	-	36.5
Topashaw	28+900, 00-061, T9	12/16/99	PC	2	-	-	-	-	36.9

Topashaw	11+670, 99-102, T2-C1	7/14/99	PC	1	-	-	-	-	-1.47
Topashaw	11+670, 99-102, T2-C1	8/10/99	PC		-	-	-	-	-
Topashaw	23+600, 98-200, T6	4/22/98	PC	1	-	6.8	13.9	-	41.8
Topashaw	23+600, 98-200, T6	4/22/98	PC	2	-	6.8	13.9	-	90.7
Topashaw	23+600, 98-200, T6	4/22/98	PC	3	-	6.8	13.9	-	55.0
Topashaw Trib 1	2+240, 00-001, TT1-1, d/s	1/14/99	PC	1	-	24.2	2.9	-	-
Topashaw Trib 1	2+240, 00-001, TT1-1, d/s	1/14/99	PC	2	-	24.2	2.9	38.3	-
Twin	0+200, 01-063	1/8/01	N	1	D	18.1	0.0	-	0.64
Twin	0+200, 01-063	1/8/01	N	2	W	35.0	0.0	-	4.41
Walnut	5+060, 00-057	8/16/00	N	1	D	31.4	0.6	-	-
Walnut	5+060, 00-057	8/16/00	N	2	W	-	-	-	-
Walnut	3+490, 00-058	9/6/00	N	1	W	27.5	4.8	-	-
Walnut	3+490, 00-058	9/6/00	N	2	D	-	-	-	-
Walnut	2+900, 00-059	9/5/00	N	1	D	-	-	-	-
Walnut	2+900, 00-059	9/5/00	N	2	D	27.5	2.2	-	-
Walnut	2+220, 00-060	9/7/00	N	1	D	32.8	0.0	-	-
Walnut	2+220, 00-060	9/7/00	N	2	D	24.7	0.0	-	-
Walnut Trib 1	0+760, 00-056	7/31/00	BD-SP	-	-	-	-	-	-
Yalobusha	32+900, 99-109, Y3-F, D/S Pyland	9/23/99	N	1	D	21.4	5.8	-	16.7
Yalobusha	32+900, 99-109, Y3-F, D/S Pyland	9/23/99	N	2	D	18.9	5.9	-	-

D = dry test
W = wet test
PC = Porters Creek clay formation.
N = Naheola formation.
Sh = shale.
SC = sandy clay
BD-SP = beaver dam, sand.
Dep = depositional.

Table 13 - Summary of k_{sat} values.

Location	**Formation**	**Permeability (k_{sat}), in (m/s)**
Bear	Naheola	1.64×10^{-09}
Bear	Naheola	3.05×10^{-09}
Bear	Naheola	5.30×10^{-09}
Buck	Conglomerate	1.42×10^{-08}
Buck	Conglomerate	4.99×10^{-08}
Cane	Porters Creek Clay	5.86×10^{-09}
Johnson	Naheola	3.04×10^{-09}
Johnson	Naheola	3.46×10^{-09}
Mud	Naheola	8.27×10^{-09}
Mud	Naheola	8.31×10^{-09}
Mud	Naheola	2.85×10^{-08}
North Topashaw	Naheola	6.39×10^{-09}
Topashaw T4	Porters Creek Clay	5.17×10^{-09}
Topashaw T4	Porters Creek Clay	9.55×10^{-09}
Topashaw Trib TT1A	Porters Creek Clay	8.26×10^{-09}
Topashaw Trib TT1A	Porters Creek Clay	6.12×10^{-09}
Yalobusha	Naheola	2.42×10^{-10}
Mean	**Naheola**	$\mathbf{6.82 \times 10^{-09}}$
Mean	**Porters Creek Clay**	$\mathbf{6.99 \times 10^{-09}}$

Table 14 - Summary of modeling results.

Location	Formation	Results of modeling
Bear	Naheola/ Porters Creek Clay	No failure
Big	Naheola	Mass Failure mechanism
Buck	Conglomerate	Shallow (<0.1 m) failures
Cane	Porters Creek Clay	No failure
Johnson	Naheola	No failure
Mud	Naheola	No failure
Topashaw	Porters Creek Clay	No failure
Topashaw Tributary 1A	Porters Creek Clay	No failure
Yalobusha	Naheola	Shallow (<0.1 m) failures

Table 15 - Results of knickpoint stability modeling on Big Creek.

Event date	Peak stage (m)	Minimum Factor of Safety	Predicted failure length (m)	Observed retreat (m)	Survey date
1-26-99	3.1	0.91	1.39	Unknown	2-1-99
3-13-99	0.6	1.07	0.5	0.46	3-25-99
4-6-99	1.0	1.08	0.5 x 2	1.2	7-12-99
6-27-99	0.5	1.97	0		
7-11-99	0.5	1.87	0		
1-5-00	0.9	0.93	0.8	0.86	3-3-00
1-6-00	0.8	0.98	0.9		
4-2-00	1.4	0.98	0.49	1.33	4-12-00
4-14-00	0.4	2.23	0	0.49	6-30-00

APPENDIX I: ArcView GIS - Help File

The mapping project contained in this report was created in ArcView GIS 3.2 software. If the user is unfamiliar with ArcView GIS, it would be very helpful to read "Introduction to ArcView" in the ArcView Help files under the Contents tab (see graphic below). This will give the user a basic understanding of the components of an ArcView project.

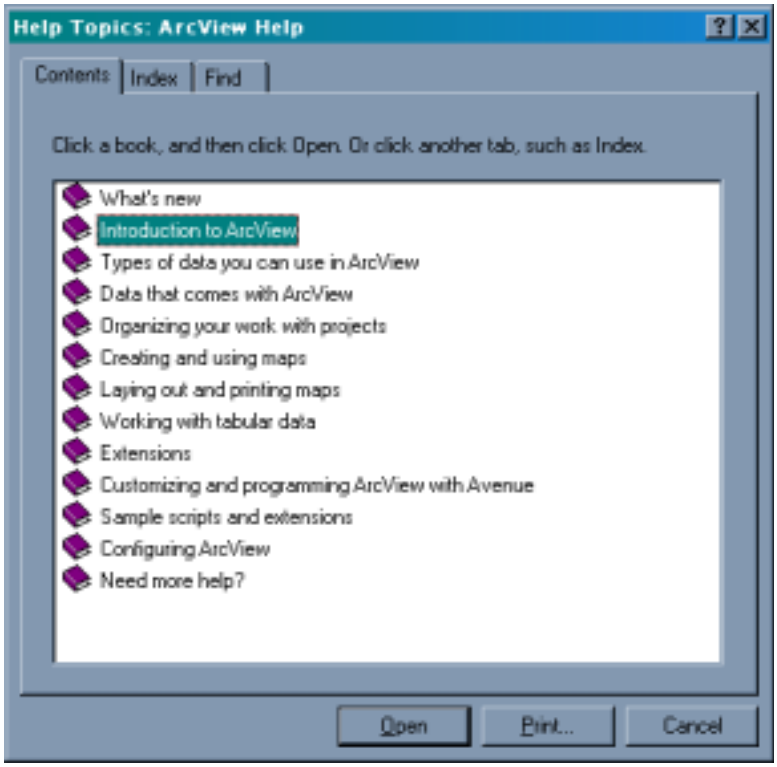

It is recommended that the user copy the folder "Yalo-Gis", and all its contents, from the CD Rom provided onto his/her hard drive and work from that location. This ensures that the project runs smoothly, and that an unchanged copy of the project is retained on the CD Rom in the event that the working copy is altered. Changes to the working copy could result in permanent changes to the maps contained within.

Navigating Through the Project

This project consists of three Views with corresponding Layouts (printable maps). The following discussion will help the user navigate through this project.

To open the project:

1. Open ArcView
2. Under File, select Open Project
3. Navigate to the project's location (where you placed the "Yalo-Gis" folder)
4. Highlight the project's name (yalo-lat-long.apr)
5. Click OK

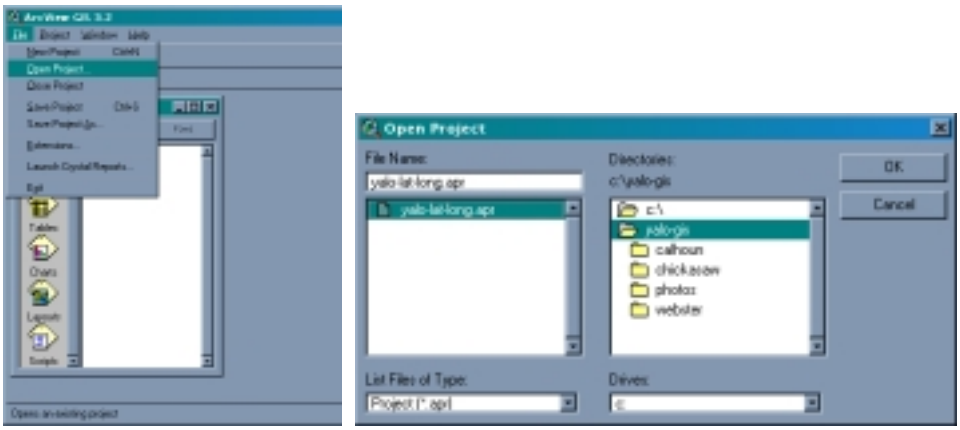

When the project opens, you see several document types that are available in ArcView. In this particular project only the "Views" and "Layouts" document types are significant.

Views

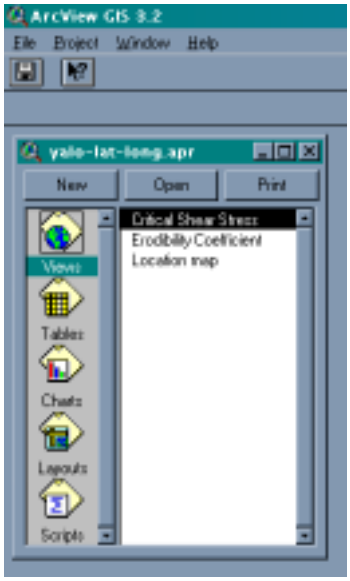

Layouts

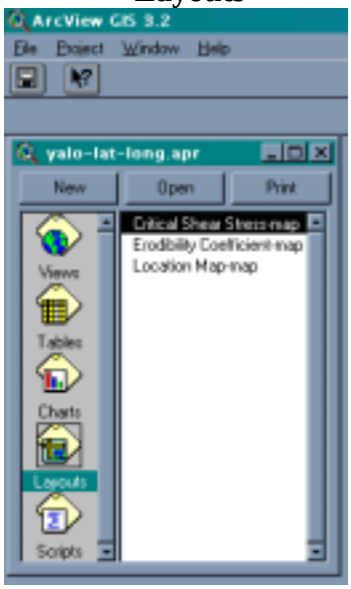

There are three Views and three Layouts that can be opened in this project (see above). The Views are the working files of the project. The Layouts are the designed maps that are suitable for printing.

When a View is opened the user will see the graphic features on the right and a table of contents (TOC) on the left see figure below). The TOC lists the "themes" that make up each View. The checked boxes in the TOC mean that those themes are turned on. To turn on/off a theme, check/uncheck the box.

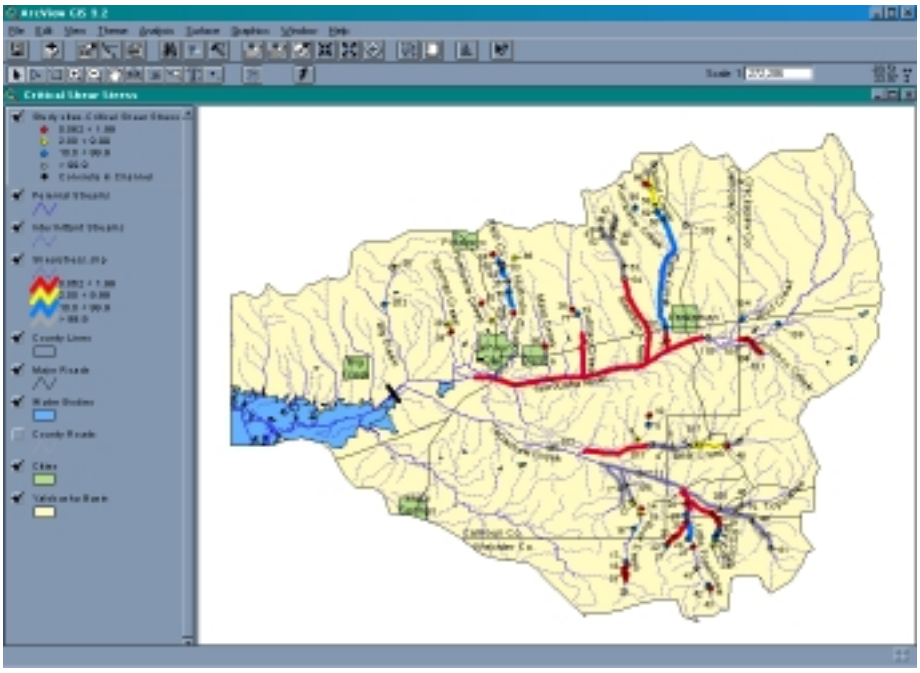

Viewing Data Tables

The “Study Sites” theme in this project (at the top of the TOC in every View) has an associated data table that lists a summary of the field data collected during this study.

To access this data table:

1. Make sure that the “Study Sites” theme is turned on (its box is checked).
2. Click on the “Study Sites” theme in the TOC to make it active.
3. You can see that the theme is active because it seems to pop out from the rest of the themes in the TOC.
4. Click on the data table button  in the toolbar; the fifth from the left in the top row in the above figure (see ArcView help for buttons and their functions).
5. The theme’s table will open, and its window can be resized to allow for viewing of multiple windows.

The graphics below show the user how the interaction of a theme and its associated data table works. In the graphic on the left, certain study sites were selected by drawing a box around them with the selection tool  . When selected, the sites are highlighted purple (ArcView’s default highlight color is yellow, but has been set to purple in this project for better contrast). When the data table is then opened, the records corresponding to the selected sites are also highlighted. Click the ‘promote’ button  to move all selected records to the top of the data table.

This interaction also works in reverse. In the graphic on the right each record in the data table containing information on Bear Creek is selected using the pointer tool  . Hold down the Shift key on your keyboard while clicking records to select multiple records at one time. In response, the sites on Buck Creek are highlighted in the View.

Sites were selected

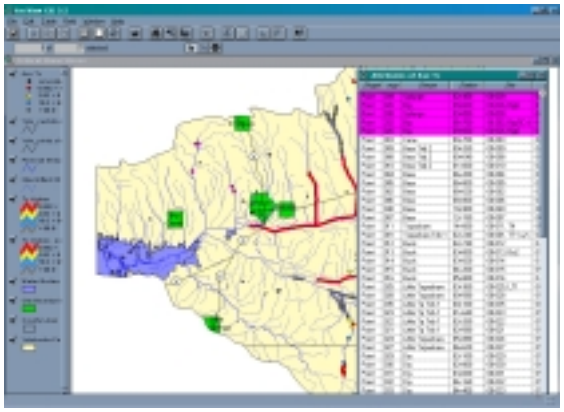

Records were selected

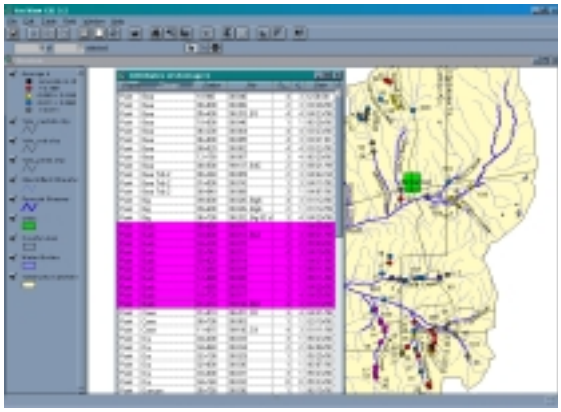

Additionally, one can sort the data table by any column. First click the header of the column of column of interest. Then click either the ascending or descending tool  . In the graphic below the data was sorted by station number. First the column 'Site__' was selected, then the sort ascending  button was clicked.

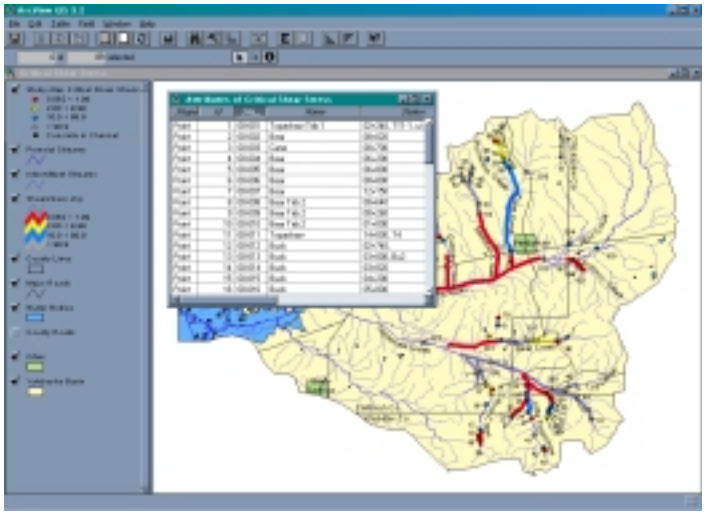

Viewing Digital Photos

Within each View it is possible to view digital photos of the study sites (see graphic below). The following discussion describes how to view the jpeg images.

To view the photo link:

1. Open any View
2. Make the "Study Sites" theme active in the TOC.
3. Click on the button that looks like a lightning bolt  to activate the photo link tool.
4. Next click on any site in the View. A jpeg photo of the site selected will open within the View. The photo's window can be resized and zoomed in/out (see the graphic below).

** Note: There are 17 sites for which a photo is not available. If one of these sites is selected, an error message will appear stating that the jpeg was not found.

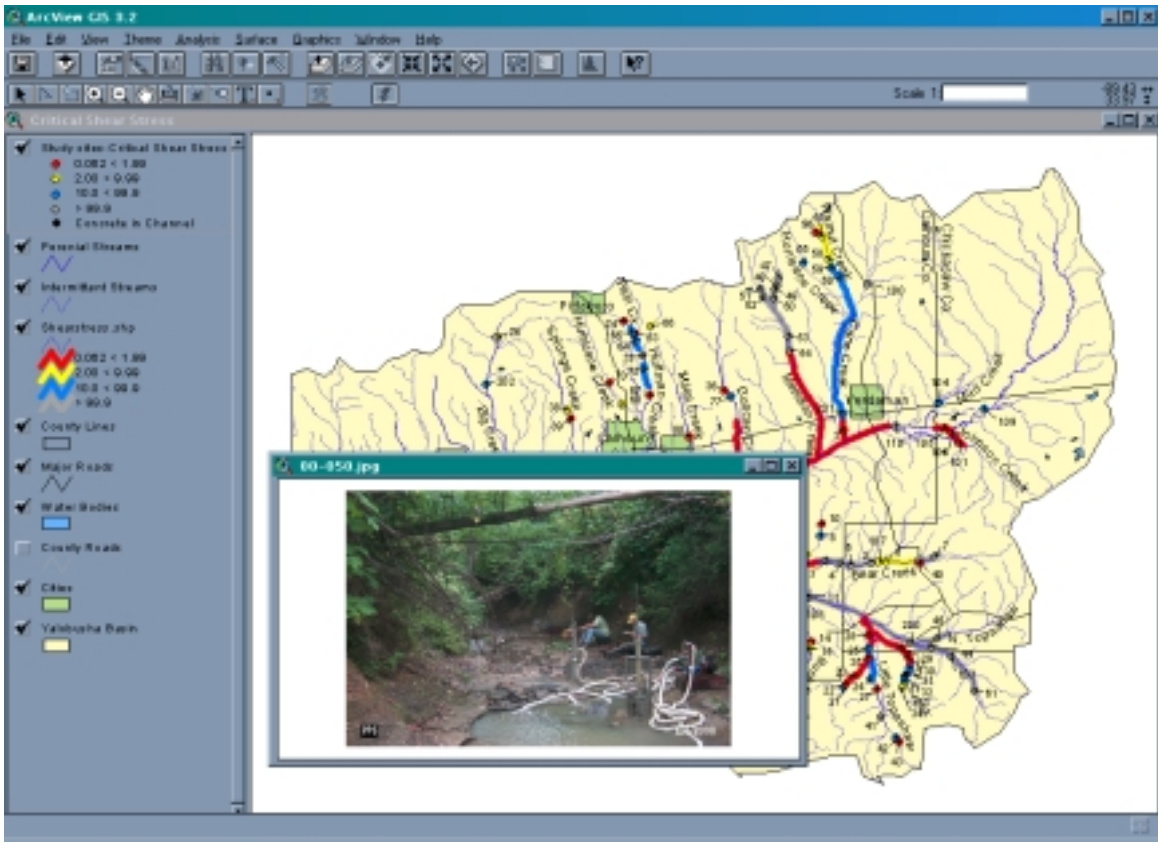

Viewing Intensive Site Photos and Graphs

Within the "Location Map" View it is possible to view digital photos of each intensive site and associated knickzone. In addition, graphs of thalweg and knickpoint migration rates are available for viewing (see graphic below). The following discussion describes how to view these documents.

To view the intensive site photos and graphs:

1. Open the "Location Map" View.
2. Make the "Knick Zones" theme active in the TOC.
3. Click on the button that looks like a lightning bolt  to activate the photo link tool.
4. Then click on any knickzone in the View. Knickzones are represented as hollow squares on the map. A Microsoft Word document will open containing a photo of the knickzone and one or more surveys of knickpoint migration. To return to ArcView simply close or minimize Microsoft Word.

** Note: This function of the project assumes that Microsoft Word is installed on your PC in the location C:\Program Files\Microsoft Office\Office. If your machine does not have Microsoft Word installed, this function will not work. However, photos of the sites can still be viewed by making the "Study Sites" theme active, selecting the photo link tool, and clicking on a study site.

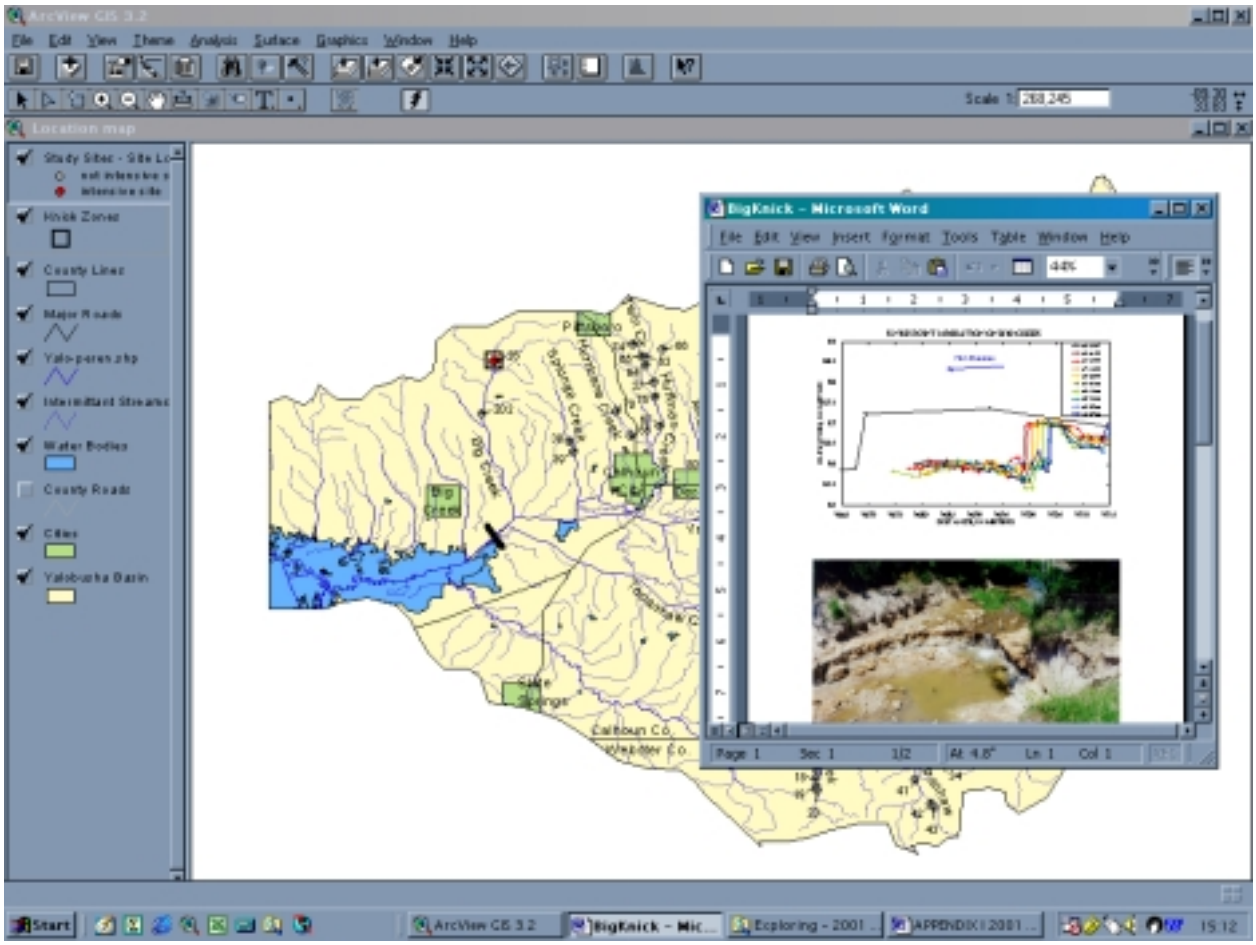

Data Sources

The data files used to create this ArcView project were obtained from the Mississippi Automated Resource Information System (http://www.maris.state.ms.us/). The Standard County Data Release files were downloaded for the following counties in Mississippi: Calhoun, Chickasaw, and Webster. Each county file contains ten standard data layers from which all views and maps in this project were created. In addition, the statewide hydrologic unit data file was download, from which the Yalobusha Drainage Basin was extracted. All files were downloaded in a Lat/Long format suitable for ArcView applications. Additional file formats are available for download from this organization.

The study sites were placed in the project by the project creator. River kilometer distance measurements and map features such as bridges and road intersections determined their locations. It is possible for ArcView to calculate the approximate latitude and longitude values for the study sites based on their locations on the map. However, users are strongly cautioned that these values will not be exact, due to the fact that lat/longs were not initially used to locate sites on the map.

APPENDIX II: On the Origin of Secondary Scour Associated With Migrating Knickpoints
by Carlos V. Alonso

This appendix examines the hydrodynamic processes in the flow region upstream of a knickpoint where secondary scour is usually observed to develop (Figure II-1). The relation between the hydrodynamic processes and bed-scouring forces in this region is evaluated by treating the abrupt bed step at the knickpoint as a free overfall.

The flow over an idealized two-dimensional free overfall in an infinitely wide channel is shown in Figure II-2. Steady, uniform flow with a unit-width discharge q_w approaches the brink over the undisturbed bed with slope S_0. The free overfall at the brink causes the flow to rapidly accelerate over the distance L between the brink and the point where the flow passes through either the critical depth h_c in subcritical flows, or the normal depth h_n in supercritical flows, whichever the case may be. Previous researchers have studied this phenomenon at length; the first rigorous treatments were given by Rouse (1936, 1937). He was the first to show that pressure through the nappe is not zero at the brink, and to present an accurate analysis of the pressure distribution within the region of accelerated flow. More recently, Rajaratnam and Muralidhar (1968) carried out detailed measurements of velocity, pressure, and bed shear stress distributions within this reach. The following discussion draws from the results and conclusions reported by these investigators.

The pressure at the bed is zero at the brink because this point is exposed to atmospheric conditions, and it converges to the hydrostatic value in the uniform flow region (Figure II-2). It should be noted here that this characterization holds true only for cases when the knickpoint is not submerged to the point that downstream conditions control flow over the knickpoint. The curvilinear flow in the reach L is directed decidedly downwards and the mean velocity components parallel, u, and normal, v, to the bed are distributed as shown in Figure II-3. It is apparent from Figure II-3 that as the brink is approached, the product $v\partial u/\partial x$ is very small and can be justifiably neglected. Therefore, the Reynolds equations governing the steady, rapidly accelerated flow in the reach L can be expressed as:

$$\frac{\partial u}{\partial x}+\frac{\partial v}{\partial y}=0 \tag{i}$$

$$u\frac{\partial u}{\partial x}=-g\frac{\partial \eta}{\partial x}-\frac{1}{\rho}\frac{\partial p}{\partial x}+\frac{1}{\rho}\frac{\partial \tau_{yx}}{\partial y} \tag{ii}$$

$$u\frac{\partial v}{\partial x}+v\frac{\partial v}{\partial y}=-g\frac{\partial \eta}{\partial y}-\frac{1}{\rho}\frac{\partial p}{\partial y}+\frac{1}{\rho}\frac{\partial \tau_{zx}}{\partial z} \tag{iii}$$

where x, y and z are the coordinate axes with origin at the brink (Figure II-2), g is the acceleration due to gravity, η is the potential energy elevation referred to an arbitrary datum, ρ is the density of water, p is the mean pressure, and τ_{ij} is the total shear stress component parallel to the axis j and acting on the plane normal to the axis i. Depth-averaging Equation (i) over an arbitrary section $0 \le x \le L$ and realizing that $\partial v/\partial y \to 0$ everywhere as $x \to L$ yields,

$$q_w = U(x)\,h(x) \tag{iv}$$

where U is the cross-sectional average velocity. Similarly, depth-averaging each term in Equation (ii) gives:

$$\int_0^h u\frac{\partial u}{\partial x}\,dy = \frac{d}{dx}\left(\beta h U^2\right) \tag{v}$$

$$-\int_0^h g\frac{\partial \eta}{\partial x}\,dy = -\int_0^h g\left[-S_0\right]dy = g\,S_0\,h(x) \equiv g\,S_0\,h\left(x\to\infty\right) = \frac{\tau_{B,\infty}}{\rho} \tag{vi}$$

$$-\frac{1}{\rho}\int_0^h \frac{\partial p}{\partial x}\,dy = -\frac{1}{\rho}\frac{\partial}{\partial x}\int_0^h p\,dy = -\frac{1}{\rho}\frac{dP}{dx} \tag{vii}$$

$$\frac{1}{\rho}\int_0^h \frac{\partial \tau_{yx}}{\partial y}\,dy = \frac{1}{\rho}\int_0^h \delta\left[\tau_{yx}(x)\right] = -\frac{\tau_B(x)}{\rho} \tag{viii}$$

where β is the momentum correction coefficient (Chow, 1959), $\tau_{B,\infty}$ is the bed shear stress in the approaching uniform flow, P is the pressure force per unit width acting on the cross section (Figure II-2), and τ_B is the bed shear stress in the region of accelerated flow. For the purposes of the present analysis, it is justifiable to assume that $\beta \approx 1$. Substituting this value and Equations (iv) - (viii) into Equation (ii) results in:

$$\tau_B(x) - \tau_{B,\infty} = -\frac{d}{dx}\left(\rho\, q_w U\right) - \frac{dP}{dx} \tag{ix}$$

The pressure force per unit width is roughly approximated as $P = p_B\, h/2$ to take advantage of the bed-pressure data, p_B, measured by Rajaratnam and Muralidhar (1968).

Next, let's define:

$$\Delta\tau_B(x) = \tau_B(x) - \tau_{B,\infty} \tag{x}$$

$$M(x) = \rho\, q_w\, U(x) \tag{xi}$$

where M is the momentum flux, and $\Delta\tau_B$ is the increase in bed shear stress in the region of accelerated flow. Introducing Equations (x) - (xi) into Equation (ix), the latter can be rewritten as:

$$\Delta\tau_B(x) = -\frac{d}{dx}M(x) - \frac{d}{dx}P(x) \tag{xii}$$

The variation of each term in Equation (xii) with *x/L* is plotted in Figure II-4. It is apparent from this plot that the first term on the R.H.S. is always positive, while the second term is always negative. Consequently, bed shear stress increases as *x* decreases because flow momentum increases while the pressure force decreases. Thus, both flow acceleration and

decreasing bed pressure are equally responsible for the increase in bed shear stress as the brink is approached. On the other hand, it can be seen that the R.H.S. of Equation (xii) converges to zero in the upstream uniform flow region where, as expected, the bed shear stress is dominated by gravitational forces (i.e., $\tau_B(x) = \tau_{B,\infty}$).

Next, let's consider the transversal forces on the flow pattern within the reach *L*. It should be noted that the L.H.S. of Equation (iii) represents the vertical convective acceleration, a_y, acting on a fluid particle. The two-dimensional flow assumption introduced above renders the last term on the R.H.S. of Equation (iii) identically zero. Hence, this equation reduces to:

$$a_y = -g\frac{\partial \eta}{\partial y} - \frac{1}{\rho}\frac{\partial p}{\partial y} = -g\left[1 + \frac{\partial}{\partial y}\left(\frac{p}{\gamma}\right)\right] \qquad \text{(xiii)}$$

This relationship is similar to that used by Rouse (1937), the only difference being his choice of $+y$ as the vertical distance below the free surface. Equation (xiii) states that at sections where the pressure increases with *y* near the bed (see Figure II-2) the fluid particles experience a downwards-vertical acceleration considerably greater than gravity.

Obviously, in the presence of a rigid bed the fluid particles are prevented from reacting to this acceleration and thus the streamlines close to the bed remain parallel to the bed. However, this is not necessarily true for an erodible bed. To illustrate this point, let's assume that a bed-material cluster gets scoured away by the augmented bed-shear forces near the brink. The bed cavity left behind by the entrained cluster will enable the near-bed fluid to enter the cavity, driven by the force $f_y = \rho a_y$, and thus create a recirculating pattern similar to that described by Bennett (1999) for the case of developing headcuts. This recirculating flow will further scour the initial cavity resulting in a deepening scour pool.

In summary, the increase in bed shear stress near the brink of the primary knickpoint can trigger point scour that will grow as the result of near-bed streamlines impinging on the cavity left behind by the entrained bed material. Once this secondary pool is initiated, subsequent runoff events will either expand the pool or generate headcut migration upstream from the primary knickpoint. This concept appears to be supported by the above analysis and the secondary scour patterns displayed in Figure II-1.

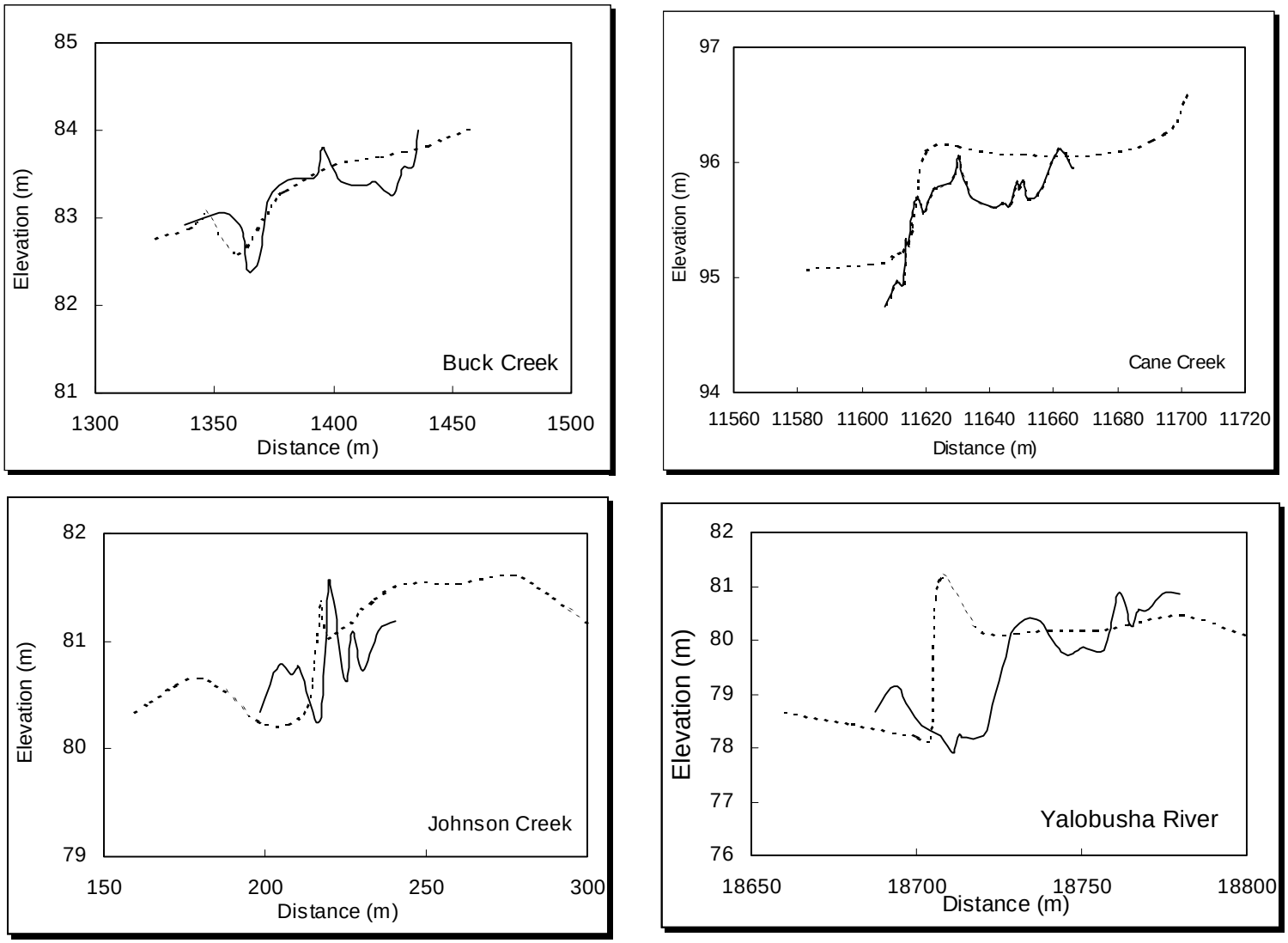

Figure II-1 - The onset of secondary scour upstream of migrating knickpoints is apparent in this contrast of surveys taken in 1997 (dashed lines) and 1999 (solid lines).

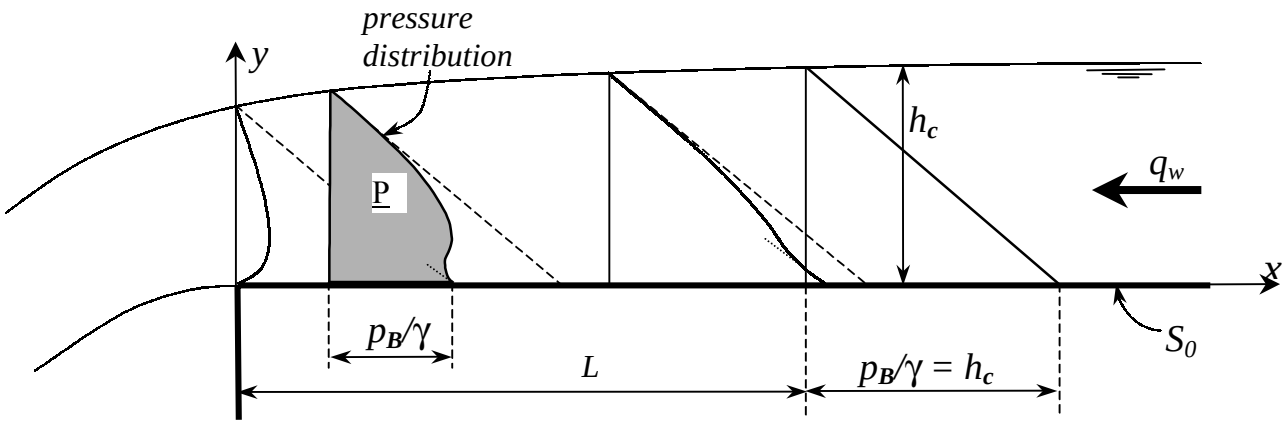

Figure II-2 - Surface profiles and pressure distributions at a free overfall.

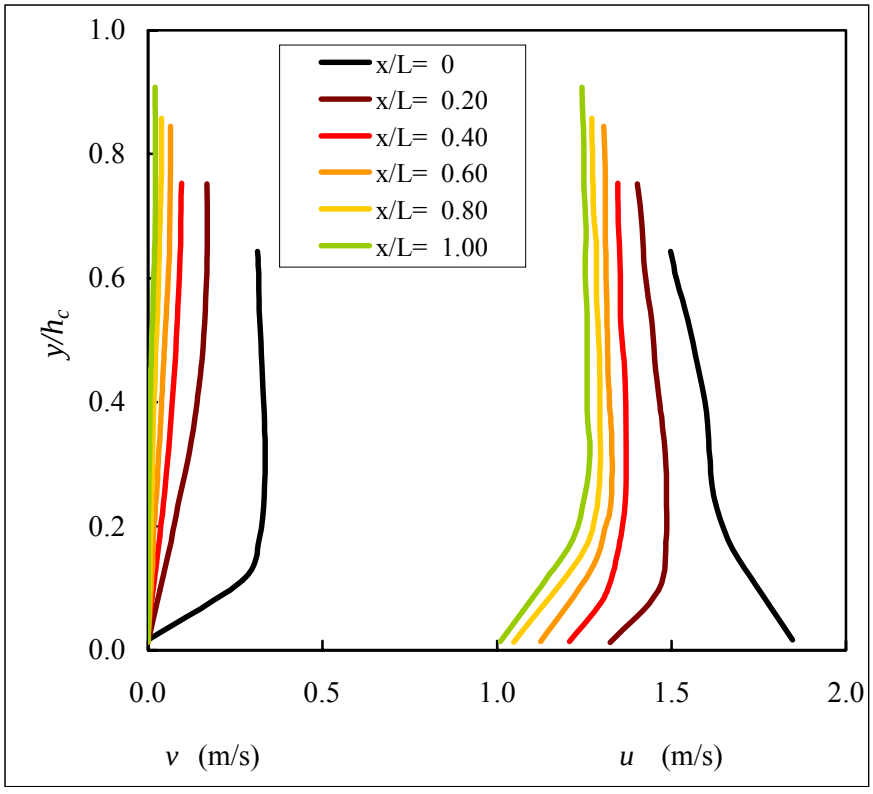

Figure II-3 - Distribution of vertical and horizontal-velocity components at the free overfall (adapted from Rajaratnam and Muralidhar, 1968).

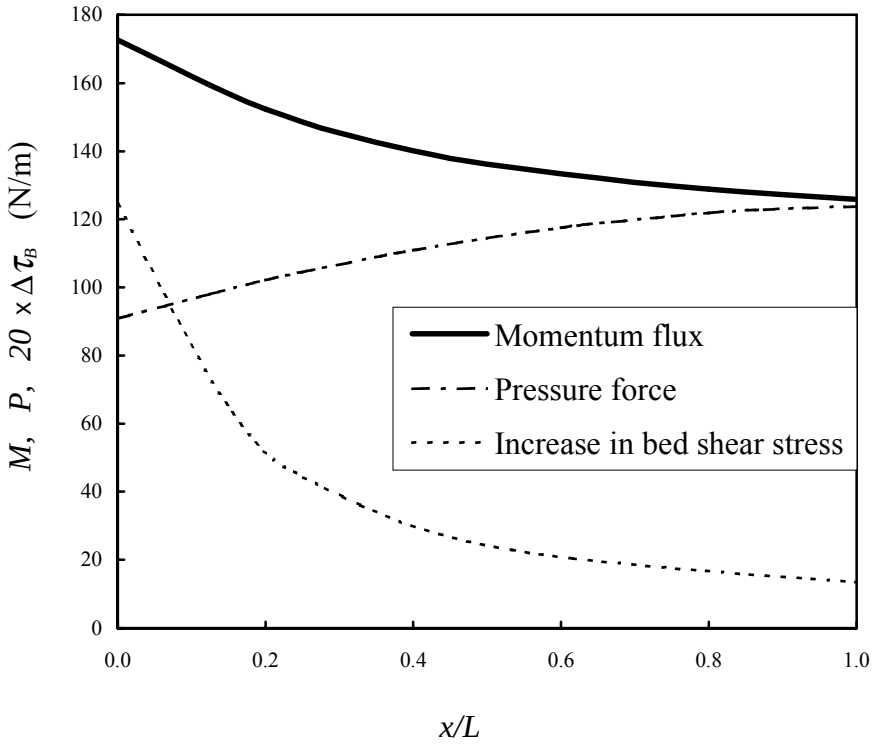

Figure II-4 - Momentum flux, cross-sectional pressure force per unit width, and bed shear stress in the region of accelerated flow computed from measurements reported by Rajaratnam and Muralidhar (1968).